Editorial Board

Environmental Research & Technology

TABLE OF CONTENTS

RESEARCH ARTICLE

Assessing pretreated municipal solid waste degradation by BMP and fibre analysis

Asif A. Siddiqui[1,*]

[1] Aligarh Muslim University, Department of Civil Engineering, Aligarh 202002, INDIA

ABSTRACT

Landfill continues to be the major method of Municipal solid waste (MSW) disposal in the UK and many other countries despite considerable efforts to limit its use. The EU Landfill Directive requires, amongst other things, that waste is treated to reduce its biodegradability prior to disposal to landfill. This pre-treatment is often achieved through what is generically termed mechanical-biological treatment. Predicting the biodegradability or degradation potential of these pre-treated wastes is important for the long term management and aftercare of landfill sites. To address this, a series of biochemical methane potential (BMP) tests have been undertaken to characterize the anaerobic biodegradation potential of two mechanically biologically treated (MBT) waste samples in terms of biogas yield, solids composition (loss on ignition, total carbon, cellulose, hemicellulose and lignin contents), and assessment of leachate characteristics during the biodegradation process. Experimental results from a long term study of MBT wastes treated to different standards are analyzed and compared. The relationship between biogas potential and solids composition was investigated, and carbon and nitrogen mass balances are discussed. The biogas potential was shown to correlate well with the ratio of cellulose plus hemicellulose to lignin, loss on ignition and total carbon content of the waste indicating a clear link between these parameters. The results indicate that solids composition of MBT wastes may provide a useful indication of the biodegradation potential. The mass balance indicates that a large proportion of carbon and nitrogen remain locked up in the waste material and is not released.

Keywords: Biodegradability, BMP, landfill, leachate, MBT waste

1. INTRODUCTION

Legislation (e.g. the EU landfill directive) in some parts of the world now requires municipal solid waste (MSW) to be processed prior to landfilling to reduce its biodegradability. This pre-processing may be achieved through what is generically termed mechanical-biological treatment. The biochemical methane potential (BMP) test measures the methane or biogas that can potentially be produced under anaerobic conditions by a known quantity of waste. This test is well recognized to provide a reliable estimate of organic waste biodegradability (e.g. [1-3]). BMP tests are bioassays in which a waste sample is incubated in a temperature controlled system, with nutrients and bacteria added to optimize conditions for microbial methanogenesis. The organic matter found in solid waste includes cellulose, hemicellulose and lignin as described in [4]. Reference [5] have shown that cellulose and hemicellulose contributes between 45 - 60% of MSW and are major biodegradable constituents responsible for up to 90% of methane production in landfills. As cellulose and hemicellulose degrades, most of the lignin remains and its percentage in the MSW increases. The relative concentrations of cellulose (C), hemicellulose (H) and lignin (L) have previously been used to assess the degree of decomposition of landfilled waste (e.g. [6, 7]). Over the past decade, field scale studies (e.g. [8, 9]) and laboratory scale studies (e.g. [10-15]) have operated MSW landfills as bioreactors to enhance the degradation process and accelerate waste stabilization, with the aim of bringing the landfill to a stable, non-polluting state in a relatively short time.

Data and experience on the performance of pre-treated MSW landfills i.e. those filled exclusively with MBT waste, is not currently available. Reference [16] investigated the impact of biological pre-treatment on leachate quality. Limited data are available on the long term leachate quality and gas generating potential of

MBT waste, based on small scale studies (e.g. [17-22]). Most of these studies did not capture the complete stabilization process and it remains unclear how the solids composition change with the progression of decomposition of an MBT waste.

To address this, a series of BMP tests have been undertaken to characterize the anaerobic biodegradation potential of two MBT waste samples pre-treated to different standards. This characterization includes measurement of biogas yield, changes in solids composition, and assessment of leachate characteristics during the biodegradation process. The relationship between biogas potential and solids composition was investigated, and carbon and nitrogen mass balances are discussed.

2. MATERIALS AND METHOD

2.1. Waste samples

Two mechanically sorted and pre-treated waste samples were studied: UK MBT waste and German MBT waste. The waste UK MBT waste was obtained from a large scale waste pre-treatment facility New Earth Solutions plant in Southern England. This is a fully enclosed facility that takes non-source segregated household wastes. These are initially shredded and screened for ferrous metals and non-biodegradable material recovery. The remaining degradable fraction undergo a six week dynamic processing phase involving aeration and, close temperature and moisture control to stabilize the waste.

The waste German MBT waste was obtained from Hannover Waste Treatment Centre, a mechanical-biological treatment facility in Hannover, Northern Germany. During the mechanical stage of the process, waste was sorted, shredded and screened, and recyclable materials and metals were removed. The remaining degradable waste fraction was anaerobically digested in fermentation tanks for a period of three weeks. The digested material was extracted and transferred to an aerobic post treatment area where it was composted in enclosed windrows for approximately 6 weeks.

2.2. Synthetic leachate

To enhance the decomposition of the waste by anaerobic bacteria, synthetic leachate containing mineral nutrients and trace elements dissolved in deionised water as described in [23] was used in this study and the details are given in Table 1.

2.3. BMP reactors set up and operation

The BMP reactors were made from 1000 ml Nalgene bottles attached to a gas collection system that allowed the volume of gas produced during anaerobic degradation to be measured. The test set-up comprised 12 BMP reactors (B1 to B12) each filled with 140 g of dried MBT waste sample. To accelerate degradation of the waste by anaerobic bacteria, 500 ml of synthetic leachate containing anaerobically digested sewage sludge seed (10% by vol.) was added to each reactor placed in a water bath at 30°C to promote mesophilic methanogenic conditions. Individual reactors were sacrificed sequentially during the test to observe solids compositional changes and leachate characteristics at different stages of degradation to allow leachate and solid compositional changes to be tracked. Each waste sample was also analyzed for total carbon, total nitrogen, loss on ignition (LOI), cellulose, hemicellulose and lignin, and the leachate samples were analyzed for pH, volatile fatty acids (VFAs), total organic carbon (TOC), dissolved organic carbon (DOC), inorganic carbon (IC), total nitrogen (TN) and ammoniacal nitrogen (NH_4-N). Biogas samples taken from each BMP reactor were analyzed for methane (CH_4) and carbon dioxide (CO_2).

2.4. Analytical procedure

The biogas that accumulated in the head space of each BMP gas collection burettes was collected in a gas tight syringe and its composition (CH_4 and CO_2) determined by gas chromatography in Varian CP3800 GC fitted with a HaySep C column and a molecular sieve 13x (80-100 mesh) operated at a temperature of 50°C. Argon was used as a carrier gas at a flow of 50 ml/minute. Leachate samples were analyzed for pH using a Jenway Model 3010 digital pH meter. TOC, DOC, IC and TN analyses of leachate samples were carried out using a high temperature Dohrmann-Rosemount DC-190 TOC analyzer equipped with a Dohrmann ozonator for TN analysis. NH_4 –N was measured by steam distillation using a Foss Tecator Kjeltec System 1002 distilling unit. VFA composition was determined by gas chromatography using a Shimadzu-2010 GC.

Table 1. Recipe of synthetic leachate

Reagent	Conc. (mg L^{-1})	Reagent	Conc. (mg L^{-1})
$K_2HPO_4.3H_2O$	330.000	$MnCl_2.4H_2O$	0.500
NH_4Cl	280.000	$CuCl_2.2H_2O$	0.038
$MgSO_4.7H_2O$	100.000	$(NH_4)6MoO_{24}.4H_2O$	0.050
$CaCl_2.2H_2O$	10.000	$AlCl_3.6H_2O$	0.090
$FeCl_2.4H_2O$	2.000	$NiCl_2.6H_2O$	0.142
H_3BO_3	0.050	$Na_2SeO_3.5H_2O$	0.164
$ZnCl_2$	0.050	$CoCl_2.6H_2O$	2.000
EDTA	1.000		

Waste solids were analyzed for LOI, TC, TN, cellulose, hemicellulose and lignin contents. Prior to the analyses for LOI, TC and TN, all non grindables (metal, glass, ceramic and stone) were removed from the sample. The remaining waste was dried at 70°C and milled to a fine powder using a Foss Knifetec 1095 mill in conjunction with a Foss Cyclotec 1093 mill. LOI content was measured by ignition of dried sample at 550°C in a muffle furnace for two hours. TC and TN contents of the samples were measured using a CE Instruments Flash EA 1112 Elemental Analyser (Thermo Finnigan). Fibre analysis using the FibreCap test method was performed for the measurement of cellulose, hemicellulose and lignin content as described in [27] and [28].

Table 2. Elemental and fibre analysis data

Chemical analysis	Concentration (% dry mass)	
	UK MBT waste	German MBT waste
Cellulose, %	10.24	7.96
Hemicellulose, %	4.54	3.91
Lignin, %	12.63	13.01
(C+H)/L ratio	1.17	0.91
Total carbon, %	22.68	19.85
Total nitrogen, %	1.81	1.52
Loss on ignition, %	42.91	34.84

3. RESULTS AND DISCUSSION

3.1. Biogas volume and composition

The net biogas yield attributable to 140 g dried waste sample in each reactor was determined by subtracting the measured biogas yield of the control bottles from the total biogas produced by each reactor. The volume of biogas collected was standardized to dry gas at STP as explained in [29]. Gas production started virtually immediately the reactors were assembled; methanogenic conditions were rapidly established. The acidogenic phase was virtually absent, probably due to the partial degradation of some organic compounds during the pre-treatment phase. This is in agreement with the findings of [18-20] and [21]. Biogas production for the MBT wastes increased in a similar trend but at different rates and most of the gas had been produced by day 100. Thereafter, gas production continued at a much lower rate until day ~200 when it had effectively ceased for both wastes. A similar observation for the gassing rate was made by [24] regarding the continuation of low level emissions in landfills over the long term. The UK MBT waste produced considerably more biogas, reaching approximately 45.54 L kg⁻¹ dry matter (DM) after 347 days. In contrast, biogas production from the German MBT waste was 16.39 L kg⁻¹ DM after 279 days. The biogas yield of UK MBT waste is greater than in some other studies (e.g. [17, 19]), but within the range reported by [20] and [22].

The higher gas production potential in the UK MBT waste is due to the more limited biological pre-treatment process used and correlates with the higher values of the organic content i.e. the LOI, cellulose and TC contents in Table 2. The gas composition in both waste samples was similar with the methane content in the range of 58% - 62% and the carbon dioxide content 35 - 40%. The cumulative gas volume for raw MSW (collected from White's Pit waste processing plant in Southern England) degraded anaerobically for 919 days as reported in [28] was significantly higher (243.55 L kg⁻¹ DM) which is attributable to the higher organic waste composition in the raw MSW. This reduced gassing potential of the MBT wastes demonstrates diversion of the degradable fraction from disposal to landfill as a result of the biological pre-treatment process, but also that landfill gas control measures will still be required to prevent fugitive gas emissions from landfill.

Fig 1. Leachate VFA and pH in BMP reactors for the UK MBT waste

The higher gas production potential in the UK MBT waste is due to the more limited biological pre-treatment process used and correlates with the higher values of the organic content i.e. the LOI, cellulose and TC contents in Table 2. The gas composition in both waste samples was similar with the methane content in the range of 58% - 62% and the carbon dioxide content 35 - 40%. The cumulative gas volume for raw MSW (collected from White's Pit waste processing plant in Southern England) degraded anaerobically for 919 days as reported in [28] was significantly higher (243.55 L kg⁻¹ DM) which is attributable to the higher organic waste composition in the raw MSW. This reduced gassing potential of the MBT wastes demonstrates diversion of the degradable fraction from disposal to landfill as a result of the biological pre-treatment process, but also that landfill gas control measures will still be required to prevent fugitive gas emissions from landfill.

3.2. Leachate Characteristics

The pH of the leachate decreased slightly at the start of the degradation process due to the built up of VFAs during the first week due to the accumulation of hydrolytic products, and started to decrease thereafter as the methanogens utilized these as a substrate for conversion to biogas. Final stable values of pH were between 7.5 and 7.7, similar to those found in previous studies (e.g. [10, 14-15]). The decrease in VFA composition is consistent with an increase in pH and biogas production as shown in Fig

1. The low VFA concentration is an indication that most of the available organic matter has been converted into biogas and that biological stabilization has been achieved. The TOC concentration increased at the start due to the rapid release and hydrolysis of organics from the waste into the leachate. It was then decreased slowly in accordance with the progression of microbially mediated stabilization processes to about 465 and 198 mg L^{-1} by the end of the test for the UK and German MBT wastes respectively (Fig 2). The lower organic content of the leachate associated with the MBT wastes are in agreement with the findings of [16] and [20], but the values are in excess of those observed by [17] and [22].

The organic strength i.e. TOC of the leachate from the German MBT waste was low compared with that from the UK MBT waste, consistent with the reduced organic content of the German waste owing to the different biological processing steps used during pre-treatment. Most of the TN was found to be in the form of ammoniacal nitrogen. After the initial increase, TN and NH$_4$-N remained stable until the end of the tests. This is in agreement with the findings of [25] and [26]. These results indicate that the leaching potential of nitrogen from the German MBT waste was less than that from the UK MBT waste and is due to the lower initial TN content of the German MBT waste.

3.3. Solids Composition

The cellulose and hemicellulose values show a decreasing trend while lignin increased (becoming a greater proportion of the remaining waste) being a recalcitrant material (Fig 3). This is consistent with the depletion of cellulose and hemicellulose as about 50 to 60% of cellulose and 40 to 45% of the hemicellulose degraded over the whole period of test for the MBT wastes. The cellulose content decreased from 10.2% to ~ 3.8% and from 7.9% to ~3.9% for the UK and German MBT wastes respectively. The hemicellulose content decreased from 4.5% to about 2.5% and from 3.9% to 2.4% for the two wastes respectively. The presence of cellulose and hemicellulose that is not degraded can be explained by the fact that lignin forms a physical barrier around some cellulose and hemicellulose which eliminates microbial access. The lignin content increases due to a relative decrease in cellulose and hemicellulose contents and the lignin enrichment of the remaining solids. A strong linear correlation was found between the biogas potential and the (C+H)/L ratio for the wastes. Decreasing (C+H)/L ratios correlate well with decreasing biogas potential. For both the wastes, a good correlation was found when comparing the biogas potential to LOI and TC content of the wastes. The LOI content of the solid waste samples showed a decreasing trend over the test period, which is consistent with the depletion of TC. Therefore, the changes in solids composition e.g. (C+H)/L ratio, LOI and TC are interrelated and there is a clear link between these parameters and biogas potential (Fig 4).
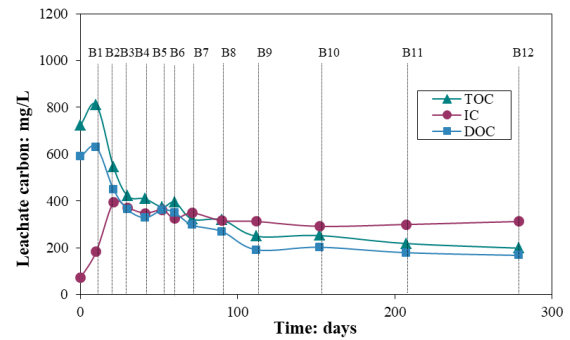
Fig 2. Leachate carbon in BMP reactors for the German MBT waste
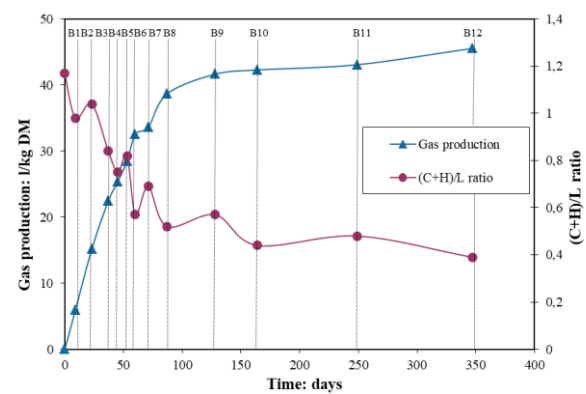
Fig 3. (C+H)/L ratio and gas production in BMP reactors for the UK MBT waste
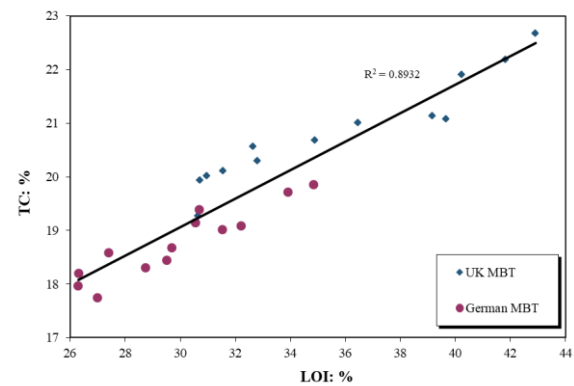
Fig 4. Correlation between LOI and TC contents of the UK and German MBT wastes

3.4. Carbon and nitrogen mass balance analysis

Carbon and nitrogen mass balance calculations for the UK and German MBT wastes are summarized in Tables 3 and 4 respectively. The mass balance shows that 85 - 90 % of the carbon initially in waste remained there, 10% was removed in the biogas, and less than 1% was transferred into the leachate. About 90 % of the nitrogen remained in the waste at the end of degradation and 5% transferred into the leachate, with 5% unaccounted for.

Table 3. Summary of carbon mass balance in the UK and German MBT wastes

Parameter	UK MBT waste	German MBT waste
$C_{initial\ waste}$, g kg^{-1} DM	226.8	198.5
$C_{synthetic\ leachate}$, g kg^{-1} DM	1.78	1.49
C_{CH4}, g kg^{-1} DM	15.13	5.18
C_{CO2}, g kg^{-1} DM	9.03	3.42
$C_{leachate}$, g kg^{-1} DM	2.71	1.82
$C_{degraded\ waste}$, g kg^{-1} DM	192.7	179.7
C_{CaCO3}, g kg^{-1} DM	0.32	0.28
C_{MgCO3}, g kg^{-1} DM	0.03	0.09
Mass balance error, g kg^{-1} DM	8.66	9.5
Mass balance error, %	3.8	4.7

Table 4. Summary of nitrogen mass balance in the UK and German MBT wastes

Parameter	UK MBT waste	German MBT waste
$N_{initial\ waste}$, g kg^{-1} DM	18.1	15.2
$N_{synthetic\ leachate}$, g kg^{-1} DM	0.34	0.24
$N_{degraded\ waste}$, g kg^{-1} DM	16.1	13.9
$N_{leachate}$, g kg^{-1} DM	1.49	0.65
Mass balance error, g kg^{-1} DM	0.85	0.89
Mass balance error, %	4.6	5.8

4. CONCLUSIONS

The biogas yield and leachate characteristics have demonstrated that pre-treatment of raw MSW substantially reduces the gas generating potential and leachate strength.

Degradability of MBT waste was evaluated using LOI, TC, biogas potential, cellulose, hemicellulose and lignin contents of decomposing waste in small scale BMP reactors. A strong correlation was found between the biogas potential and the (C+H)/L ratio. The initial cellulose and hemicellulose contents of the pre-treated wastes were reduced, but in the degraded state were very similar to degraded MSW indicating that the same state of final decomposition is achieved. LOI content of the waste samples decreased with the progression of degradation which is consistent with the depletion of the TC content. The biogas potential was shown to correlate well with LOI and TC content of the waste. The BMP test results indicate that changes in LOI, TC and (C+H)/L ratio and biogas potential are inter-related and solids composition of MBT waste may provide a useful indication of the biodegradation potential.

The carbon and nitrogen mass balances indicate only a small proportion of the carbon and nitrogen in the system is unaccounted for. A large proportion of carbon and nitrogen remain locked up in the waste material and is not released.

REFERENCES

[1]. S.T. Wagland, S.F. Tyrrel, A.R. Godley and R. Smith, "Test methods to aid in the evaluation of the diversion of biodegradable municipal waste (BMW) from landfill," Waste Management, Vol. 29 (3), pp. 1218–1226, 2009.

[2]. A.R. Godley, A. Graham and K. Lewin, "Estimating biodegradable municipal solid waste diversion from landfill: Screening exercise to evaluate the performance of biodegradable waste test methods," *Environment Agency R&D Technical Report*, P1-513 (EP 0173) phase 1, 2005.

[3]. T.L. Hansen, J.E. Schmidt, I. Angelidaki, E. Marca, J.C. Jansen, H. Mosbæk and T.H. Christensen, "Method for determination of methane potentials of solid organic waste," *Waste Management*, Vol. 24 (4), pp. 393 - 400, 2004.

[4]. M.A. Barlaz, "Carbon storage during biodegradation of municipal solid waste components in laboratory scale landfills," *Global Biogeochemical Cycles,* Vol. 12 (2), pp. 373-380, 1998.

[5]. M.A. Barlaz, A.P. Rooker, P. Kjeldsen, M.A. Gabr and R.C. Borden, "A Critical Evaluation of Factors Required to Terminate the Post-Closure Monitoring Period at Solid Waste Landfills," *Environmental Science and Technology*, Vol. 36 (16), pp. 3457 – 3464, 2002.

[6]. M.S. Hossain, M.A. Gabr and M.A. Barlaz, "Relationship of compressibility parameters to municipal solid waste decomposition," *ASCE Journal of Geotechnical and Geoenvironmental Engineering,* Vol. 129 (12), pp. 1151 – 1158, 2003.

[7]. T.D. Baldwin, J. Stinson and R.K. Ham, "Decomposition of specific materials buried within sanitary landfills," *Journal of Environmental Engineering,* Vol. 124 (12), pp. 1193- 1202, 1998.

[8]. C.H. Benson, M.A. Barlaz, D.T. Lane and J.M. Rawe, "Practice review of five bioreactor/recirculation landfills," *Waste management,* Vol. 27 (1), pp. 13-29, 2007.

[9]. J.W.F. Morris, N.C. Vasuki, J.A. Baker and C.H. Pendleton, "Findings from long-term monitoring studies at MSW landfill facilities with leachate recirculation," *Waste Management*, Vol. 23 (7), pp. 653–666, 2003.

[10]. W.R. Valencia van der Zon, H. Woelders, H.J. Lubberding and H.J. Gijzen, "Achieving "Final Storage Quality" of municipal solid waste in pilot scale bioreactor landfills," *Waste Management*, Vol. 29 (1), pp. 78-85, 2009.

[11]. V. Francois, G. Feuillade, G. Matejka, T. Lagier and N. Skihiri, "Leachate recirculation effects on waste degradation: study on columns," *Waste Management*, Vol. 27 (9), pp. 1259-1272, 2007.

[12]. A.S. Erses, T.T. Onay and O. Yenigun, "Comparison of aerobic and anaerobic degradation of municipal solid waste in bioreactor landfills," *Bioresource Technology*, 99 (13), 5418–5426, 2008.

[13]. M.S. Bilgili, A. Demir and B. Özkaya, "Influence of leachate recirculation on aerobic and anaerobic decomposition of solid wastes," *Journal of Hazardous Materials*, Vol. 143 (1-3), pp. 177-183, 2007.

[14]. D.T. Sponza and O.N. Ăgdăg, "Impact of leachate recirculation and recirculation volume on stabilization of municipal solid wastes in simulated anaerobic bioreactors," *Process Biochemistry*, Vol. 39 (12), pp. 2157-2165, 2004.

[15]. M. Warith, "Bioreactor Landfills: experimental and field results," *Waste Management*, Vol. 22 (1), pp. 7-17, 2002.

[16]. H.D. Robinson, K. Knox, B.D. Bone and A. Picken, "Leachate quality from landfilled MBT waste," *Waste Management*, Vol. 25 (4), pp. 383-391, 2005.

[17]. M. van Praagh, J. Heerenklage, E. Smidt, H. Modin, R. Stegmann and K.M. Persson, "Potential emissions from two mechanically–biologically pretreated MBT wastes," *Waste Management*, Vol. 29 (2), pp. 859–868, 2009.

[18]. K. Sormunen, J. Einola, M. Ettala and J. Rintala, "Leachate and gaseous emissions from initial phases of landfilling mechanically and mechanically-biologically treated municipal solid waste residuals," *Bioresource Technology*, Vol. 99 (7), pp. 2399-2409, 2008.

[19]. G. De Gioannis, A. Muntoni, G. Cappai and S. Milia, "Landfill gas generation after mechanical biological treatment of municipal solid waste: estimation of gas generation constants," *Waste Management*, Vol. 29 (3), pp. 1026-1034, 2009.

[20]. R. Bayard, J. de Araujo Morais, M. Rouez, U. Fifi, F. Achour and G. Ducom, "Effect of biological pretreatment of coarse MSW on landfill behaviour: laboratory study," *Water Science and Technology*, Vol. 58 (7), pp. 1361-1369, 2008.

[21]. A. Bockreis and I. Steinberg, "Infuence of mechanical-biological waste pre-treatment methods on the gas formation in landfills," *Waste Management*, Vol. 25 (4), pp. 337–343, 2005.

[22]. K. Leikam and R. Stegmann, "Influence of mechanical–biological treatment of municipal solid waste on landfill behavior," *Waste Management and Research*, Vol. 17 (6), pp. 424–429, 1999.

[23]. L. Florencio, J. A. Field and G. Lettinga, "Substrate competition between methanogens and acetogens during the degradation of methanol in UASB reactors," *Water Research*, Vol. 29 (3), pp. 915-922, 1995.

[24]. K. Knox and H.D. Robinson, "MBT and thermal treatment of MSW residues: a comparative study of energy balance and long-term pollution potential of leachates," Proceedings Sardinia 2007, Eleventh International Waste Management and Landfill Symposium, Cagliari, Italy, 2007.

[25]. N.D. Berge, D.R. Reinhart and T.G. Townsend, "The fate of nitrogen in bioreactor landfills," *Critical Reviews in Environmental Science and Technology*, Vol. 35 (4), pp. 365-399, 2005.

[26]. J.P.Y. Jokela and J.A. Rintala, "Anaerobic solubilisation of nitrogen from municipal solid waste," *Reviews in Environmental Science and Biotechnology*, Vol. 2 (1), pp. 67-77, 2003.

[27]. B. Zheng, D.J. Richards, D.J. Smallman and R.P. Beaven, "Assessing MSW degradation by BMP and fibre analysis," *Waste and Resource Management*, Vol. 160 84), pp. 133-139, 2007.

[28]. L.K., Ivanova, D.J. Richards and D.J. Smallman, "Assessment of the anaerobic biodegradation potential of MSW," *Waste and Resource Management*, Vol. 161 (3), pp. 167-180, 2008.

[29]. A.A. Siddiqui, "Pretreated municipal solid waste behaviour in laboratory scale landfill," *International Journal of Sustainable Development and Planning*, Vol. 9 (2), pp. 263-276, 2014.

RESEARCH ARTICLE

Removal of indigo dye by photocatalysis process using Taguchi experimental design

Gamze Dogdu Okcu[1,*] (ID), Tugba Tunacan[2] (ID), Emre Dikmen[1] (ID)

[1] Bolu Abant Izzet Baysal University, Environ. Eng. Dept., Golkoy Campus, 14030 Bolu, TURKEY
[2] Bolu Abant Izzet Baysal University, Industrial Eng. Dept., Golkoy Campus, 14030 Bolu, TURKEY

ABSTRACT

The major concern of the present research is degradation of hazardous and stable Indigo dye used in industrial denim dying process. For this purpose, a heterogeneous photocatalysis process was carried out to treat aqueous solution of Indigo dye using pure titanium dioxide (TiO_2) in a batch reactor system under ultraviolet A (UVA) light for 210 min. In the study, individual and synergistic effects of factors such as TiO_2 dosage, pH, and initial dye concentration were scrutinized. Moreover, Taguchi statistical method was performed to optimize influential parameters. The results obtained from the study that TiO_2 concentration had the most effective factor on the Indigo dye degradation. The optimal conditions for dye removal were A (pH) at level 2 (4), B (initial dye concentration) at level 1 (10 mg L^{-1}) and C (TiO_2 concentration) at level 4 (1.5 g L^{-1}). The results presented that the theoretically predicted value for degradation efficiency (100%) was confirmed by the experimental value (100%).

Keywords: Indigo dye, optimization, photocatalytic degradation, Taguchi method, water treatment

1. INTRODUCTION

The textile manufacturing and clothing sector has strategic importance in terms of exports, investments, employment, the value added in the manufacturing sector for the Turkish economy. According to the European Statistical Office (Eurostat), Turkey's clothing exports to the European Union ranked third with around EUR 9.1 billion (9%) after China, Bangladesh in 2017 [1].

Jeans which are sold two billion every year all around the world are the most worn clothing among people. However, one jean alone requires 10.000 L of water, 0.5 kg of chemicals, pesticides, dyes, strong detergents and road and fuel cost due to transportation thus, they cause to enormous disaster [2]. Dyes are major responsible of the water pollution that are generally non-biodegradable and hardly degradable substances due to their synthetic origin and complex aromatic structures [3].

The denim dyeing industry generally use indigo blue is a kind of organic structural dye that has toxic properties in aquatic systems [4]. Indigo ($C_{16}H_{10}N_2O_2$) is belonging to the vat-indigoids class of dyes that is

produced naturally by plants or manufactured synthetically in large quantities (20 million kg annually) [5, 6]. Indigo blue is practically insoluble in water (2 ppm) and has no affinity for cellulose fibers in such a state. Thus, it needs to be reduced to its soluble form (leuco from) by a powerful reducing agent such as sodium dithionite ($Na_2S_2O_4$) before dying. This agent helps to convert Indigo dye into a water soluble form. So, the dye can develop a chemical affinity with the cellulose fiber [7, 8]. Moreover, indigo dyes create dye rich effluents that resulted with various environmental problems [9]. These dyes are generally disposed in natural streams that are easily accessed by people for drinking, washing or personal cleaning activities. Hence, this type of water pollution poses threats to human health. Also the disposal of synthetic dyes into the water system damages photochemical activities of aquatic ecosystem by preventing light penetration solubility of gases [10, 11]. Indigo dye is very stable molecule that is difficult to remove using traditional biological treatment methods [12]. Thus, it is necessary to treat colored wastewater before discharging it to the environment and water resources [13].

Degradation and decolorization of indigo dye and indigo rich wastewater can be treated by physicochemical methods like adsorption/biosorption [6, 14], ozonation [15], coagulation/flocculation [16, 17], Fenton/Foto-Fenton [18], photocatalysis [5, 19-21], electrochemical treatment methods [12], membrane bioreactors [8], biological process [6, 9]. However, cost of regeneration, secondary pollutants, limited versatility, interference by other wastewater constituents, necessities for reagents, and generation of large quantity of sludge are fundamental disadvantages of these conventional techniques coupled with the increment costs due to handling, treatment and disposal [22, 23]. Nowadays, effective, simple and low cost technologies are tried to find as a solution by researchers to eliminate indigo dye from wastewater.

Advanced Oxidation Processes (AOPs) generally based on the production of hydroxyl radicals ($\bullet OH$) can be considered as a promising alternative for the treatment of stable, non-biodegradable pollutants [24, 25]. Among the existing AOPs, heterogeneous photocatalysis is an effective technique that comprises a semiconductor catalyst such as TiO_2, ZnO, CdS which works with ultraviolet light (UV) to degrade pollutants [26]. Titanium dioxide (TiO_2) has been widely used catalyst due to its biological and chemical stability, relatively high photocatalytic activity, non-toxic nature, low-cost and long span [27].

The multivariate optimization methods have various benefits compared to traditional one-at-a-time method because they help us to get a greater set of data with fewer experimental runs [13]. The main principles of Taguchi methods are to obtain information about main effects and synergistic effects of design parameters from minimum number of experiments [28]. In this study, all of the operational parameters were optimized by using Taguchi design to achieve the maximum removal of Indigo dye from the aqueous solution. This technique has been used in the literature by other researchers for optimization of the experimental factors in advanced oxidation processes [29-31]. To the best of our knowledge, the optimization of process parameters for the dye degradation by Taguchi method is very scarce and there is no report in the literature on the optimization of photocatalytic degradation of commercial grade indigo dye in aqueous heterogeneous suspension by TiO_2/ultraviolet A (UVA) with Taguchi experimental design. For this reason, an orthogonal array experiment design L_{25} comprising of each experimental variable with different levels was applied. Moreover, for the determination of optimal photocatalysis conditions (pH, initial dye concentration and TiO_2 concentration) for maximum degradation of Indigo dye, Taguchi's signal-to-noise ratio (S/N) and the analysis of variance (ANOVA) was used. Also, a confirmation test with the optimal levels

of process parameters was done in order to demonstrate the performance of Taguchi's optimization method [31].

2.   MATERIALS AND METHOD
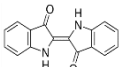
2.1. Chemicals and reagents

A TiO_2 photocatalyst (Sigma-Aldrich Inc., St. Louis, MO, USA; Product Code: 14021) was used as received. Other chemicals were of analytical grade and used without purification. Commercial synthetic Indigo dye (Molecular formula: $C_{16}H_{10}N_2O_2$) dissolved in water (40%) containing some impurities in solution which was supplied from Realkom Denim Textile Factory (Düzce, Turkey) to simulate realistic operating conditions. Table 1 shows the chemical structure of the original Indigo dye. Other chemicals such as NaOH and H_2SO_4 (assay 97%) used for adjusting pH were obtained from Merck (Darmstadt, Germany). All chemicals were used as received without further treatment. All solutions and reaction mixtures were prepared using purified water (spec. resistivity: 18.2 MΩ cm; Merck Millipore, Burlington, MA, USA).

2.2. Experimental setup and procedure

Photocatalytic experiments were performed in a 4.6 L (operating volume: 1 L) cylindrical, (14 cm D × 30 cm L) batch photoreactor (Fig 1) maintained at 25±1ºC by circulating the coolant (water) through inlets of the inner cylinder. The photoreactor was constructed from three parts: i) an external Pyrex glass; ii) a Pyrex glass thimble, where the head part is fitted to the outside container to form a gastight seal and running water is passed through the thimble to cool the reaction solution and iii) an empty quartz chamber, in which a Philips PL-L UVA 36 W lamp (315 to 380 nm; 110 μW cm^{-2}) was placed. The reactor was also equipped with a control system, a water level sensor system and a water-inlet and outlet. A gas inlet opening supplies air from a diffuser system of 3.5 L min^{-1} capacity during experiments. The reactor was wrapped in aluminum foil to prevent UV ray penetration. For irradiation experiments, the desired concentrations of Indigo solution were prepared from 1000 mg L^{-1} of stock solution daily in amber-glass vessels, and the system was stirred and had air bubbled through – in order to increase the oxygen transfer to the solution – following the addition of TiO_2 for at least 30 minutes in the dark to allow the system to reach equilibrium in case of adsorption. This time was chosen so that under stirring in the dark no more dye molecules could be adsorbed by the photocatalyst. For comparison, irradiation experiments without adding TiO_2 were also performed.

Table 1. Chemical structure of Indigo

Name	Molecular structure	Chemical structure	Molecular weight (g mol^{-1})	λmax (nm)
Indigo, Indigotin	$C_{16}H_{10}N_2O_2$		262.26	610

The pH of the reaction mixture was adjusted by adding 1 N of NaOH and 1 N of H_2SO_4. The extent of substance conversion under radiation was determined by withdrawing aliquots after specific reaction time intervals, where the starting time was defined as the beginning of irradiation. Samples were centrifuged in a stoppered tube for 15 minutes at 5000 rpm to remove the TiO_2 from the solution.

Optimization of photocatalysis conditions were initially done using a spectrophotometer (Merck Pharo 100, Germany) and measuring the optical density (OD) of samples at its λ_{max} of 610 nm, which is the given maximum absorption wavelength for Indigo molecules for 210 minutes irradiation. Calibration plot based on Beer-Lambert's law was established by relating the absorbance to the concentration. This was also confirmed by a spectrum reading from the spectrophotometer. The percentage of degradation of Indigo was calculated using Eq 1:

$$Percentage\ of\ degradation\ of\ Indigo = \frac{c_i - c_f}{c_i} \qquad (1)$$

where C_i and C_f are the initial and final Indigo concentrations in the reaction mixture, respectively.
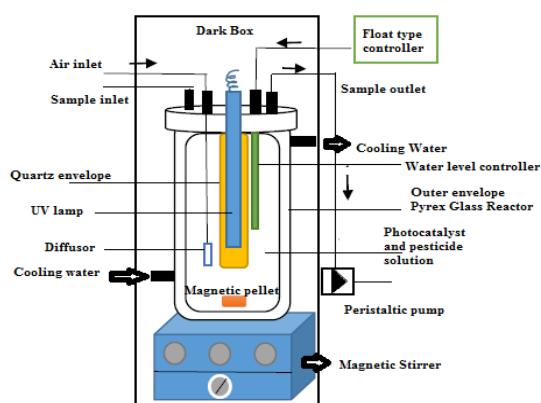

Fig 1. Schematic diagram of photocatalytic reactor

The photocatalytic experiments were performed using aqueous solutions of Indigo dye at different initial pH values (2-10), dye concentrations (10-50 mg L^{-1}) and catalyst dosages (0-2.0 g L^{-1}).

2.3. Taguchi orthogonal array experimental design

The Taguchi method is a powerful design that has been extensively used in engineering analysis. The method reduces the number of tests by using orthogonal arrays and minimizes the effects of the uncontrollable factors [32, 33]. Japanese scientist Dr. Genichi Taguchi developed this statistical experimental design method that enables to examine

the parameters affecting an experiment in two groups, that is controllable and uncontrollable. Also, it allows studying multiple parameters at two or more levels [34]. The fundamental aim of the Taguchi method is to find out the best combination of design parameters and reduce the variation for quality [35].

Experiment with one variable or one factor at a time is a traditional approach that is time consuming and labor-intensive [36]. Recently, the systematic orthogonal array (OA) is frequently used to optimize and design experiments in Taguchi method. The OA is a kind of experiment where the columns for the independent variables are "orthogonal" to one another [31]. The analysis of variance (ANOVA) and signal-to-noise ratio (S/N) are generally used to analyze the results of designed experiments. Hence, process parameters can be easily identified that have important contribution on the process [37]. According to previous works about Indigo dye removal using photocatalysis process [9, 18], main operational parameters and their levels were selected and given in Table 2.

In this study, for optimizing the experimental variables of Indigo removal three factors (pH, initial dye concentration and TiO_2 concentration) in five levels were studied with fractional factorial design leading to twenty-five experiments (L_{25} design, Table 3). Three-five level factors are arranged in an L_{25} orthogonal array table. L indicates the Latin square and 25 means replication number of the experiment. The number in table implies the level of factors [38]. Experimental data were analyzed using the Minitab software (version 17-trial edition).

3. RESULTS AND DISCUSSION

3.1. Determination of optimal conditions using Taguchi method

Taguchi method enables to identify the optimal conditions of photocatalysis experiment and it determines the parameters having the most significant effect on the dye removal. The structure of Taguchi's L_{25} design and the results of experiments are given in Table 3. Each run of the matrix indicates one test run. However, the sequence in which these tests were applied was randomized. A range of values from 16% to 100% was obtained from the removal efficiency. This statistical experiment design is considered as a strong predictive model because it allows evaluation by separating the controllable and uncontrollable factors. In this study, there are no uncontrollable variables. Hence, the controllable variables are taken as pH, initial concentration of the Indigo dye, and TiO_2 concentration.

Table 2. Process parameters and their levels

Parameters	Symbol	Level 1	Level 2	Level 3	Level 4	Level 5
pH	A	2	4	6	8	10
Indigo concentration (mg L^{-1})	B	10	20	30	40	50
TiO_2 concentration (g L^{-1})	C	0	0.5	1	1.5	2

Table 3. Full factorial design with orthogonal array of Taguchi L$_{25}$ (5^3)

Exp. no.	Factor A	Factor B	Factor C	Response (%)	S/N (dB)	Mean value	Predic-tive S/N ratio	Predictive Mean value
1	1	1	1	53.81	34.62	53.81	33.44	55.75
2	1	2	2	58.76	35.38	58.76	37.97	73.63
3	1	3	3	99.56	39.96	99.56	39.47	89.61
4	1	4	4	74.67	37.46	74.67	37.76	79.67
5	1	5	5	80.52	38.12	80.52	36.90	68.66
6	2	1	2	100.00	40.00	100.00	39.74	97.33
7	2	2	3	100.00	40.00	100.00	40.83	104.22
8	2	3	4	100.00	40.00	100.00	40.44	104.51
9	2	4	5	99.90	39.99	99.90	38.16	90.09
10	2	5	1	24.38	27.74	24.38	28.56	28.13
11	3	1	3	100.00	40.00	100.00	39.33	97.28
12	3	2	4	99.34	39.94	99.34	38.52	88.47
13	3	3	5	71.31	37.06	71.31	37.57	84.28
14	3	4	1	16.43	24.32	16.43	26.55	18.91
15	3	5	2	40.92	32.24	40.92	31.59	39.08
16	4	1	4	100.00	40.00	100.00	39.86	95.68
17	4	2	5	81.46	38.22	81.46	38.51	82.39
18	4	3	1	26.27	28.39	26.27	28.81	27.25
19	4	4	2	45.86	33.23	45.86	32.43	44.00
20	4	5	3	48.89	33.78	48.89	34.02	53.17
21	5	1	5	100.00	40.00	100.00	42.25	107.78
22	5	2	1	52.68	34.43	52.68	32.14	43.54
23	5	3	2	79.03	37.96	79.03	37.08	70.52
24	5	4	3	72.09	37.16	72.09	37.26	76.28
25	5	5	4	64.07	36.13	64.07	36.96	69.75

In the Taguchi design, the terms "signal" and "noise" represent the desirable and undesirable values for the output characteristic, respectively. S/N ratio gives the measurement of the quality characteristic deviating from the desired value. The S/N ratio is defined as ratio between desirable results (signal) to undesirable results (noise). Maximum S/N ratio gives the optimum conditions [39]. In the study, the maximum dye removal efficiency is tried to measure, so the performance formula of "bigger characteristics are better" was applied as objective function to define S/N ratios.

$$\frac{S}{N}[dB] = -10\log\left[\frac{1}{n}\sum_{i-1}^{n}1/y_i^2\right] \qquad (2)$$

where y_i is the characteristic property, n is the replication number of the experiment.

Table 4 shows the S/N ratio for removal of the solution containing Indigo dye calculated using Eq 2. The mean S/N ratio for each level of the parameters was summarized as S/N response, which was shown in Table 3.

The optimum condition is A2, B1 and C4. According to S/N ratio, the optimal parameters (conditions) for dye removal are A (pH) at level 2 (4), B (initial dye concentration) at level 1 (10 mg L^{-1}) and C (TiO$_2$ concentration) at level 4 (1.5 g L^{-1}). Based on the optimum conditions, 100.0% dye removal can be obtained.

Table 4. S/N response table for % dye removal

Levels	Control factors		
	% dye removal		
	A	B	C
Level 1	37,11	**38,92**	29,9
Level 2	**37,55**	37,6	35,76
Level 3	34,71	36,67	38,18
Level 4	34,72	34,43	**38,71**
Level 5	37,14	33,6	38,68
Delta	2,83	5,32	8,81
Rank	3	2	1

Bold values shows the optimal levels of control factors

3.2. Statistical Analysis

ANOVA helps to determine the effects of each parameter on the variance of the results, regarding the total variance of all the parameters [31]. Actually, the main aim of the ANOVA is to extract from the results how much variations each factor causes relative to the total variation observed in the result [28]. Table 5 shows the ANOVA results for Indigo dye removal efficiency in the photodegradation process.

The significance of the experimental parameters was found out by using analysis of variance. The analysis was evaluated for confidence level 95%, that is for significance level of $\alpha=0.05$. The p values <0.05 represents the significance of the parameters. It points out that there is only a 5% chance that a p value this large could occur due to noise.

Hence, the ANOVA results show that the most significant factor contributing the Indigo dye removal is TiO_2 concentration (C), followed by initial Indigo concentration (B) as shown in Table 5. However, according to F-test, pH (A) is statistically insignificant on the degradation of Indigo dye by photocatalysis process. So, the most effective parameters were selected based on their F values.

The main effect plot of the process parameters on the dye removal efficiency is clearly illustrated in this Fig 2 and Fig 3. Concentration of TiO_2 as a catalyst has a significant role in the efficiency of photocatalytic process. The effect of different doses of catalyst from 0 to 2.0 g L^{-1} was tested in the study. When the catalyst concentration increases, that is found to be the most significant factor among all; the S/N ratio also increases. As shown in Fig 2 and Fig 3., with increasing catalyst concentration at 1.5 g L^{-1}, the reaction rate increases, because with an increasing amount of catalyst more dye molecules are adsorbed onto the catalyst surface and dye removal in the area of irradiation n increases. Moreover, the catalyst has high accessible surface area at the beginning of the photocatalysis process [27].

Secondly, in order to investigate the effectiveness of photocatalytic oxidation with increasing dye concentration, experiments were conducted for 10 to 50 mg L^{-1} concentrations of Indigo dye. As illustrated in Fig 2, when the dye concentration increases, the S/N ratio decreases sharply. This indicates that degradation is achieved better at lower dye concentrations. Reference [31] reported that when the Carmoisine dye increased from 20 to 30 mg L^{-1}, S/N ratio decreased for Fenton and photo Fenton processes. Furthermore, Reference [24] stated that when the concentration of a kind of textile dye, Bezacryl Yellow (BZY) increased from 10 mg L^{-1} to 117 mg L^{-1} in the presence of TiO_2, the dye removal decreased from 100% to 57%.

Table 5. ANOVA results by Taguchi method and regression equations

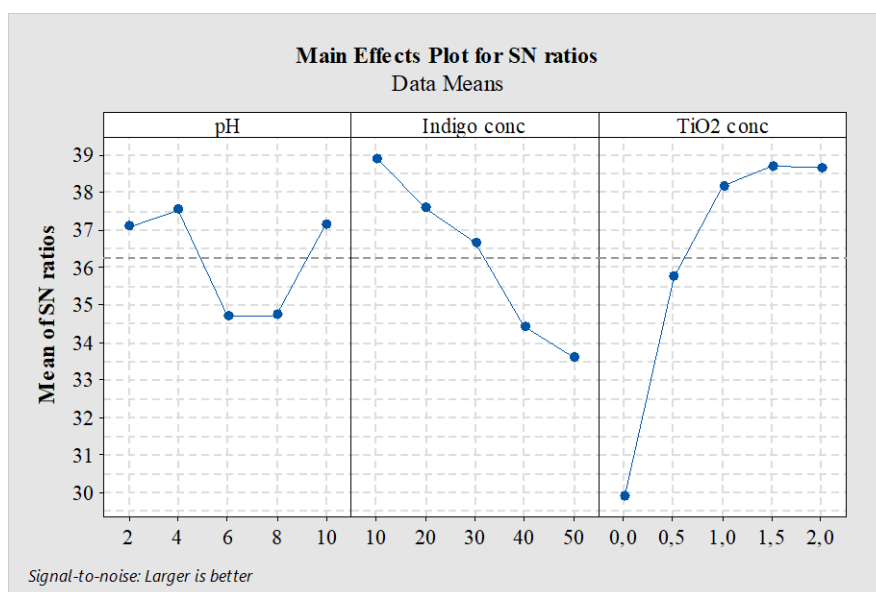| Factors	For Taguchi method				
	d.f.	Adj SS	Adj MS	F-value	P-value
pH (A)	1	291.4	291.4	1.22	0.281
Indigo conc (mg L^{-1}) (B)	1	4481	4481	18.83	0.000
TiO2 conc (g L^{-1}) (C)	1	8006.6	8006.6	33.65	0.000
Error	21	4996.7	237.9		
Total	24	17775.8			

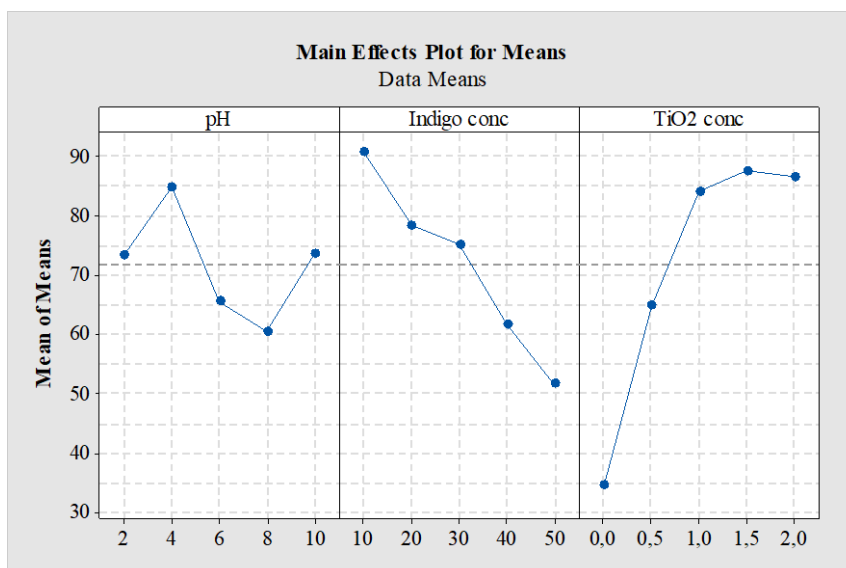**Fig 2.** Effects of process parameters on S/N in photocatalysis process

Fig 3. Effect of process parameters on Means in photocatalysis process

pH value has been frequently observed due to dependency of charged substrates such as dyes to the photocatalytic degradation efficiency. S/N value is found to be larger at the pH 4 as shown in Fig. 2. After this point, the S/N ratio decreases with sharper slope, which means the degradation is performed better at lower pH value. The zero point of charge (pH_{zpc}) for TiO2 is approximately pH of 6.50, hence negatively charged molecules are more readily degraded at acidic pH values when the photocatalyst surface is positively charged [30]. Reference [3] reported that as the pH increased from 1.0 to 2.0, the biosorption capacity of Spirulina pacifica reached a maximum value of 86.08% (17.22 mg g^{-1}) for Indigo dye. Although the pH is an extremely important parameter for photocatalysis experiments, it has less significance on the removal of Indigo dye compared to other factors such as catalyst or dye concentration. As illustrated in Fig 3, S/N ratio increases again at pH 10 at lower dye concentration (10 mg L^{-1}) and higher catalyst concentration (2.0 g L^{-1}). It is thought that the molecular characteristic of Indigo dye, the type of degradation process, and other experimental factors affects the degradation parameters and their influence levels.

3.3. The Results of Multivariable Regression Model

The experimental results are given by multivariable linear regression model analysis that is conducted to determine the effects of pH, TiO_2 and initial dye concentration on Indigo removal. SPSS (version 17-trial edition) software was used to set regression model. In order to establish a multiple regression model, linear and "step-by-step" model were used. As a result of regression analysis, 2 different models were set and accuracy of prediction values for each model was presented in Table 6.

Variables for each model are summarized in Table 7. The interaction of TiO_2 and initial dye concentration is statistically significant on the removal of dye removal as shown in Table 7 ($p<\alpha$, $\alpha=0.05$). Second model has the highest R^2 ratio that can express the 70% of the results of variance. Hence, it is decided to use Model 2 for prediction model.

Table 6. The multivariable regression model for Indigo dye removal

Model	R	R2	R2 Change	Adjusted R2	F	P
1	0.671	0.45	0.45	0.427	18.85	0
2	0.838	0.703	0.252	0.675	18.642	0

Table 7. The coefficients of variables in Model 2

Variables	Unstandardized Coefficients		Standardized Coefficients	T	P	Pearson-Corelation	
	B	Std. Error	Beta	t	p	Pearson-Corelation	p
(Constant)	74.691	8.492		8.796	0		
TiO_2 conc. (g L^{-1})	25.309	4.385	0.671	5.771	0	0.785	0
Initial dye conc. (mg L^{-1})	-0.947	0.219	-0.502	-4.318	0	-0.688	0.007

Table 7 summarizes the data of the coefficients of variables that were used in Model 2. The variables enable to interpret results according to the standardized regression coefficients. When the variables were arrayed in accordance with relative significance order, it was determined that the first interpretive variable was TiO_2, and the second variable was the initial dye concentration. In the regression model, the level variables for pH weren't seen to have any relation to dye removal.

It was determined that the t-test results regarding the significance of the regression coefficients indicated the same order and that p <0.05 was statistically significant. Furthermore, when the t-test values were examined, it appeared that TiO_2 linearly affects the dye degradation, but the concentration has an inverse interaction on the dye removal. This was also

determined in the Taguchi experimental design. The prediction model established by using the coefficients of the variables is as follows;

$$Y = 74.691 + 25.309*(TiO_2) - 0,947*(\text{Initial dye concentration}) \quad (3)$$

In addition, when the Pearson-correlation coefficients were analyzed, it was observed that the amount of TiO_2 and initial dye concentration had strong effects on the outcome variable and it was statistically significant ($p<\alpha$, $\alpha=0.05$). The coefficient calculated for pH was -0.235 (p = 0.281), so that the effect on the result was weak and this correlation was statistically insignificant. Since there wasn't any direct relationship for pH variable, new regression models were established via "curve prediction" model by using only this variable. The summary information on these models is summarized on the Table 8 and Fig 4.

Table 8. Results for all estimated models for pH and dye removal efficiency

| Model	R	R²	F	t	P
Linear	0.128	0.016	0.383	-0.619	0.542
Logarithmic	0.127	0.016	0,376	-0.613	0.546
Inverse	0.106	0.011	0.263	0.513	0.613
Quadratic	0.15	0.023	0.254	-0.483	0.778
Cubic	0.299	0.09	0.689	1.079	0.569
Compound	0.092	0.008	0.196	27.776 (p=0)	0.662
Power	0.12	0.015	0.339	-0.582	0.566
S	0.129	0.017	0.392	0.626	0.537
Growth	0.092	0.008	0.196	-0.442	0.662
Exponential	0.092	0.008	0.196	-0.442	0.662
Logistic	0.092	0.008	0.196	27.776 (p=0)	0.662
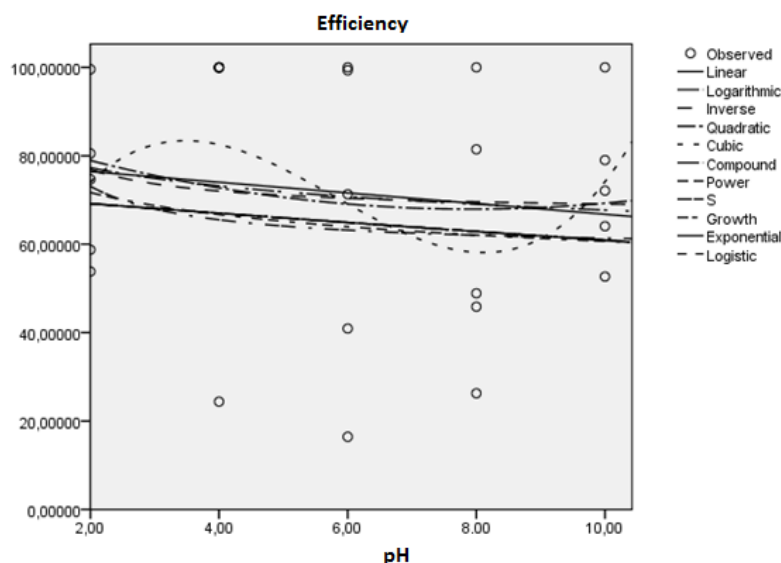
Fig 4. Results for all estimated models for pH and dye removal efficiency

When F, t and p values belongs to all models were investigated, there weren't seen any statistically significant effect of pH on the removal of dye. Two different p values were calculated for compound and logarithmic functions. One of them was calculated for general model, and other one was for predictive coefficient. While these estimated coefficients are significant, they are considered statistically insignificant since they predominantly deviate from actual values together with these coefficients. When the all situations were evaluated, it has been decided that it is more appropriate to predict the efficiency of dye removal by using other variables other than pH.

4. CONCLUSIONS

In this study, the obtained results show that a kind of textile vat dye, Indigo blue can be efficiently degraded by heterogeneous photocatalysis process in aqueous suspension of TiO_2 as photocatalyst under UVA irradiation. Based on the S/N ratio method, the degradation of Indigo dye was found to dependent on the initial dye concentration and TiO_2 concentration. The optimal conditions for dye removal were A (pH) at level 2 (4), B (initial dye concentration) at level 1 (10 mg L^{-1}) and C (TiO_2 concentration) at level 4 (1.5 g L^{-1}). The results indicate that TiO_2 concentration is the most effective compared to the other experimental parameters. Under the above optimum conditions, 100% Indigo dye degradation was achieved within 210 minutes.

ACKNOWLEDGEMENT

REFERENCES

[1]. Eurostat, "A closer look at clothes and footwear in the EU," Available: http://ec.europa.eu/eurostat/en/web/products -eurostat-news/-/EDN-20180227-1, (accessed 27 February 2018).

[2]. K. Hendaoui, F. Ayari, I.B. Rayana, R.B. Amar, F. Darragi and M. Trabelsi-Ayadi, "Real indigo effluent decontamination using continuous electrocoagulation cell: Study and optimization using Response Surface Methodology," *Process Safety and Environmental Protection*, Vol. 116, pp. 578-589, 2018.

[3]. A. Yalcuk and G. Dogdu Okcu, "Biosorption of Indigo and Acid Yellow 2G (Y2G) dyes from aqueous solutions using a commercial powder form of ecologically pure Hawaiian Spirulina pacifica (HSP)," *Desalination and Water Treatment*, Vol. 79, pp. 386-399, 2017.

[4]. R. Qu, B. Xu, L. Meng, L. Wang and Z. Wang, "Ozonation of indigo enhanced by carboxylated carbon nanotubes: Performance optimization, degradation products, reaction mechanism and toxicity evaluation," *Water Research*, Vol. 68, pp. 316–327, 2015.

[5]. C.G. Joseph, Y.L. Sharain-Liew, A. Bono and L.Y. Teng, "Photodegradation of Indigo Dye Using TiO2 and TiO2/Zeolite System," *Asian Journal of Chemistry*, Vol. 25(15), pp. 8402-8406, 2013.

[6]. P.O. Bankole, A.A. Adekunle, O.F. Obidi, O.D. Olukanni and S.P. Govindwar, "Degradation of indigo dye by a newly yeast, Diutina rugosa from dye wastewater polluted soil," *Journal of Environmental Chemical Engineering*, Vol. 5(5), pp. 4639-4648, 2017.

[7]. S. Hammami, M.A. Oturan, N. Oturan, N. Bellakhal and M. Dachraoui, "Comparative mineralization of textile dye indigo by photo-Fenton process and anodic oxidation using boron-doped diamond anode," *Desalination and Water Treatment*, Vol. 45, pp. 297–304, 2012.

[8]. C.F. Couto, L.S. Marques, J. Balmant, A.P. de Oliveira Maia, W.G. Moravia, M. Cristina and S. Amaral, "Hybrid MF and membrane bioreactor process applied towards water and indigo reuse from denim textile wastewater," *Environmental Technology*, Vol. 39(6), pp. 725-738, 2018.

[9]. A.M. Chia and I.R. Musa, "Effect of indigo dye effluent on the growth, biomass production and phenotypic plasticity of Scenedesmus quadricauda (Chlorococcales)," *Anais da Academia Brasileira de Ciências*, Vol. 86(1), pp. 419-428, 2014.

[10]. M.T. Yagub, T.K. Sen, S. Afroze and H.M. Ang, "Dye and its removal from aqueous solution by adsorption: a review," *Advances in Colloid and Interface Science*, Vol. 209, pp. 172-184, 2014.

[11]. B. Naroozi and G.A. Sorial, "Applicable models for multi-component adsorption of dyes: a review," *Journal of Environmental Science*, Vol. 25(3), pp. 419-429, 2013.

[12]. A. Trujillo-Ortega, S.A. Martinez Delgadillo, V.X. Mendoza-Escamilla, M. May-Lozano and C. Barrera-Diaz, "Modeling the removal of indigo dye from aqueous media in a sonoelectrochemical flow reactor," *International Journal of Electrochemical Science*, Vol. 8(3), pp. 3876–3887, 2013.

[13]. J. Zolgharnein and M. Rastgordani, "Optimization of simultaneous removal of binary mixture of indigo carmine and methyl orange dyes by cobalt hydroxide nano-particles through Taguchi method," *Journal of Molecular Liquids*, Vol. 262, pp. 405-414, 2018.

[14]. N. Gupta, A.K. Kuswaha and M.C. Chattopadhyaya, "Application of potato (Solanum tuberosum) plant wastes for the removal of methylene blue and malachite green dye from aqueous solution," *Arabian Journal of Chemistry*, Vol. 9(1), pp. S707-S716, 2016.

[15]. M.A. García-Morales, G. Roa-Morales, C. Barrera-Díaz, V. Martínez Míranda, P. Balderas Hernández and T.B. Pavón Silva, "Integrated Advanced Oxidation Process (Ozonation) and Electrocoagulation Treatments for Dye Removal in Denim Effluents," *International Journal of*

Electrochemical Science, Vol. 8, pp. 8752-8763, 2013.

[16]. K. Hendaoui, F. Ayari, I.B. Rayana, R.B. Amar, F. Darragi and M. Trabelsi-Ayadi, "Real indigo dyeing effluent decontamination using continuous electrocoagulation cell: Study and optimization using Response Surface Methodology," *Process Safety and Environmental Protection*, Vol. 116, pp. 578-589, 2018.

[17]. C.Z. Liang, S.P. Sun, F.Y. Li, Y.K. Ong and T.S. Chung, "Treatment of highly concentrated wastewater containing multiple synthetic dyes by a combined process of coagulation/flocculation and nanofiltration," *Journal of Membrane Science*, Vol. 469, pp. 306-315, 2014.

[18]. P.T. Almazán-Sánchez, P.W. Marin-Noríega, E. González-Mora, I. Linares-Hernández, M.J. Solache-Rios, I.G. Martínez-Cienfuegos and V. Martínez-Miranda, "Treatment of Indigo-Dyed Textile Wastewater Using Solar Photo-Fenton with Modified Clay and Copper-Modified Carbon," *Water, Air, & Soil Pollution*, Vol. 228(294), pp. 294-308, 2017.

[19]. A. Hassan Ali, "Study on the photocatalytic degradation of indigo carmine dye by TiO2 photocatalyst," *Journal of Kerbala University*, Vol. 11(2), pp. 145-153, 2013.

[20]. Z. Zainal, L.K. Hui, M.Z. Hussein, Y.H.T. Yap, A.H. Abdullah and I. Ramli, "Removal of dyes using immobilized titanium dioxide illuminated by fluorescent lamps," *Journal of Hazardous Materials*, Vol. 125(1-3), pp. 113-120, 2005.

[21]. O.T. Alaoui, Q.T. Nguyen and T. Rhlalou, "Preparation and characterization of a new TiO2/SiO2 composite catalyst for photocatalytic degradation of indigo carmin," *Environmental Chemistry Letters*, Vol. 7(2), pp. 175-181, 2009.

[22]. S.V. Mohan, S. Veer Raghavulu, S. Srikanth and P.N. Sarma, "Bioelectricity production by mediatorless microbial fuel cell under acidophilic condition using wastewater as substrate: Influence of substrate loading rate," *Current Science*, Vol. 92(12), pp. 1720-1726, 2007.

[23]. Y. Saatçi, Ö. Hanay, "Color removal from ındigo dye containing wastewater by electro-fenton process," *Erciyes Üniversitesi Fen Bilimleri Enstitüsü Dergisi*, Vol. 29, pp. 129-134, 2013.

[24]. L. Khenniche, L. Favier, A. Bouzaza, F. Fourcade, F. Aissani and A. Amrane, "Photocataytic degradation of bezacryl yellow in batch reactors- feasibility of the combination of photocatalysis and a biological treatment," *Environmental Technology*, Vol. 36(1-4), pp. 1-10, 2015.

[25]. C.G. Maia, A.S. Oliveira, E.M. Saggioro and J.C. Moreira, "Optimization of the photocatalytic degradation of commercial azo dyes in aqueous TiO2 suspensions," *Reaction Kinetics, Mechanisms and Catalysis*, Vol. 113(1), pp. 305-320, 2014.

[26]. J.R. Alvarez-Corena, J.A. Bergendahl and F.L. Hart, "Advanced oxidation of five contaminants in water by UV/TiO2: Reaction kinetics and byproducts identification," *Journal of Environmental Management*, Vol. 181, pp. 544-551, 2016.

[27]. A. Sraw, A. Pal Toor and R.K. Wanchoo, "Adsorption kinetics and degradation mechanism study of water persistent insecticide quinalphos: for heterogeneous photocatalysis onto TiO2," *Desalination and Water Treatment*, Vol. 57(36), pp. 16831-16842, 2016.

[28]. N. Daneshvar, A.R. Khataee, M.H. Rasoulifard and M. Pourhassan, "Biodegradation of dye solution containing Malachite Green: Optimization of effective parameters using Taguchi method," *Journal of Hazardous Materials*, Vol. 143(1-2), pp. 214-219, 2007.

[29]. A. Arimi, M. Farhadian, A.R.S. Nazar and M. Homayoonfal, "Assessment of operating for photocatalytic degradation of a textile dye by Fe2O3/TiO2/clinoptilolite nanocatalyst using Taguchi experimental design," *Research on Chemical Intermediates*, Vol. 42(5), pp. 4021-4040, 2016.

[30]. O. Prieto, J. Fermoso, Y. Nuñez, J.L. del Valle and R. Irusta, "Decolouration of textile dyes in wastewaters by photocatalysis with TiO2," *Solar Energy*, Vol. 79(4), pp. 376-383, 2005.

[31]. M.R. Sohrabi, A. Khavaran, S. Shariati and S. Shariati, "Removal of Carmoisine edible dye by Fenton and photo Fenton processes using Taguchi orthogonal array design," *Arabian Journal of Chemistry*, Vol. 10(2), pp. S3523-3531, 2017.

[32]. T. Kıvak, "Optimization of surface roughness and flank wear using the Taguchi method in milling of Hadfield steel with PVD and CVD coated inserts," *Measurement*, Vol. 50, pp. 19-28, 2014.

[33]. E. Canıyılmaz and F. Kutay, "An Alternative Approach to Analysis of Variance in Taguchi Method," *Journal of the Faculty of Engineering and Architecture of Gazi University*, Vol. 18, pp. 51-63, 2003.

[34]. P.J. Ross, Taguchi Techniques for Quality Engineering: Loss Function, Orthogonal Experiments, Parameter and Tolerance Design, 2nd ed., NY: McGraw-Hill, New York, USA. 1996.

[35]. C.B. Raj and C.H.L. Quen, "Advanced oxidation processes for wastewater treatment: optimization of UV/H2O2 process through a statistical technique," *Chemical Engineering Science*, Vol. 60(19), pp. 5305–5311, 2005.

[36]. S. Rashidi, M. Nikazar, A.V. Yazdi and R. Fazaeli, "Optimized photocatalytic degradation of Reactive Blue 2 by TiO2/UV process," *Journal of Environmental Science and Health, Part A*, Vol. 49(4), pp. 452-462, 2014.

[37]. Y.H. Andrew Liou, P.P. Lin, R.R. Lindeke, H.D. Chiang, "Tolerance specification of robot kinematic parameters using and experimental design technique the Taguchi method," *Robotics and Computer-Integrated Manufacturing*, Vol. 10 (3), pp. 199-207, 1993.

[38]. K.D. Kim, D.N. Han and H.T. Kim, "Optimization of experimental conditions based on the Taguchi robust design for the formation of nano-sized silver particles by chemical reduction method," *Chemical Engineering Journal*, Vol. 104 (1-3), pp. 55-61, 2004.

[39]. P.H. Sreeja, and K.J. Sosamony, "A Comparative Study of Homogeneous and Heterogeneous Photo-Fenton Process for Textile Wastewater Treatment," *Procedia Technology*, Vol. 24, pp. 217-223, 2016.

Environmental Research & Technology

RESEARCH ARTICLE

Characterization of sludge waste products from wastewater treatment plant of Khenifra city in Morocco

Mohamed Aadraoui[1,*] (iD) , Jamila Rais[1] (iD) , Mohamed Elbaghdadi[1] (iD) , Abdellah Ouigmane[2] (iD) , Mohamed Mechadi[3] (iD)

[1] Georesources and Environment Team, Faculty of Science and Technics, University Sultan Moulay Slimane, Beni Mellal, B.P.Box 523, Béni Mellal 23030, MOROCCO.
[2] Environmental & Agro-Industrial Processes Team, Faculty of Science and Technics, University Sultan MoulaySlimane, Beni Mellal, MOROCCO.
[3] Transdisciplinary Team of Analytical Science for Sustainable Development, Department of Chemistry and Environment,Faculty of Science and Technics, University Sultan Moulay Slimane, Beni Mellal, MOROCCO.

ABSTRACT

To promote the utilization of sewage sludge as alternative building materials, a study was carried out to examine the characteristics of sewage sludge from wastewater treatment plant of khenifra city, Morocco. Experiments were performed for determining the mineralogical composition, chemical properties, loss of weight, the rate of the calcium carbonate and moisture. Furthermore, the geotechnical parameters deal with the Atterberg limits, water content and Sand equivalent of the sewage sludge material. The purpose of this paper is to present the available information on the various components of sewage sludge to explore the possibility of exploiting this waste in building materials

Results show that sewage sludge has neutral pH value around 6.93 and contains organic matter. Moreover, the sludge is composed of a significant amount of oxides and metals. The value of net calorific value (NCV) is 1888.91 Kcal kg⁻¹. As well as, the mineralogical composition of sludge has been determined by X-rays diffraction (XRD) show the presence of quartz (SiO_2), hematite (Fe_2O_3), aluminum oxide (Al_2O_3) and calcite (CaO_3).The result of the geotechnical properties of sewage sludge obtained indicates a very high value for a liquid limit of 126%, a plastic limit of 100% and the plasticity index of 25% and 128% water content.
Based on the data obtained from the characteristics of sewage sludge produced by wastewater treatment plant in the Khenifra city, the utilization of sewage sludge into building materials such as in brick making, ceramics making and in the manufacture of cement are possible, because sludge composition is similar to the raw to construction materials.

Keywords: Characterization, recycling, sewage sludge, wastewater treatment plant

1. INTRODUCTION

Rapid increase in industrial development, population growth and improvements in life style are among the factors leading to higher wastewater production. Consequently, the wastewater treatment results in generating huge amount of sewage sludge worldwide [1]. In Morocco, the annual production of sewage sludge exceeds 2 million tons of dried sludge in 2015. While the amount of sewage sludge produced in 2025 is estimated to reach 3.4 million tons as a result of the rapid progress of urbanization and the continuous improvement of sewage treatment facilities [2.3]. Among all the sewage sludge disposal methods at present, the most common techniques to discard of sludge are sanitary landfills, in addition to some being used in agriculture as organic fertilizer and for soil management [4, 5]. In the meantime, more stringent environmental regulations which govern the disposal of sewage sludge have resulted in limitations on sewage sludge disposal options [6]. These methods of managing the sewage sludge might have adverse impacts on the environment. As a consequence of these problems related to the disposal of sewage sludge, another a new technique of sewage sludge

disposal is based on the utilization of sludge in construction materials. However, the physicochemical characteristic and mineralogical property of the sludge is similar to the construction material investigated in literature [7]. Several research work has been done on the use of this waste in construction materials, to make filler in asphalt concrete applications [8], in brick making [9, 10, 11], in ceramic making [12, 13], and in the manufacture of cement [14, 15, 16], cementitious materials [17, 18], or for the manufacture of aggregates and lightweight aggregates [19, 20].

The main objective of this study is to evaluate the characteristics of sewage sludge such as the properties mineralogical, characterization of the physicochemical and also the geotechnical parameters to solve the problem of sludge disposal due to the growing amount of sludge as well as environmental protection issues and to reduce costs of the handling of sewage sludge is becoming one of the most significant challenges in wastewater management, therefore, reuse or recycling of sewage sludge to develop sustainable construction materials as proved to be a practical solution for disposal and environmental problem.

2. MATERIALS & METHOD

The sample of the sewage sludge used in this work was sampled from the wastewater treatment plant (WWTP) located in the Khenifra city, Morocco. The WWTP is a sewage treatment plant by processes biological according to standardized conditions of AFNOR EN 1085 [21].

The sludge was dried in air are brought to the laboratory, for to characterize the physical properties, chemical analysis, and geotechnical parameters. For this purpose, the collected samples were dried at a temperature equals of 105°C for 48 hours, the sludge dried has undergone a pulverization in a porcelain mill and it sieved to obtain a particle size less than 200 μm using a metallic sieve. In the laboratory basic physical parameters was determined; pH was determined by pH meter, moisture content was determined according to NF EN 13037 standard [22],

and conductivity ratio was determined according to the standard LST EN 1745 [23].

The major chemical compounds such as (Cr, Co, Cu, Zn, Pb, and Cd) of the dry sludge have been analyzed by inductively coupled plasma-atomic emission spectrometry (ICP-AES) equipment. The net calorific value (NCV) is determined by calorimetric bomb type 6100 calorimeter.

The mineralogical composition is determined by X-ray diffraction (Bruker X-ray diffractometer equipment) in a radiation of half an hour scanning, which explores in the interval of 2θ angles from 10° to 90°.

The particle size distribution was measured by conventional sieving for the 63 to 2000 μm fractions sieves, according to NLT 104/91 standard [24] and ASTM standard [25].

Limits of Atterberg corresponding to the thresholds of the passage of the solid state in a plastic state and to the plastic state in the liquid state. The interval between these two limits allows to obtain the index of plasticity. These limits were determined by the Casagrande method [26, 27, 28, 29].

The water content is defined as the ratio of the mass of the pore fluid to the mass of the solid particles, expressed as a percentage. The water content was determined using the oven-drying method BS1377 [29]. The mass of the solid particles in the sludge specimen equals the residual mass after drying in an oven at a temperature of 110 ± 5°C for a period of 8–16 h according to ASTM D2216 standard [30, 31]. The sand equivalent was determined according to NLT 113/87 standard [24], a quick procedure for determining the percentage of fines elements contained in a material [32].

3. RESULTS & DISCUSSION

3.1. Physical characteristics

Table 1 shows the physical characteristics such as pH, moisture content, net calorific value, volatile matter, loss on ignition and rate of the calcite of the sewage sludge.

Table 1. Physical characteristics of the sewage sludge

Parameters	Content	Literature results [7]	Literature results [33]	Literature results [34]
pH	6.93	6.82	6.85	7-7.5
Conductivity (mS m^{-1})	4.51	-	3.27	-
Moisture[a] (%)	23.33	2.35	-	74
NCV (Kcal kg^{-1})	1888.91	-	-	-
Volatile matter[b] (%)	51.90	2.66	-	-
Loss on ignition[c] (%)	44	8.96	-	-
Rate of the CaCO$_3$	16.55	-	-	5.98

[a]Heated at 105±5 °C for 24 hours   [b]Combusted at 550±5 °C for 2 hours   [c]Combustedat 550±5 °C for 4 hours

The results of pH (6,93) indicated that the average near the neutrality, this value is close to those found in literature; Ahmad et al.[7], Naamane et al. [33] and Malliou et al. [34] found respectively 6.82, 6.85, 7 as a values of pH in their studies. The moisture content of

dried sample is 23.33, the same result was found by Modolo et al. [35]. The volatile matter present in the sludge is 51.9 % indicates that the sludge is inorganic in nature, whereas loss on ignition is 44 %. The rate of carbonate found is 16.55%, which is the same result

obtained by Aadraoui et al. [36]. NCV found is 1888Kcal.kg-1, the value of NCV compared with results found in other studies; Husillos-Rodriguez et al. [37] found 1999 Kcal kg^{-1}, Zhang et al.[38] found 5972 Kcal kg^{-1}, Samolada et al. [39] found 3487 and Zhao et al. [40] found 4497 Kcal kg^{-1}. This can be explained by the presence of significant amounts of soil in the sludge. Indeed, the mineral matter influences the NCV of a material. The Fig. 1 shows the result of particle size distribution of the sludge.
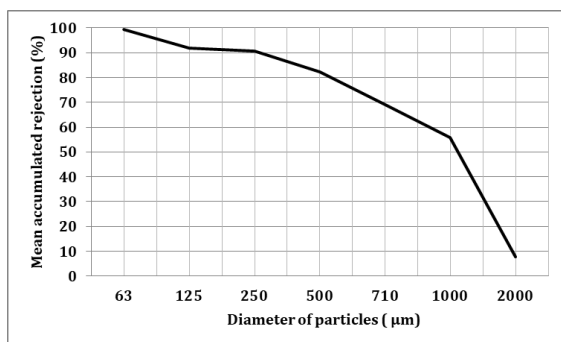

Fig 1. Sludge grain size distribution

About 78% of sand (distributed as follows, coarse sand is 25%, medium sand is 17% and fine sand is 36%) ranging between 150-75μm and also around 22% for clay and silt fractions its diameter is lower than 63 μm, are constituted principal composition of the sludge of this study. Furthermore, it was similar to that of fine agglomerate according to results obtained in the study by Valls et al. [41].

3.2. Chemical characteristics

The Table 2 shows the ICP–AES analysis results for the sewage sludge. The results indicated the presence of high quantity of Ca, Fe, Mg, Na and K. In general, the concentration of these elements was the same result obtained by Naamane et al. [42, 43, 44], Tantawy et al. [45] and Cyr et al. [46]. The high concentration of the calcium and iron in the sewage sludge is owing to the utilize of ferric salts during wastewater treatment. Thus, these results provided a presence of heavy metals such as Zn, Cu, Pb, Cd and Co. these toxic elements may be due to domestic detergents (may be which contain several chemical elements such as linear alkylbenzene sulfonates, nonylphenol and alkylphenol ethoxylates), or by the erosion of the system of piping or by pluvial waters [47]. On the other hand, the sludge tends to accumulate high concentrations of heavy metals, because of the physical-chemical processes that are involved in wastewater treatment plant [48, 49].

Table 2. Results of Heavy metal in sewage sludge

Non-toxic elements			Toxic elements		
Elements	Content (mg kg^{-1})	Literature results [42]	Elements	Content (mg kg^{-1})	Literature results [42]
Fe	14860	34.16	Zn	1386.67	3.82
Ca	64633.33	657.245	Cu	211.33	1.84
Mg	6833.33	69.422	Ba	337.93	0.53
Al	3942.53	-	Pb	100.88	1.04
K	1435.66	18.966	Cr	31,52	0.79
Na	1600.66	79.239	Cd	131.18	0.04
Mn	156.56	0.33	Co	3.106	0.02

3.3. Oxide composition

The results of the X-ray diffraction (XRD) patterns of the sewage sludge are shown in Fig 2. The major chemical composition of the sludge is present in figure 2, showed the presence of calcite ($CaCO_3$) and quartz (SiO_2), aluminum oxide (Al_2O_3) and hematite (Fe_2O_3) are the main components of the sludge, same results obtained by Al-Sharif et al. [50], De-Lima et al. [51] and Aadraoui et al. [52]. This component produces during wastewater treatment because of the using of coagulant as the aluminum oxide and iron oxide [47], it is noted that components of the waste sludge which is similar to the primary components found in the ordinary Portland cement and also in the silty fractions of clays [53, 54].

3.4. Geotechnical parameters

Some geotechnical properties of sewage sludge tested are listed in Table 2. The plasticity characteristics assessed using the Atterberg limit tests, indicated a liquid limit of 126.08% and a plastic limit of 100.49 %. The plasticity index of 25%, based on those results on the classification of Casagrande, it can be concluded that the sewage sludge mostly a similar behavior within soils elastic silts and organic clay of very high plasticity [32, 55]. In addition, the liquidity index about -1.42 % was given that this sewage sludge is largely solid [52], according to the result of the consistency index about to 3.72 %, this sewage sludge is solid. However, the equivalent of sand around to 15% was confirmed the sewage sludge sample is plastic, this result correlated with those of the plastic soil [52], according to the classification of Casagrande, the sewage sludge is the similar composition with of soils elastic silts clays to high plasticity. Laboratory test results demonstrated that the sludge was high in water content near at 128.45%.
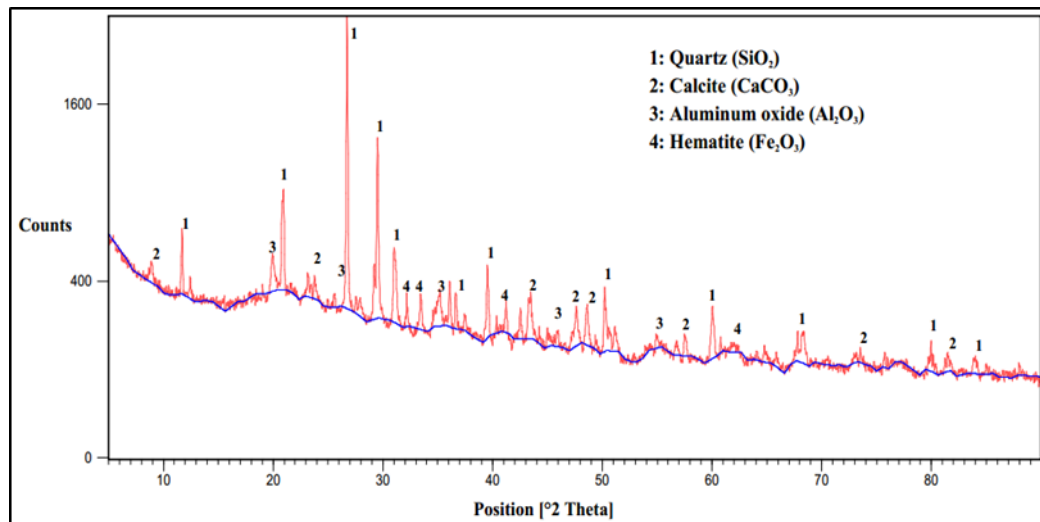
Fig 2. XRD patterns of sewage sludge

Table 2. Geotechnical properties of the sewage sludge

Parameters		Mean (%)
	Liquid limit (L_L)	126.08
	Plastic limit(P_L)	100.49
Limits of Atterberg	Plasticity Index (P_I)	25.60
	Liquidity index (L_I)[a]	-1.42
	consistency index(C_I)[b]	3.72
Equivalent of sand		15
Water content (W) (%)		128.45
[a]$L_I = \frac{(W - P_L)}{(L_L - P_L)}$	[b]$C_I = \frac{(L_L - W)}{(L_L - P_L)}$	

4. CONCLUSIONS

The results of this research are the first step in the study of the characterization of the sewage sludge generated by wastewater treatment plants of Khenifra City. Since the calorific value is low and the sewage sludge contains the mineral material it may be used as raw materials in construction. The following conclusions can be made from the studies carried out:

1. This sewage sludge contains high organic substances and heavy metals;
2. This sewage sludge composes of SiO_2, Al_2O_3, and small amounts of Fe_2O_3, the sum of SiO_2, Al_2O_3, and Fe_2O_3 satisfies requirements stated for pozzolanic;
3. This sewage sludge mainly contains Ca, Fe, Mg, Na, P and K, and as minor constituents, it contains Zn, Pb, Cu, Ti, Ba, Cr, Mn, and Ni;
4. The geotechnical parameters according to the classification of Casagrande showed that the sewage sludge consisted of high values of liquid limits and plastic limits.

Based on these results, the next step in our work (which will be the subject of the next publication) is the use of this waste sludge as an additive in construction materials (in the manufacture of cement, manufacture of brick and of aggregates), to assess the effect of this sludge on the cement and also know about the added sludge dose that would be ideal and similar to the standards of building materials.

REFERENCES

[1]. S. Amir , Contribution à la Valorisation de Boues de Stations D'épuration par Compostage: Devenir des Micropolluants Metalliques et Organiques et Bilan Humique du Compost. Doctoral dissertation, Thèse Doctorale Sciences Agronomiques–L'Institut National Polytechnique de Toulouse. Toulouse, pp 341, 2005.

[2]. L. El Fels, Suivi physico-chimique, microbiologique et écotoxicologique du compostage de boues de STEP mélangées à des déchets de palmier: validation de nouveaux indices de maturité, Doctoral dissertation, École Doctorale Sciences de l'univers, de l'environnement et de l'espace Toulouse, 159341302, pp. 295, 2014.

[3]. A. Jouraiphy, Compostage des boues actives-déchets verte: analyses physicochimiques, microbiologiques, toxicologiques, bilan humique et valorisation agronomique,UFR, Ecologie et Fonctionnement des Ecosystèmes Terrestres, Spécialité Sciences Agronomiques et Environnement, pp. 168, 2017.

[4]. S.J. Young and R. P. Res, "An LCA of alternative wastewater sludge treatment scenarios," *Resources, Conservation and Recycling*, Vol 35, pp. 191-200, 2002.

[5]. M.A. S´anchez-Monedero, C. Mondini, M.D. Nobili, L. Leita and A. Roig, "Land application of biosolids. Soil response to different stabilization degree of the treated organic matter," *Waste Management*, Vol. 24, pp. 325-332, 2004.

[6]. H. Ødegaard, B. Paulsrud and I. Karlsson," Wastewater sludge as a resource: sludge disposal strategies and corresponding treatment technologies aimed at sustainable handling of wastewater sludge," *Water Science and Technology*, Vol. 46, pp. 295-303, 2002.

[7]. T. Ahmad, K. Ahmad and M. Alam, "Characterization of water treatment plant's sludge and its safe disposal options," *Procedia Environmental Sciences*, Vol. 35, pp. 950-955, 2016.

[8]. M.H. Al Sayed, I.M. Madany, and A.R.M. Buali, "Use of sewage sludge ash in asphaltic paving mixes in hot regions," *Construction and Building Materials*, Vol. 9, pp. 19-23, 1995.

[9]. D.F. Lin, H.L. Luo and Y.N. Sheen, "Glazed tiles manufactured from incinerated sewage sludge ash and clay," *Journal of the Air & Waste Management Association*, Vol. 55, pp 163-172, 2005.

[10]. K.-Y. Chiang, P.-H. Chou, C.-R. Hua, K.-L. Chien and C. Cheeseman, "Lightweight bricks manufactured from WTS and rice husks," *Journal of Hazardous Matererials*, Vol. 171, pp. 76-82, 2009.

[11]. C.-H. Weng, D.-F. Lin and P.-C. Chiang, "Utilization of sludge as brick materials," *Advances in Environmental Research*, Vol. 7, pp. 679-685, 2003.

[12]. S.R. Teixeira, G.T.A. Santos, A.E. Souza, P. Alessio, S.A. Souza, and N.R. Souza, "The effect of incorporation of a Brazilian WTPs sludge on the properties of ceramic materials," *Applied Clay Science*, Vol. 53, pp. 561-565, 2011.

[13]. O. Kizinievic, R. Zurauskiene, V. Kizinievic, R. Zurauskas, "Utilisation of sludge waste from water treatment for ceramic products," *Construction and Building Materials*, Vol. 41, pp. 464-473, 2013.

[14]. O. Van, G. Hendrik and A.C. Padovani. "Cement manufacture and the environment: part I: chemistry and technology," Journal of Industrial Ecology, Vol. 6 (1), pp. 89-105, 2002.

[15]. C.-L. Yen, D.-H. Tseng, T.-T. Lin, " Characterization of eco-cement paste produced from waste sludges", *Chemosphere*, Vol. 84, pp. 220-226, 2011.

[16]. N. H. Rodríguez., S. M. Ramírez, M.T.B. Varela, M. Guillem, J. Puig, E. Larrotcha and J. Flores, "Evaluation of spray-dried sludge from drinking water treatment plants as a prime material for clinker manufacture." *Cement and Concrete Composite*, Vol. 33, pp. 267–275, 2011.

[17]. M. Alqam, A. Jamrah and H. Daghlas, "Utilization of cement incorporated with water treatment sludge", *Jordan Journal of Civil Engineering*, Vol. 5 (2), pp. 268–277, 2011.

[18]. H. El-Didamony, K.A. Khalil and M. Heikal, "Physico-chemical and surface characteristics of some granulated slag–fired drinking water sludge composite cement pastes," *HBRC Journal*, Vol. 10, pp. 73–81, 2014.

[19]. C.-H. Huang and S.-Y. Wang, "Application of WTS in the manufacturing of lightweight aggregate," *Construction and Building Materials*, Vol. 43, pp. 174–183, 2013.

[20]. A. Sales, F.R. De Souza and F.R. Almeida, "Mechanical properties of concrete produced with a composite of water treatment sludge and sawdust," *Construction and Building Materials,* Vol. 25(6), pp. 2793–2798, 2011.

[21]. AFNOR, La Norme européenne EN 1085, 2007.

[22]. NF EN 13037 February, Soil amendments and crop supports - Determination of pH - Organic amendments and culture, 2012.

[23]. LST EN 1745."Masonry and masonry products – methods for determiningdesign thermal values", pp. 64, 2002.

[24]. Normas NLT. II – Ensayos de Suelos. Centro de Estudios y Experimentacio´n de Obras Pu´blicas. Laboratorio de Geotecnia. 2a Ed. Madrid, 1992.

[25]. ASTM, 1985. ASTM C188-84. Standard Test Method for Density of Hydraulic Cement. Annual Book of ASTM Standards. Section 4,Construction. American Society for Testing and Materials, Philadelphia, USA.

[26]. G. Maria, F. Jannuzzi, F.A.B. Danziger and I.S.M. Martins, "Geological–geotechnical characterisation of Sarapuí II clay," *Engineering Geology*, Vol. 190, pp. 77–86, 2015.

[27]. E. Hrubesova, B. Lunackova and O. Brodzki, "Comparison of Liquid Limit of Soils Resulted from Casagrande Test and Modified Cone Penetrometer Methodology," *Procedia Engineering*, Vol. 142, pp. 364-370, 2016.

[28]. E. Karakan and S. Demir, "Liquid limit determination of various sand clay mixtures by Casagrande and fall cone test methods," *Balıkesir Üniversitesi Fen Bilimleri Enstitüsü Dergisi*, Vol. 20, pp. 361-371, 2018.

[29]. BS1377, "Methods of Test for Soils for Civil Engineering Purposes.Part 2: Classification Tests. British Standards Institution", London, 1990.

[30]. ASTM D2974-07a, "Standard test methods for moisture, ash, and organic matter of peat and other organic soils", 2007.

[31]. H.S. Kim, G.-C. Cho, J.Y. Lee and S.J. Kim, "Geotechnical and geophysical properties of deep marine fine-grained sediments recovered during the second Ulleung Basin Gas Hydrate expedition, East Sea, Korea", *Marine and Petroleum Geology*, Vol. 47, pp. 56–65, 2013.

[32]. M. Ignacio, L.F. Arevalo and F. Romero, "Characterization and possible uses of ashes from wastewater treatment plants", *Waste Management*, Vol. 25, pp. 1046–1054, 2005.

[33]. S. Naamane, Z. Rais and M. Chaouch, "Incorporation of wastewater sludge treated by water washout in cement", *Journal of Materials and Environmental Science*, Vol. 5 (S2), pp. 2515-2521, 2014.

[34]. O. Malliou, M. Katsioti,, A. Georgiadis and A. Katsiri, "Properties of stabilized/solidified admixturesof cement and sewage sludge", *Cement & Concrete Composites*, Vol. 29, pp. 55–61, 2007.

[35]. R. Modolo, V.M. Ferreira, L.M. Machado, M. Rodrigues and I. Coelho, "Construction materials as a waste management solution for cellulose sludge", *Waste Management*, Vol. 31, pp. 370–377, 2011.

[36]. M. Aadraoui, M. Elbaghdadi, J. Rais, A. Barakat, W. Ennaji, L.A. Karroum and H. Oumenskou, "Effect of incineration of sewage sludge on the evolution of physicochemical characterization and mineralogical properties," Journal of Materials and Environmental Science, Vol. 8, pp. 2800-2806, 2017.

[37]. N.H. Rodriguez, S. Martinez-Ramirez, M.T. Blanco-Varelaa, S. Donatello, M. Guillem J. Puig, C. Fos, E. Larrotcha and J. Flores "The effect of using thermally dried sewage sludge as an alternative fuel on Portland cement clinker production," *Journal of Cleaner Production*, Vol. 52, pp. 94-102, 2013.

[38]. L. Zhang, Xiao, B., Hu, Z., Liu, S., Cheng, G., He, P., & Sun, L., "Tar-free fuel gas production from high temperature pyrolysis of sewage sludge". Waste management, Vol. 34, pp. 180-184, 2014.

[39]. M.C. Samolada, A. A. Zabaniotou, "Comparative assessment of municipal sewage sludge incineration, gasification and pyrolysis for a sustainable sludge-to-energy management in Greece," *Waste management*, 34 (2014) 411-420.

[40]. P. Zhao, Y. Shen, S. Ge, K.Yoshikawa, "Energy recycling from sewage sludge by producing solid biofuel with hydrothermal carbonization," *Energy Conversion and Management*, Vol. 78, pp. 815–821,2014.

[41]. S. Valls, A. Yagüe, E. Vazquez and C. Mariscal, "Physical and mechanical properties of concrete with added dry sludge from a sewage treatment plant," *Cement and Concrete Research*, Vol. 34, pp. 2203 – 2208, 2004.

[42]. S. Naamane, Z. Rais, M. Taleb, N.H. Mtarfi and M. Sfaira, "Sewage sludge ashes: Application in construction materials", *Journal of Materials and Environmental Science*, Vol. 7 (1), pp. 67-72, 2016.

[43]. S. Naamane, Z. Rais and M. Taleb, "The effectiveness of the incineration of sewage sludge on the evolution of physicochemical and mechanical properties of Portland cement," *Construction and Building Materials*, Vol. 112, pp. 783–789, 2016.

[44]. S. Naamane, Z. Rais, N.H. Mtarfi, M. El Haji and M. Taleb, "Valorization of wastewater sludge in cement CPJ45," *Physical and Chemical News*, Vol. 74, pp. 44-50, 2014.

[45]. M.A. Tantawy, A.M. El-Roudi, Elham M. Abdalla, and M.A. Abdelzaher, "Evaluation of the Pozzolanic Activity of Sewage Sludge Ash, International Scholarly Research Network," *ISRN Chemical Engineering*, Vol. 2012, pp. 8, 2012.

[46]. M. Cyr, M. Coutand and P. Clastres, "Technological and environmental behavior of sewage sludge ash (SSA) in cement-based materials," *Cement and Concrete Research*, Vol. 37, pp. 1278-1289, 2007.

[47]. P. Hsiau and S. Lo "Extractabilities of heavy metals in chemically-fixed sewage sludges," *Journal of Hazardous Materials*, Vol. 58, pp. 73–82, 1998.

[48]. D. Fytili, A. Zabaniotou, "Utilization of sewage sludge in EU application of old and new methods—A review," *Renewable and Sustainable Energy Reviews*, Vol. 12, pp. 116–140, 2008.

[49]. J.C. Lynn, R. K. Dhira, G. S. Ghataora and R.P. West, "Sewage sludge ash characteristics and potential for use in concrete, Sewage sludge ash characteristics and potential for use in concrete," *Construction and Building Materials*, Vol. 98, pp. 767–779, 2015.

[50]. M. Al-Sharif and M.F. Attom, "Geoenvironmental application of burned wastewater sludge ashin soil stabilization," *Environmental Earth Sciences*, Vol. 71, pp. 2453–2463, 2014.

[51]. J.F. De Lima, D. Ingunza and M. Del Pilar, "Effects of sewage sludge ash addition in Portland cement concretes," International Conference on Civil, London 13–14th March, Atlantis Press, Materials and Environmental Sciences, pp. 189–191, 2015.

[52]. M. Aadraoui, M. Elbaghdadi, J. Rais, A. Barakat,W. Ennaji, L.A. Karroum, H. Oumenskou, A. Ouigmane, M. Mechadi and S. Didi, "Characteristics of sewage sludge produced from wastewater treatment plant in the Moroccan city Khouribga," *Desalination and Water Treatment*, Vol. 112, pp. 179-185, 2018.

[53]. J.A. Cusido and C. Soriano, "Valorization of pellets from municipal WWTP sludge in lightweight clay ceramics", *Waste Management*, Vol. 31, pp. 1372–1380, 2011.

[54]. C.A. Velis, C. Franco-Salinas, C. OSullivan, J. Najorka, A.R. Boccaccini and C.R. Cheeseman, "Up-cycling waste glass to minimal water adsorption/absortion lightweight aggregate by rapid low temperature sintering: optimization by dual process-mixture response surface

methodology," *Environmental Science and Technology*, Vol. 48, pp. 7527–7535, 2014.

[55]. C. Brendan and O. Kelly, "Geotechnical properties of municipal sewage sludge," *Geotechnical and Geological Engineering*, Vol. 24, pp. 833–850, 2006.

Environmental Research & Technology

RESEARCH ARTICLE

Biodegradation behavior of two different chitosan films under controlled composting environment

Emine Altun[1] (iD), Eda Celik[1,2] (iD), Hulya Yavuz Ersan[1,2,*] (iD)

[1] Hacettepe University, Institute of Science, Bioengineering Division, 06800, Beytepe, Ankara, TURKEY
[2] Hacettepe University, Faculty of Engineering, Chemical Engineering Department, 06800, Beytepe, Ankara, TURKEY

ABSTRACT

Chitosan has applications in different industries, due to the superior properties, causing an increase in the production of chitosan containing waste. Although composting is the most suitable method for biodegradable wastes like chitosan, less is known about the degradation of chitosan within the composting environment. In this study, biodegradation behavior of bare chitosan films and neutralized chitosan films were investigated under controlled composting environment according to international standards. CO_2 emission data showed higher degradation rate of bare chitosan films compared with neutralized chitosan films, which was also supported by SEM images and digital photographs in addition to the TGA and FTIR results. It can be concluded that the biodegradation rate of chitosan films under the composting environment is highly related to the amount of glycerol present in the films and the extraction rate of glycerol from film structure.

Keywords: Biodegradation, biopolymer, chitosan, composting

1. INTRODUCTION

Recently, with increasing economic growth, rapidly growing population, with the alteration of the standard of living, the amount of solid waste is increasing along with the changes in its composition. A large part of the generated solid waste is plastics, generally petrochemical-derived synthetic polymers. The overuse of plastic products causes some difficulties in waste management since they are not biodegradable. So, such wastes cause pollution of soil, groundwater and surface water resources. For this reason, the use of biodegradable polymers for various applications has become widespread. Chitosan is one of the most important biopolymers, which is deacetylated form of chitin, has applications in various fields such as medical, food and chemical industries due to mainly its biocompatible, biodegradable, antimicrobial, and nontoxic properties [1]. The form of the chitosan-based products in these areas can be diversified membranes, gels, films and hydrogels related to the intended purpose. The film is

the preferred form of chitosan, incorporating with or without other polymers, essential oils, etc., in different areas like chemical engineering, medical, biotechnology, especially in the food industry as a packaging material [2-5]. Chitosan-based films have selective permeability to gases besides to non-toxic, biodegradable and antimicrobial nature thus they have great potential as a packaging material to extend of food shelf life [6-9]. For this reason usage of chitosan films will increase and in the meanwhile requirement to dispose of chitosan containing waste also.

Composting is a decomposition process of organic materials into stable humus that can be used to improve soil fertility [10, 11]. Composting is a suitable method for the disposal of biodegradable organic waste like chitosan containing wastes providing not only environmental benefits but also economic benefits [12]. There are only a few studies about biodegradation of chitosan in soil and the composting environment in the literature. Dean et al. [13] have reported that addition of nanoclay to chitosan films

had no significant effect on degradation both in soil and composting conditions, which was prepared using melt processing method with or without glycerol as a plasticizer. Another study by Xie et al. [14] which has reported that the addition of glycerol and unmodified nanoclay caused to increase of biodegradation degree, mainly related to the addition of unmodified nanoclay. As a consequence, the chitosan biodegradation mechanism in a composting environment is not well defined yet. Therefore, we aimed to contribute to the studies related to the understanding of the biodegradation of chitosan in the composting environment by investigating the effect of neutralization of chitosan films since it was reported that neutralized films have no antimicrobial activity [4].

In this study, the effect of the neutralization process on biodegradation behavior of chitosan films, under controlled composting environment was investigated. Biodegradation of chitosan films, obtained with and without neutralization process, were investigated under controlled composting conditions according to international standards. In order to compare biodegradation behaviors of bare chitosan and neutralized chitosan films within composting environment, the amount of emitted CO_2, proof of the biodegradation by microbial activity, was evaluated in addition to characterization studies performed by FTIR, TGA, and SEM.

2. MATERIALS & METHOD

2.1. Preparation of films

Chitosan films were produced by the solvent casting method. Acetic acid (Sigma Aldrich) was used as a solvent and glycerol (Glycerol solution 84-88%, Sigma Aldrich) as a plasticizer. A 1% (w/v) chitosan (low molecular weight, with degree of deacetylation 75-85%, Sigma Aldrich) film solution was prepared with 1% (v/v) acetic acid solution [15]. After totally dissolving chitosan, glycerol was added at 0.2% (v/v). Solutions were filtered and then poured into petri dishes followed by drying of films at room temperature. After drying, for neutralization of chitosan films, the films were kept in 0.1 M NaOH solution for 30 minutes and then washed with distilled water and re-dried [16].

2.2. Composting system and biodegradation analysis

Biodegradation of films was investigated by measuring CO_2 emissions from composting reactors according to ASTM D-5338 and ISO 14855: 1, 2012 standards [17, 18]. Among the six parallel composting reactors used, two reactors were containing bare chitosan films, two were containing neutralized chitosan films while the remaining two were used as positive and negative controls containing cellulose and polyethylene films, respectively. Reactors were designed to incorporate 180 g total dry solids of compost and 30 g total dry solids of films according to the compost to polymer ratio given in the ASTM D-5338 and ISO 14855: 1, 2012 standards. Before

biodegradation analysis, the films were cut to obtain a size of 1.5 cm x 1.5 cm of each piece of films. Mature compost was taken from a commercial composting plant that processes municipal solid wastes to high quality compost via tunnel composting system.

To obtain aerobic conditions, the air system was designed to send compressed air that provides CO_2-free, H_2O saturated air to each of the reactors at a sufficient airflow rate. Each reactor's air flow rate was regulated with a volumetric gas flow meter. Reactors were mixed periodically to obtain homogenous content. The temperature of the reactors was maintained at 58±2°C according to standards. During the process, moisture content was maintained over 50%. pH was measured throughout the process and digital photographs were taken at different time periods. The amount of CO_2, emitted as a biodegradation product, was measured by an infrared CO_2 analyzer (Model 902P O_2/CO_2 Analyzer, Quantek Instruments, USA).

2.3. SEM

Film samples were collected during the biodegradation process, rinsed with distilled water, air-dried, and coated with gold for sample imaging. Images of samples were obtained by scanning electron microscopy (SEM) using Nova™ NanoSEM 430 (FEI Company, USA).

2.4. FTIR

Fourier transform infrared (FTIR) spectra were measured on FTIR spectrophotometry (Nicolet 6700, Thermo Scientific) in the range of 4000 to 400 cm^{-1} for bare chitosan and neutralized chitosan films.

2.5. Thermal analysis

Thermal properties of the bare chitosan and neutralized chitosan films were investigated by thermogravimetric analysis (TGA) using TGA SII Exstar 6000 TG/DTA 6300. TGA was performed under a nitrogen atmosphere (10 mL min^{-1}) and film samples were heated to 600°C at a rate of 10°C min^{-1}.

3. RESULTS & DISCUSSION

In order to compare biodegradation behavior of bare and neutralized chitosan films digital photographs and SEM images, FTIR spectra and TGA thermograms of samples and carbon dioxide emission data were given below.

3.1. Digital photographs and SEM images

SEM images and digital photographs of bare chitosan film samples collected during the degradation process at different time periods are given in Fig 1. SEM images of bare chitosan films showed that the films had a homogeneous structure before degradation. After 5 days of biodegradation regular structure of film surfaces started to change. At the end of the first week, films were highly degraded, so it was not

possible to take of bare chitosan film samples after 7 days. Different days were selected depending on the maximum CO_2 emissions for bare chitosan films. Size of films decreased during biodegradation as observed by digital photographs and by SEM images.

SEM images and digital photographs of neutralized chitosan film samples collected at different times of biodegradation are given in Fig 2. For neutralized chitosan films, same days were selected to compare the results with bare chitosan films. Digital

photographs of neutralized chitosan films showed that the films were retained their structure for a long time when compared with bare chitosan films. Therefore, sampling from the reactors containing neutralized chitosan films was able to be continued to the end of the composting process. Correspondingly, the results of SEM analysis showed that at the end of the biodegradation process only a small amount of degradation has occurred.
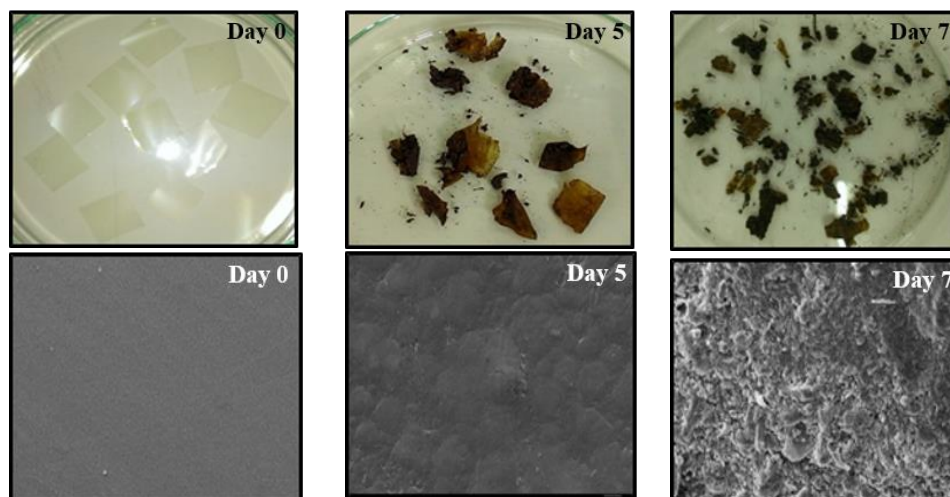

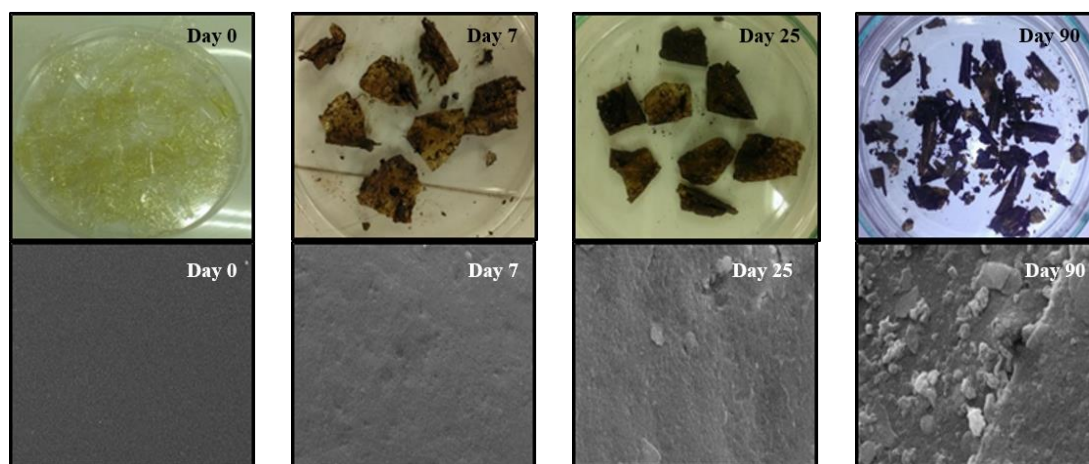**Fig 1.** Digital photographs and SEM images of bare chitosan film samples

Fig 2. Digital photographs and SEM images of neutralized chitosan film samples

3.2. FTIR spectra

The absorption bands (1160-1140 cm^{-1}) corresponding to the FTIR spectra of C-O-C bond between the glucosidic units were used to represent the degradation of films due to microbial activity [19]. The decrease in intensity of the peak at 1150 cm^{-1} for bare chitosan films was attributed to the biodegradation of films by microbial activity (Fig 3, a and b). The intensity of the peak was not changed for neutralized chitosan films so it can be concluded that the films were not degraded by microorganisms (Fig 3, c and d).

3.3. Thermal Analysis

TGA of bare chitosan films and neutralized chitosan films that were collected before and after biodegradation process was carried out. Before degradation, weight loss was observed in three regions as 0-100°C, 150-200°C and 250-300°C for bare chitosan film samples corresponding to moisture loss, evaporation of glycerol [20] and degradation of chitosan respectively (Fig 4). Results of TG analysis emphasized that the degradation of chitosan films pursues upon glycerol molecules because the peak that corresponds to the evaporation of glycerol was disappeared for the samples of bare chitosan films after degradation. Meanwhile, there were only two peaks for neutralized films and the third peak corresponding to the evaporation of glycerol was already absent before degradation. Therefore, limited

degradation could only be observed due to the lack of glycerol within the neutralized samples. Supporting these findings, it has been previously reported that using glycerol as a plasticizer makes films more hydrophilic and increase the biodegradation rate of films by microbial activity [21, 22]. Xie et al. [14] have reported that plasticized chitosan-based nano-biocomposites degraded more easily than unplasticized chitosan due to the presence of glycerol.
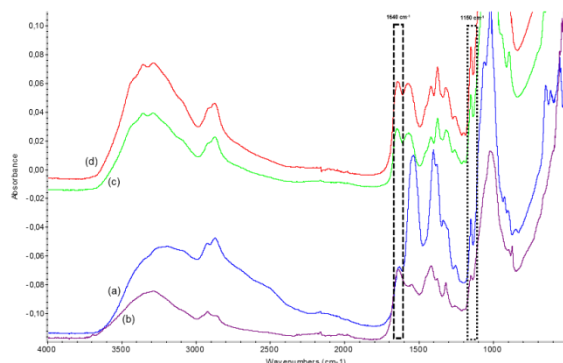

Fig 3. FTIR spectra of bare chitosan films (a) before and (b) after the degradation process; neutralized chitosan films (c) before and (d) after degradation process
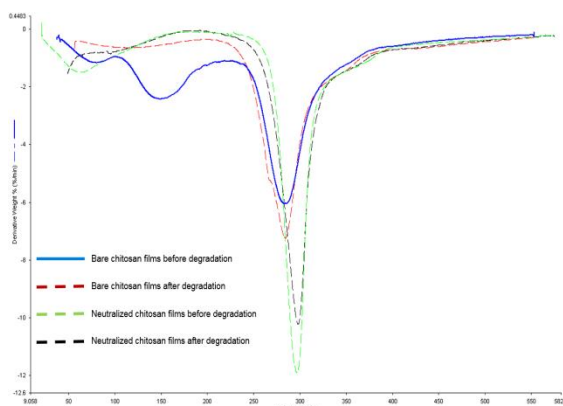

Fig 4. TGA thermograms of bare chitosan films and neutralized chitosan films before and after degradation
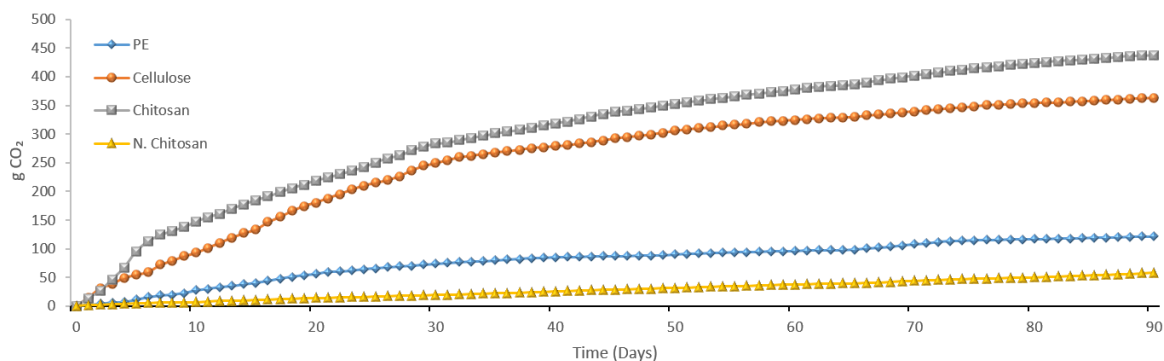
3.4. CO_2 Emissions

CO_2 emission data given in Fig 5 showed a high degradation rate of bare chitosan films compared with neutralized chitosan films especially during the first week of the process supporting the result given above. The probable reason for the lack of biodegradability after neutralization could be the elimination of glycerol during the neutralization step, the presence of which promotes microbial degradation. Therefore it can be concluded that the presence of glycerol is so dominant in biodegradability of chitosan films that the effect of the change in antimicrobial properties couldn't even be recognized in which case reverse data would be expected. Plasticization with glycerol makes films easily accessible for the microbial attack through the increase of water vapor permeability. The amount of carbon available to be metabolized to CO_2 in neutralized films would be less hence it is reasonable to observe less carbon dioxide emission from neutralized films containing reactor. But being even smaller than that of the negative control reactor may not be related only to the lack of glycerol. Microorganisms in the composting environment are mainly responsible for the biodegradation process of organic materials. Therefore it is reasonable to identify the microbial diversity, which has a major role in the degradation process. Further research is needed to understand the role of microorganisms and enzymes in the biodegradation of chitosan in the composting environment.

Fig 5. Cumulative CO_2 values (per vessel)

4. CONCLUSIONS

It was observed that the biodegradation rate of bare chitosan films is higher than that of neutralized chitosan films. Therefore, it can be concluded that the biodegradation rate of chitosan films under the composting environment is highly related to the amount of glycerol present in the films, and the extraction rate of glycerol from film structure but not the antimicrobial properties at all. Further research is needed to identify the microbial diversity, enzymes, plasticizer amount and film synthesizing techniques that play a role in the degradation process in order to increase the biodegradation rate of chitosan in the composting environment.

ACKNOWLEDGEMENT

REFERENCES

[1]. S.-H. Lim, and S.M. Hudson, "Review of Chitosan and Its Derivatives as Antimicrobial Agents and Their Uses as Textile Chemicals," Journal of Macromolecular Science Polymer Reviews, Vol. 43(2), p. 223-269, 2003.

[2]. M., Guo, T.Z. Jin, L. Wang, O.J. Scullen and C.H. Sommers "Antimicrobial films and coatings for inactivation of Listeria innocua on ready-to-eat deli turkey meat," Food Control, Vol. 40, pp. 64-70, 2014.

[3]. D.E. Altiok and F. Tihminlioglu, "Physical, antibacterial and antioxidant properties of chitosan films incorporated with thyme oil for potential wound healing applications," Journal of Materials Science Materials in Medicine, Vol. 21(7), pp. 2227-2236, 2010.

[4]. P. Fernandez-Saiz, J.M. Lagaron and M.J. Ocio, "Optimization of the biocide properties of chitosan for its application in the design of active films of interest in the food area," Food Hydrocolloids, Vol. 23(3), pp. 913-921, 2009.

[5]. T. Freier, H.S. Koh, K. Kazazian and M.S. Shoichet, "Controlling cell adhesion and degradation of chitosan films by N-acetylation," Biomaterials, Vol. 26(29), pp. 5872-8 2005.

[6]. J. Bonilla, E. Fortunati, L. Atarés, A. Chiralt and J.M. Kenny, "Physical, structural and antimicrobial properties of poly vinyl alcohol–chitosan biodegradable films," Food Hydrocolloids, Vol. 35, pp. 463-470, 2014.

[7]. P. Fernández-Saiz, G. Sánchez, C. Soler and J.M. Lagaron, "Chitosan films for the microbiological preservation of refrigerated sole and hake fillets," Food Control, Vol. 34(1), pp. 61-68, 2013.

[8]. Q. Ma, Y. Zhang, F. Critzer, P.M. Davidson, S. Zivanovic and Q. Zhong, "Physical, mechanical, and antimicrobial properties of chitosan films with microemulsions of cinnamon bark oil and soybean oil," Food Hydrocolloids, Vol. 52, pp. 533-542, 2016.

[9]. Z.H. Zhang, Z. Han, X.A. Zeng, X.Y. Xiong and Y.J. Liu, "Enhancing mechanical properties of chitosan films via modification with vanillin," International Journal of Biological Macromolecules, Vol. 81, pp. 638-43, 2015.

[10]. C.M. Mehta, U. Palni, I.H. Franke-Whittle and A.K. Sharma, "Compost Its role, mechanism and impact on reducing soil-borne plant," Waste Management, Vol. 34, pp. 607-622, 2014.

[11]. P.M. Dees and W.C. Ghiorse, "Microbial diversity in hot synthetic compost as revealed by PCR-amplified rRNA sequences from cultivated isolates and extracted DNA," FEMS Microbiology Ecology, Vol. 35, pp. 207-216, 2001.

[12]. I. Leceta, P. Guerrero, S. Cabezudo and K. de la Caba, "Environmental assessment of chitosan-based films," Journal of Cleaner Production, Vol. 41, pp. 312-318, 2013.

[13]. K. Dean, P. Sangwan, C. Way, X. Zhang, V.P. Martino, F. Xie, P.J. Halley, E. Pollet and L. Avérous, "Glycerol plasticised chitosan: A study of biodegradation via carbon dioxide evolution and nuclear magnetic resonance," Polymer Degradation Stability, Vol. 98(6), pp. 1236-1246, 2013.

[14]. D.F. Xie, V.P. Martino, P. Sangwan, C. Way, G.A. Cash, E. Pollet, K.M. Dean, P.J. Halley and L. Avérous, "Elaboration and properties of plasticised chitosan-based exfoliated nano-biocomposites," *Polymer*, Vol. 54(14), p. 3654-3662, 2013.

[15]. I. Leceta, P. Guerrero, and K. de la Caba, "Functional properties of chitosan-based films," *Carbohydrate Polymers*, Vol. 93(1), pp. 339-46, 2013.

[16]. A.P. Martínez-Camacho, M.O. Cortez-Rocha, J.M. Ezquerra-Brauer, A.Z. Graciano-Verdugo, F. Rodriguez-Félixa, M.M. Castillo-Ortega, M.S. Yépiz-Gómez and M. Plascencia-Jatomea, "Chitosan composite films: Thermal, structural, mechanical and antifungal properties," *Carbohydrate Polymers*, Vol. 82(2), pp. 305-315, 2010.

[17]. D5338-98 American Society for Testing Materials (ASTM), Standard Test Method for Determining Aerobic Biodegradation of Plastic Materials under Controlled Composting Conditions. ASTM International, West Conshocken, PA, 2003.

[18]. EN ISO 14855-1, Determination of the Ultimate Aerobic Biodegradability and Disintegration of Plastic Materials under Controlled Composting Conditions—Method by Analysis of Evolved Carbon dioxide-Part 1: General method. 2012.

[19]. M. Kammoun, M. Haddar, T.K. Kallel, M. Dammak and A. Sayari "Biological properties and biodegradation studies of chitosan biofilms plasticized with PEG and glycerol," *International Journal of Biological Macromolecules*, Vol. 62, pp. 433-8, 2013.

[20]. M. Kurek, C.H. Brachais, C.M. Nguimjeu, A. Bonnotte, A. Voilley, K. Galić, J.-P. Couvercelle and F. Debeaufort, "Structure and thermal properties of a chitosan coated polyethylene bilayer film," Polymer Degradation and Stability, Vol. 97(8), pp. 1232-1240, 2012.

[21]. R. Lamim, R.A. de Freitas, E.I. Rudek, H.M. Wilhelm, O.A. Cavalcanti and T.M.B. Bresolin, "Films of chitosan andN-carboxymethylchitosan. Part II: effect of plasticizers on their physiochemical properties," *Polymer International,* Vol. 55(8), pp. 970-977, 2006.

[22]. N. Suyatma, L. Tighzert and A. Copinet, "Effects of hydrophilic plasticizers on mechanical, thermal, and surface properties of chitosan films," *Journal of Agricultural and Food Chemistry*, Vol. 53, pp. 3950-3957, 2005.

Environmental Research & Technology

RESEARCH ARTICLE

Study of the chemical durability of a hollandite mineral leached in both static and dynamic conditions

Fairouz Aouchiche[1] [iD], Nour-el-hayet Kamel[1,*] [iD], Dalila Moudir[1] [iD], Yasmina Mouheb[1] [iD], Soumia Kamariz[1] [iD]

[1]Algiers Nuclear Research Centre, Division of Nuclear Techniques, 2. Bd Frantz Fanon, P.O.Box: 399, Alger-RP, Algiers, ALGERIA

ABSTRACT

Hollandite is a ceramic used for the confinement of cesium. In this study, we synthesized a hollandite of chemical formula: $K_{0.28}Ba_{0.76}Ti_{7.10}Cu_{0.9}O_{16}$, where K simulates cesium. This new formulation of a copper-containing hollandite was synthesized by a double calcination; the first one at 950°C during 18 h, and the second one at 1000°C during 6 h. The mineral was identified by X-ray diffraction. Various leaching tests are employed in order to assess the chemical durability of this mineral. The static test MCC1 gave elemental leaching rates of: $7.097\ 10^{-5}$ g cm^{-2} d^{-1} for Cu, $5.592\ 10^{-7}$ g cm^{-2} d^{-1} for Ti and $4.630\ 10^{-6}$ g cm^{-2} d^{-1} for Ba, after 42 days. This corresponds to dissolved elements percentages of: 5.7% Cu, 0.0007% Ti and 0.2% Ba. The equivalent amount of dissolved K is 0.0029%. A static test in the presence of a clay barrier, gave the best leaching rates (at 42nd day, NR<$3.704\ 10^{-7}$ g cm^{-2} d^{-1} of Cu, and <$1.11\ 10^{-9}$ g cm^{-2} d^{-1} of Ti and <$3.67\ 10^{-9}$ g cm^{-2} d^{-1} of Ba). This corresponds to 0.030% of Cu, 10^{-6} % of Ti and 0.002 % of Ba, and about 0.002% of K. In MCC5 dynamic test, the leaching rates of Cu, Ti and Ba reached $2\ 10^{-6}$, $1,468\ 10^{-7}$, and $1.084\ 10^{-5}$ g cm^{-2} d^{-1}, respectively, corresponding to 0.028% Cu, 0.0003% Ti, and 0.082% Ba, after seven days. The estimated K leaching rate is $3.613\ 10^{-6}$ g cm^{-2} d^{-1}, ie 0.082% K dissolved in the leachate. There is no passivation layer formation. The MCC5 test is considered as a dissolution test.

Keywords: Hollandite, cesium, leaching, MCC1, MCC5, clay

1. INTRODUCTION

Alkaline isotopes raising from many intermediate radioactive waste, such as 137 Cs, 134 Cs and 90 Sr are an issue in an environmental point of view, and their confinement for long periods of time, in durable matrix is a concern for the scientific community [1].

Many nuclear glasses and ceramic matrix as well, have been proposed to embed such radioactive elements. The ceramics have the advantage to be more chemically durable and are highly resistant to radiations damages, resulting from radionuclides disintegrations in the materials during waste disposal. Among the proposed confinement materials for these alkaline elements, borosilicate, aluminosilicate and phosphate glasses, ceramics (NZP: $NaZr_2(PO_4)_3$, phosphated apatites such as $Ca_8NdCs(PO_4)_6F_2$, silicated apatitessuch as $Ca_7Nd_2Cs(PO_4)_5(SiO_4)F_2)$, zeolite cenospheres, $KCsFeZrP_3O_{12}$, etc.), and aluminosilicate glass-ceramics, have suitable properties[1–4].

Synroc ceramics which are mainly composed of hollandite, perovskite, zirconolite, and rutile can also confine Cs and Sr in the crystalline lattice of their minerals. Hollandite is a mineral belonging to Synroc. It can easily accommodate cesium in its structure. Hollandite can vary in its chemical composition leading to various material properties [5].

Natural hollandite has the chemical formula: $BaAl_2Ti_6O_{16}$. It is dedicated to the confinement of radioactive alkaline earth elements, such as cesium (Cs), rubidium (Rb) and barium (Ba) [6]. The general formula of hollandite is: $A_x(B,C)_8O_{16}$, x ≤ 2, where A cations are mono or bivalent, C cations, usually bi or trivalent, and B cations tetravalent. C cations compensate the charge for the incorporation of A cations into the structure [7]. This structure is derived from that of rutile, and consists of double chains of BO_6 octahedron. The structure symmetry can be

monoclinic (I2/M) or quadratic (I4/M), depending on the ionic radii of A, B or C cations [8–12]. According to J. Zhang et al. [13], the most widespread crystalline structure for hollandite is tetragonal, with a (I4/M) space group.

Many studies have dealt with the hollandite optimal composition.

F. Angeli et al. [14] synthesized a hollandite with the chemical formula: $Ba_x^{2+}Cs_y^{2+}M_{2x+y}^{3+}Ti_{8-2x-y}^{4+}O_{16}$ (x ≤ 2) where M is a trivalent cation (Ti^{3+}, Al^{3+} or Fe^{3+}) providing the charge compensation required for Ba and Cs loading. When M= Fe^{3+} or $Fe^{3+} + Al^{3+}$ in Ba_xCs_y $(Fe, Al)^{3+}_{2x+y}Ti^{4+}_{8-2x-y}O_{16})$ hollandite, the most significant amounts of Cs were loaded in the structure, under oxidizing sintering conditions [7, 15–18].

Joint investigations between the ANSTO (Australian Nuclear Science and Technology Organisation) and the French CEA (Commissariat àl'Enérgie Atomique)report the loading of high amounts of Cs ions within $Ba_1Cs_{0,28}Al_{1,46}Fe_{0,82}Ti_{5,72}O_{16}$ hollandite [19].

Several synthetic methods, dry and wet ones, are used to synthesize hollandite. However, most of them are wet route processes, based on sol-gel reactions in which the precursors mixtures are obtained by the alkoxide route [14, 18, 20, 21]. Otherwise, the dry method employs sintering processes, called 'oxides route' [15, 16]. This last is based on a calcination, under air or inert atmosphere, of a mixture of oxides and carbonates, followed by a sintering between 1200 and 1400 °C [16, 17].

For an optimal confinement of Cs, under the frame of (Ba-Cs) hollandite investigations, many studies seek to vary the charge compensating element (C), among many metals. Till today, copper has not been studied yet.

This study investigates the synthesis of a titaniferous hollandite with copper (Cu^{2+}) as a charge compensating element, with the chemical formula of: $K_{0.28}Ba_{0.76}Cu_{0.9}Ti_{7.10}O_{16}$, by a dry method. The precursor mixture contains titanium (Ti), barium (Ba), and copper (Cu) oxides, and potassium (K) carbonate. The ionic radii of Ti^{4+} and Cu^{2+} are relatively close to each other [7] and the tolerance factor, th, has been verified, such that one can expect a stable structure of hollandite [22].

On the other hand, to avoid process constraints due to the chemical properties of Cs_2O (low melting temperature (490°C) and high volatility), potassium is used as Cs simulator, to validate the process; and to check the possibility of formation of hollandite mineral under the chosen operating conditions.

One can note that the optimization of sintering conditions has been the subject of a previous work in our laboratory [23].

The chemical durability of hollandite is assessed by three leaching tests: the MCC1 static test, a static test in the presence of a clay barrier, and the MCC5 soxhlet dynamic test. The leaching kinetics is monitored by ICP-OES spectroscopy. The evolution of the concentration, the mass loss, and the elemental leaching rate of Cu, Ti and Ba, are calculated; and

make conclusions valuable, on the leaching behavior of the as-prepared hollandite.

2. MATERIALS & METHOD

The following commercial reagents are employed: K_2CO_3 (99% Merck), BaO (99.6% Fluka), TiO_2 (99% Merck) and CuO (99% Merck). They are dried separately in an oven at 100°C overnight, crushed using a manual agath mortar, and sieved to reach a particle size less than 60 μm. A mixture of powders, according to the stoichiometric conditions of the chosen chemical formula, is weighed. 8 wt.% of zinc stearate (Sigma-Aldrich) is added as organic binder. The mixture is homogenized using a D 4030 Controls Automatic Sieve Shaker. Pellets with 14.3 mm diameter, and of different heights are compacted using a Sodemi RD uni-axial press, at 6 t. They are calcined at 950°C for 18 h in a RHF-1600 Carbolite furnace, with a heating and cooling rate of 5 and 10 ° min^{-1}, respectively. The calcined pellets are similarly crushed, pelletized, then sintered under air at 1000°C, for 6 h, with both a heating and cooling step of 5 ° min^{-1}. Both green (d_c) and sintered (d_f) geometrical densities are measured.

The materials phases' identification is performed by X-ray diffraction analysis (XRD) with a Philips X-Pert Pro spectrometer. The X'Pert High Score Plus software, 4.1 version, is used for phase' identification [24].

The MCC1 leach test is performed in a small volume of leachate during a relatively short time period. The mineral pellets are immersed in dark opened glass vials, containing ultra-pure water (18 MΩ cm^{-1}) at ambient temperature (≅25°C). Regular samplings of 1 mL are performed at know times, not exceeding 42 days. A drop of 1N nitric acid solution is added to each sample to prevent the formation of solid layers on the sampling tubes walls.

After each sampling, the leachate volume is completed to its initial value, with ultra-pure water, in order to maintain (S_0/V_0) surface to volume ratio constant.

The starting leachate immersion volumes are calculated considering S_0/V_0= 30. This last is an important test parameter. S0: is the material surface effectively in contact with the leachate, and V_0 is the leachate volume.

The static test, performed in presence of a clay barrier, simulating an engineering barrier in storage conditions, is similar to MCC1 test. The samples are immersed in water into a clay container. This last is synthesized by calcination at 750°C in air, of natural Algerian kaolin.

The MCC5 test employs a 250 mL soxhlet extractor, working under air.Cylindrical pellets, of both known dimensions and weight, are continuously immersed in the leachate. The balloons are filled with 30 mL of ultra-pure water excess (18 MΩ cm^{-1}), to prevent both evaporation and samplings water losses.

Daily leachates samplings of 1 mL are performed in the balloon during 7 days. The balloon residues are collected after the last sampling. The balloon is

further cleaned with a 1N HNO_3 (Merck) acid solution, in order to remove walls likely deposits. The whole of liquid' residues are analyzed.

All leachates are analyzed by a32 Jobin Yvon ICP-OES spectrometer, after establishing the calibration curves of the interest elements, leached from the mineral, namely: Cu, Ti et Ba.

Standard solutions are prepared using ICP/DCP Fluka standards. The chosen concentrations are: 10, 20, 50, 80 and 100 ppm. The elemental calibrations curves of the measured intensity (I) versus the i element concentration (C_i), are fitted using LabView equipment software.

The elemental mass loss, for each i element, NL_i traduces the dissolution of a known i element [25]. It is expressed in kg m^{-2}, and given by the equation (1).

$$NL_i = \frac{C_i V_0}{S_0 F_i} \qquad (1)$$

Where C_i: is the total concentration of the i element (kg m^{-3}), V_0: the total volume of the leachate solution (m^3), S_0: the sample initial surface effectively in contact with the liquid (m^2) and F_i: the i element weight fraction in the solid phase (wt.%).

The elemental normalized leaching rate (NR_i) as a function of time expresses the material normalized dissolution rate (in kg m^{-2} s^{-1}). It is given by the equation (2)[25].

$$NR_i = \frac{dM_i}{dt} = \frac{1}{F_i S_0} \frac{dm_i}{dt} \qquad (2)$$

The i element average leaching rate is calculated by dividing the normalized mass loss by a mean time interval (Δt) starting from the initial time of leaching. It is given by the equation (3).

$$NR_{imoy} = \frac{\Delta M_i}{\Delta t} = \frac{1}{F_i S_0} \frac{\Delta m_i}{\Delta t} \qquad (3)$$

3. RESULTS & DISCUSSION

3.1. Density of the synthesized material

The hollandite crud density, d_c, is of 2.72. After the first thermal treatment, it is of 2.02; and the final sintered density is of 2.56. After the first thermal treatment, the materials density decreases highlighting the fact that a second thermal treatment is required. This last improved the material density.

V. Aubin-Chevaldonnet et al. [15] found sintered densities in the interval of 3.92-4.55, for different Ba-hollandites. These values are higher than those of the present study, due to the synthesis processemployed by these authors,which involves a sintering pressure, and thus increases density, and reduces the internal porosity. Adding to the difference in the used elements, such as Cu, which have a low atomic weight, and contributes to decreasing the sintered density.

3.2. Phases identification

Both the calcined and sintered materials XRD spectra are given in Fig 1. The calcined material phases identificationshows a main tetragonal phase, identified as $BaTi_7MgO_{16}$ hollandite skeleton,

associated to the JCPDS card number: 01-073-0499, with over 60 % [26]. The calcined pellets appear to be homogeneous. An excess of TiO_2 appears as a secondary phase, identified by the JCPDS standard number 03-065-0191.
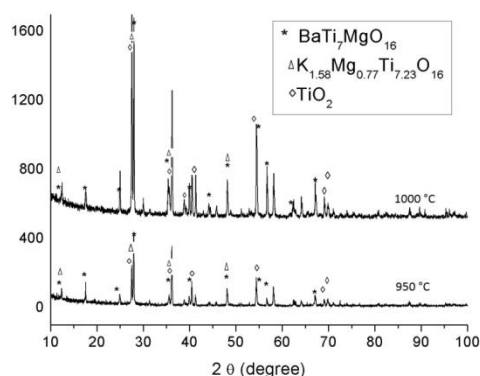

Fig 1. XRD spectra of both calcined (950 °C) and sintered (1000 °C) materials

A similar semi-quantitative composition is identified for the sintered material, with over 65 % of hollandite skeleton, shared in two phases: 46 % of tetragonal $BaTi_7MgO_{16}$ (JCPDS 01-073-0499) and 19 % of tetragonal $K_{1.58}Mg_{0.77}Ti_{7.23}O_{16}$ (JCPDS 01-084-0976). One can also observe 35 % of tetragonal TiO_2 (JCPDS 01-089-4202).

3.3. Leaching tests

MCC1 static test

During this test, the evolution of Ba, Ti and Cu concentrations as a function of time show that for the whole of elements, the elemental concentrations (C_i) are low during the first seventh days, then increase (Fig 2). They are high between the 28th and the 35th day, with maximum values. Copper is the most water-soluble element, with a maximum concentration at the 35th day: C_{Cu}=3.8335 kg m^{-3}. At this time, C_{Ba}=0.6985 kg m^{-3}, and C_{Ti}=0.0221 kg m^{-3}; being in mind that this last element is the most abundant in the solid phase.

For all elements, these values decrease at the 42nd day (1 day=86400 s).

The evolution of normalized mass losses, N_{Li}, in Ba, Ti and Cu seems to follow that of concentrations (Table 1). Until the 7th day, the values are very low. Beyond, NL_{Cu} increases rather quickly, till the 35th day, and then decreases significantly. For Ba, this evolution goes in the same way but is slower than that for Cu. For Ti, the evolution of NL_{Ti} is absent.

During this leaching stage, there is a certain balance, which shows that the leaching is very slow, or that there is a balance between the leached elements and those that eventually return to the matrix. This is probably due to a solubility competitiveness of Cu and Ba elements in the water.
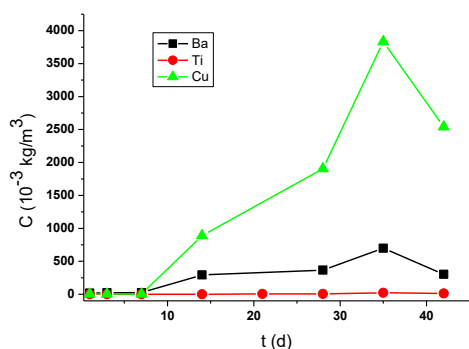
Fig 2. Evolution of Ba, Ti and Cu concentrations as a function of time, for $K_{0.28}Ba_{0.76}Ti_{7.10}Cu_{0.9}O_{16}$ hollandite leached by MCC1 test

Table1. Evolution of the normalized elemental mass loss as a function of time for Ba, Ti and Cu, for $K_{0.28}Ba_{0.76}Ti_{7.10}Cu_{0.9}O_{16}$ hollandite in MCC1 test

t (days)	NL_{Ba} (10^{-2} kg m^{-2})	NL_{Ti} (10^{-2} kg m^{-2})	NL_{Cu} (10^{-2} kg m^{-2})
1	0.0113	0.0770	0.0036
3	0.0145	0.0632	0.0018
7	0.0154	0.0672	0.0019
14	0.1885	0.2113	1.0423
21	---	0.9805	---
28	0.2354	0.0011	2.2365
35	0.4493	0.0044	4.4995
42	0.1944	0.0024	2.9807

In general, Cu is more soluble than Ba, which in turn is more soluble than Ti. The maximum elemental mass losses observed are at day 35: NL_{Ba}=0.4493 10^{-2} kg m^{-2}, NL_{Ti}=0.0044 10^{-2} kg m^{-2}, NL_{Cu}=4.4995 10^{-2} kg m^{-2}. These low values show that the matrix is less soluble in water, especially since its major element, Ti, is released in the smallest amount.

Beyond the 35th day, NLi values increase for the three elements, then decrease. At the 42nd day, they are of: 2.9807 10^{-2} kg m^{-2} for Cu, 0.1944 10^{-2} kg m^{-2}for Ba, 0.0024 10^{-2} kg m^{-2} for Ti. At this stage, the matrix elements are likely redeposited around the material, slowing down the leaching speed. A passivation layer starts to form around the material, leading the leaching medium to a steady state.

F. Angeli et al. [14] have leached a Cs-doped hollandite ceramic ($BaCs_{0.28}Fe_{0.82}Al_{1.46}Ti_{5.72}O_{16}$) at 90°C. A Ba-layer has formed around the material, and coated it, after several months of leaching. It is poor in Cs, and probably formed by $BaCO_3$, where carbon is coming from air CO_2. This layer re-dissolves when the water is renewed in the medium [27,28].

During the leaching process, there is a strong displacement of alkalis from the materials surface. G. Leturq et al. [29] show a zirconolite decalcification after leaching at 150 °C in an acidic medium, and formation of a passivation layer, rich in the least soluble alkalis (Ba). This passivation layer has been

evidenced in other studies [30, 31].In this study, NL_{Cs} is similar to that of Ba (19 10^{-5} g cm^{-2}).

In the present test, one can suppose that Cs and K moved during surface alteration, and formed Cs and/or K-reach minerals, as layers deposited on the material surface, like hydrated titanates ($Ti(OH)_4$) [29, 32].

T. Suzuki-Muresan et al. [33] conduct leaching experiments in static mode of (Cs, Ba)-hollandite during 240 days, at various pH in NaCl aqueous solutions.

The steady-state is established between 45 and 240 days, and the average NL_{Cs} ranges between (8.2 ± 0.3) 10^{-6} kg m^{-2} (pH 2.5) to (4.1 ± 0.2) 10^{-6} kg m^{-2} (pH 8.6), and NL_{Ba} from (3.7 ± 0.4) 10^{-6} kg m^{-2} (pH 2.5) to (4 ± 2) 10^{-7} kg m^{-2} (pH 8.6). These values are higher than our results, which are of NL_{Ba}=0.1944 10^{-2} kg m^{-2}, after 42 days of test in a neutral medium.

These authors have loaded hollandite with (^{137}Cs and ^{133}Ba) isotopes, and perform sorption experiments on hollandite pre-leached in aqueous solutions. Cs and Ba release is controlled by surface reactions. Leaching experiments and isotopic addition experiments (^{137}Cs and ^{133}Ba-radiotracers) indicate that Cs behavior is independent on pH-values, at the opposite of that of Ba which strongly depend on it.

The NR_i evolution for Ba, Ti and Cu as a function of time, expresses the mineral dissolution rate. The corresponding speed curves are shown in Fig 3.
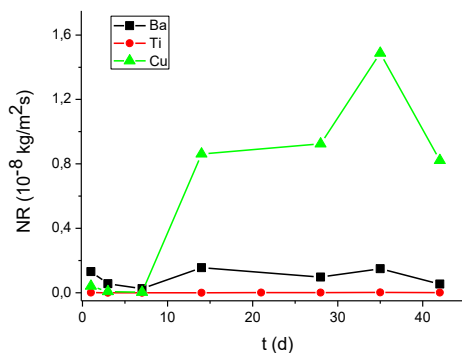

Fig 3. Evolution of the leaching rate as a function of time for Ba, Ti and Cu, for $K_{0.28}Ba_{0.76}Ti_{7.10}Cu_{0.9}O_{16}$ hollandite in MCC1 test

The maximum rates of leaching are at the 35th day, for Ti and Cu, namely: NR_{Ti}=1.157 10^{-4} kg m^{-2} s^{-1} and NR_{Cu}=1.4884 10^{-8} kg m^{-2} s^{-1}. At the end of the test, ie at the 42nd day, NR_{Cu}=8.2176 10^{-9} kg m^{-2} s^{-1}, and NR_{Ti}=6.4718 10^{-11} kg m^{-2} s^{-1}.That is a solids content of: 5.7% Cu, and 0.0007% Ti.

NR_{Ba} has a random evolution. The maximum value is at the 14th day. It is of: NR_{Ba}=1.5625 10^{-9} kg m^{-2} s^{-1}. At the end of test, ie at the 42nd day, NR_{Ba}=5.3241 10^{-10} kg m^{-2} s^{-1}. That is a solid content of: 0.2%.

Taking into account the stoichiometry of the molecule, the K dissolved amount is of 0.2064 %.

F. Angeli et al. [14] have studied the aqueous corrosion behavior of Cs-doped hollandite ceramic ($BaCs_{0.28}Fe_{0.82}Al_{1.46}Ti_{5.72}O_{16}$) at 90°C, using several

static protocols, at both various pH and S_0/V_0 ratios, for times periods ranging from six months to three years. They report that after a rapid initial Cs release, the alteration rate is extremely low over the pH range from 2 to 10 (10^{-5} g m^{-2} d$^{-1}\cong$1.1574 10^{-9} kg m^{-2} s^{-1}), and reaches 510^{-3} g m^{-2} d^{-1} at pH=1. In these experiments S_0/V_0 ratios are from 0.1 to 1200 cm^{-1}. The alteration thicknesses are of a few nanometers per year. These values are about 105 times lower than NR_{Ba} in the present study, which is about 5.3588 10^{-6} kg m$_{-2}$ s$_{-1}$, instead of the low temperature (25°C).Whilst, after 261 days of test, aCs depletion is evidenced at the surface,when leachates are replenished with fresh deionized water. The presence of a soluble Ba-bearing secondary phase was inferred.

Solomah et al. [34] perform a MCC1 test, during 120 days. They found a value of: NR_{Ba}=6.94 10^{-7} kg m-2 s-1. This value is lower than our result (5.3588 10^{-6} kg m^{-2} s^{-1} at the 42th day).

B.B. Shabalin et al. [32] assessed NR_{Cs} for $Ba_{0.9}Cs_{0.2}Fe_{2.0}Ti_{6.0}O_{16}$ ceramic, by MCC2 test at 150°C, in distilled water, during 1, 3, 7, 10, and 14 days; with S/V=0.01 mm^{-1}($\cong 10^{-5}$ m^{-1}). After 10 days, NRCs slows down: NR_{Cs}=1.1574 10^{-9} kg m^{-2} s^{-1}.

3.4. Static test in the presence of a clay barrier

The evolution of Ba and Cu concentrations as a function of time shows two minimums on the concentration curves (Fig 4). C_{Ba} stabilizes at the 42nd day at: C_{Ba}=2.288 10^{-3} kg m^{-3}. This low concentration shows the affinity of this alkaline earth element for the clay.
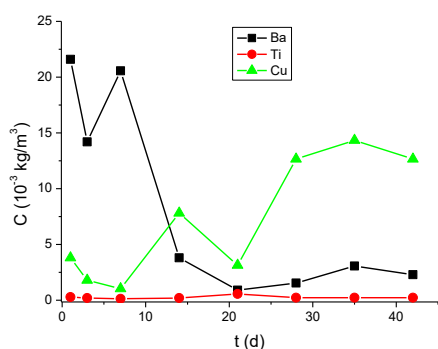

Fig 4. Evolution of the concentration as a function of time for Ba, Ti and Cu, for $K_{0.28}Ba_{0.76}Ti_{7.10}Cu_{0.9}O_{16}$ hollandite in the clay container test

In the clay container test, changes in C_{Ti} as a function of time show that C_{Ti} are the lowest concentrations. There are very weak during the whole period of test.

In opposite, for Cu, two maximum concentrations are observed on the 14th and 35th day. The final C_{Cu} value attains 12.66 10^{-3} kg m^{-3}. Cu does not have any affinity for clay.

The NL_i values follow the evolution of C_{Ba}, C_{Ti} and C_{Cu} values (Table 2), confirming that the clay slows the leaching over the 28th day of test; Ti and Ba (thus K simulator of Cs) having an affinity for the clay, at the opposite of Cu which dissolves in water. At the 42th

day, NL_{Ba}=0.0015 10^{-2} kg m^{-2}, NL_{Ti}=4.6526 10^{-7} kg m^{-2} and NL_{Cu}=0.0156 10^{-2} kg m^{-2}.

Table 2. Evolution of the elemental mass loss as a function of time for Ba, Ti and Cu, for $K_{0.28}Ba_{0.76}Ti_{7.10}Cu_{0.9}O_{16}$ hollandite in the clay container test

t (days)	NLBa (10-2 kg m-2)	NLTi (10-7 kg m-2)	NLCu (10-2 kg m-2)
1	0.0145	5,9966	0.0047
3	0.0096	4,1356	0.0022
7	0.0139	2,6881	0.0013
14	0.0026	4,0942	0.0096
21	0.0006	11.9312	0.0039
28	0.0010	4.71458	0.0156
35	0.0021	4.77662	0.0176
42	0.0015	4.65255	0.0156

The evolution of NR_{Ba} and NR_{Cu} as a function of time are shown in Fig 5. It follows an exponential law for the three studied elements. The NR_{Ti} values remain very low over time.
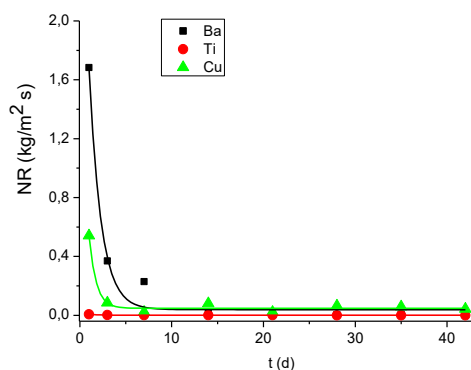

Fig 5. Evolution of the leaching rate as a function of time for Ba, Ti and Cu, for $K_{0.28}Ba_{0.76}Ti_{7.10}Cu_{0.9}O_{16}$ hollandite in the clay container test

The corresponding mathematical relations (4 and 5) are calculated by Origin 8.0 software.

$$NR_{Ba} = 3.8592\ 10^{-11} + 3.5312\ 10^{-9} exp^{\left(\frac{-t}{1.30534}\right)} \quad R^2=0.9848 \quad (4)$$

$$NR_{Cu} = 4.7931\ 10^{-11} + 1.7984\ 10^{-9}\ exp^{\left(\frac{-t}{0.77722}\right)} \quad R^2=0.9866 \quad (5)$$

The leaching rates at the end of the experiments are: NR_{Ba}=4.2455 10^{-12} kg m^{-2} s^{-1}, NR_{Ti}=1.2822 10^{-13} kg m^{-2} s^{-1} and NR_{Cu}=4.2869 10^{-11} kg m^{-2} s^{-1}. Therefore, the dissolved amounts are of: 0.0016 % Ba, 10-6 % Ti and 0.0299 % Cu. That is a quantity of dissolved K estimated to 0.0016 %.

3.5. The MCC5 dynamic test

The curves of the evolution of the concentration of Ba, Ti and Cu as a function of time are gathered in Fig 6. During the soxhlet leaching, Ba is the most trained element into the leaching waters. Its concentration reaches 22.62 10^{-3} kg m^{-3} in the first day. Then, the evolution of C has a saw teeth form. The concentration curve shows two minima, the first to the 3rd day

($17.51 \cdot 10^{-3}$ kg m^{-3}) and the 2nd, at the 6th day of test, is much more significant ($1.14 \cdot 10^{-3}$ kg m^{-3}). Then, C_{Ba} is again up to a value of $11.79 \cdot 10^{-3}$ kg m^{-3}. This indicates that this element is still dissolving around the 7nd day.
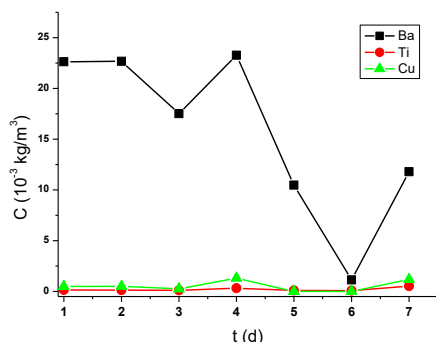

Fig 6. Evolution of the concentration as a function of time for Ba, Ti and Cu, for $K_{0.28}Ba_{0.76}Ti_{7.10}Cu_{0.9}O_{16}$ hollandite in MCC5 test

The evolution of C_{Ti} and C_{Cu} as a function of time shows that these two concentrations are very low during the whole of test, with a slight maximum on the 4th day: $C_{Timax}=0.320 \cdot 10^{-3}$ kg m^{-3} and $C_{Cumax}=1.31 \cdot 10^{-3}$ kg m^{-3}, respectively.

The evolution of NL_{Ba}, NL_{Ti} and NL_{Cu} as a function of leaching follows that of concentrations (Table 3). One can note two minimums on $NL_{Ba}=f(t)$ curve, the most important is at the 6th day with: $0.0073 \cdot 10^{-2}$ kg m^{-2}. The NL_{Ti} and NL_{Cu} values are very low, with a maximum of $0.0154 \cdot 10^{-2}$ kg m^{-2} at the 4th day. At the end of test, Ba, Ti and Cu continue to dissolve. On day 7, $NL_{Ba}=7.59 \cdot 10^{-4}$ kg m^{-2}, $NL_{Ti}=1.0 \cdot 10^{-5}$ kg m^{-2} and $NL_{Cu}=1.40 \cdot 10^{-4}$ kg m^2.

Table3. Evolution of the elemental mass loss as a function of time for Ba, Ti and Cu, for $K_{0.28}Ba_{0.76}Ti_{7.10}Cu_{0.9}O_{16}$ hollandite in MCC5 test.

t (days)	NL_{Ba} (10^{-2} kg m^{-2})	NL_{Ti} (10^{-6} kg m^{-2})	NL_{Cu} (10^{-2} kg m^{-2})
1	0.14556	2.76674	0.0058
2	0.14595	2.56911	0.0059
3	0.11268	2.17386	0.0029
4	0.14975	6.32397	0.0154
5	0.06738	1.97624	*
6	0.00734	1.58099	*
7	0.07587	10.3000	0.0140

S.P. Kumar and B. Gopal [4] have synthesized a langbeinite phosphate powder: $KCsFeZrP_3O_{12}$ by a wet route. After one month of test, the MCC5 test applied to langbeinite phosphate powder: $KCsFeZrP_3O_{12}$ gave normalized mass losses in the order of $NR_K=10^{-7}$-10^{-6} kg m^{-2}, $NR_{Fe}=10^{-9}$-10^{-7} kg m^{-2}, $NR_{Zr}=10^{-8}$-10^{-6} kg m^{-2} and $NR_P=10^{-7}$-10^{-6} kg m^{-2}, respectively; and negligible Cs rate of leaching. These values are lower than our values.

The evolution of NR_{Ti} and NR_{Cu} as a function of time is represented in Fig 7. The maximum values are at the 1st day, where they reach: $NR_{Timax}=3.2022 \cdot 10^{-11}$ kg m^{-2}

s^{-1} and $NR_{Cumax}=6.7130 \cdot 10^{-10}$ kg m^{-2} s^{-1} for Cu. Then, they decrease, and become undetectable for Cu at the 5th and 6th days.

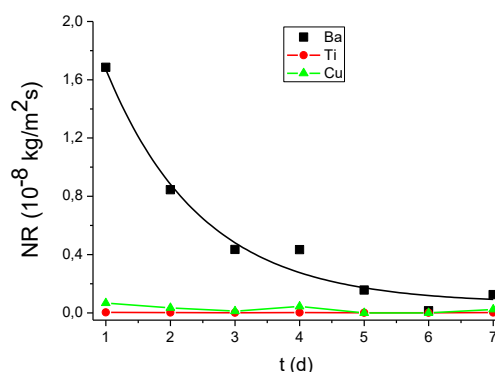**Fig 7.** Evolution of the normalized rate of leaching as a function of time of Ba, Ti and Cu, for $K_{0.28}Ba_{0.76}Ti_{7.10}Cu_{0.9}O_{16}$ hollandite in MCC5 test

At the end of MCC5 test, both NR_{Ti} and NR_{Cu} increases again: $NR_{Ti}=1.6992 \cdot 10^{-11}$ kg m^{-2} s^{-1} and $NR_{Cu}=2.3148 \cdot 10^{-10}$ kg m^{-2} s^{-1}, ie 0.00034% Ti and 0.0276% Cu, contained in the mineral.

The evolution of NR_{Ba} as a function of time follows an exponential decay law, calculated by the Origin 8.0 software ($NR_{Ba}=3.1508 \cdot 10^{-8} \exp(-t/1.48452) + 6.3535 \cdot 10^{-10}$, $R^2=0.98973$). At the end of test, $NR_{Ba}=1.25 \cdot 10^{-9}$ kg m^{-2} s^{-1}, corresponding to 0.0820% of the Ba contained in the mineral. The amount of dissolved K is therefore about 0.0822%.

Since Ba is in the geometric position of K (Cs simulator) inside the hollandite crystal, and regarding the Ba/K ratio in the mineral, the dissolution of K can be estimated to the third of $1.25 \cdot 10^{-9}$ kg m^{-2} s^{-1}, is $0.4167 \cdot 10^{-11}$ kg m^{-2} s^{-1}.

These results show that there is no passivation layer, formed during soxhlet leaching; this test being considered as an aggressive one.

In general, the literature surveys show that among the ceramics studied for Cs immobilization, the leaching tests prove the good stability of the matrices against Cs release [4, 35].

Cs-tetra-ferri-annite, $CsFe^{(II)}_3$-$Fe^{(III)}Si_3O_{10}(OH)_2$, leached by soxhlet, in neutral medium, (pH=7.05), with: m/V_0 = 1 mg cm^{-3} , gave 0.82 wt.% of Cs release [35]. Compared to the soxhlet test results in the present study (0.0820 wt.% Ba and 0.0822 wt.% K, after 7 days; m/V_0 = 7.79 mg cm$_{-3}$), our values are ten times lower compared to those of Cs-tetra-ferri-annite leaching. One can note that in our study, the main amounts of K and Ba, are released in the first day (24 h) of leaching.

4. CONCLUSIONS

In this study, we have synthesized a hollandite mineral with the chemical formula: $K_{0.28}Ba_{0.76}Ti_{7.10}Cu_{0.9}O_{16}$, where K simulates Cs. This new formulation contains copper. After a double calcination at 950°C for 18 h and a sintering at 1200°C for 6 h, the final product presents a sintered density of

2.56. XRD analysis reveals a polyphasic material with 65% of tetragonal hollandite, namely: 46% $BaTi_7MgO_{16}$ and 19% $K_{1.58}Mg_{0.77}Ti_{7.23}O_{16}$; and 35% of TiO_2.

In order to test the hollandite confinement ability, itschemical durability was assessed using three leaching tests: MCC1, MCC5 and a test in the presence of a clay barrier.

On the basis of the results, the leaching in the presence of a clay barrier shows the lowest leaching rates (at the 42nd day, $NR_{Ba} < 4.2555 \ 10^{-12}$ kg m^{-2} s^{-1}, and $NR_{Ti} = 1.2822 \ 10^{-13}$ kg m^{-2} s^{-1} and $NR_{Cu} = 4.2869 \ 10^{-11}$ kg m^{-2} s^{-1}).

MCC1 test gives slightly larger values (42nd day, $NR_{Ba} = 5.3241 \ 10^{-10}$ kg m^{-2} s^{-1}, $NR_{Ti} = 6.4718 \ 10^{-11}$ kg m^{-2} s^{-1} and $NR_{Cu} = 8.2176 \ 10^{-9}$ kg m^{-2} s^{-1}). Finally, the MCC5 test dissolves the most quantities (at the 7th day, $NR_{Ba} = 1.25 \ 10^{-9}$ kg m^{-2} s^{-1}, $NR_{Ti} = 1.6992 \ 10^{-11}$ kg m^{-2} s^{-1} and $NR_{Cu} = 2.3148 \ 10^{-10}$ kg m^{-2} s^{-1}). Obviously, Ti, Ba and therefore K have an affinity for kaolin clays.

Globally, the mineral currently studied has a good chemical durability, which is suitable in disposal conditions.It is able to well embed K (Cs simulator). Indeed, it shows K released contents less than 0.0029% in MCC1, 0.0016% in the presence of a clay barrier and 0.0822% in MCC5.

REFERENCES

[1]. I.W. Donald, Waste immobilization in glass and ceramic based hosts. Radioactive, toxic and hazardous wastes, Ed. John Wiley & Sons, Chichester, 2010.

[2]. M.I. Ojovan and W.E. Lee, An introduction to nuclear waste ımmobilisatıon, Ed. Elsevier, Amsterdam, 2005.

[3]. C. Cantale, J-P. Glatz, E.H. Toscano, A. Donato, M. Coquerelle, and J. Fuger, "Characterization of highly active waste glasses produced in a hot vitrification pilot plant," *Materials Research Society Symposium Proceedings*, Vol. 176, pp. 403-410, 1989.

[4]. S.P. Kumar and B. Gopal, "Synthesis and leachability study of a new cesium immobilized langbeinite phosphate: KCsFeZrP3O12," *Journal of Alloys and Compounds*, Vol. 615, pp. 419-423, 2014.

[5]. S. E. Kesson, "The Immobilization of Cesium in Synroc Hollandite," *Radioactive waste Management Nuclear Fuel Cycle*, Vol. 2, pp. 53-71, 1983.

[6]. A.E. Ringwood, V.M. Oversby, S.E. Kesson, W. Sinclair, N. Ware, W. Hibberson and A. Major, "immobilization of high-level nuclear reactor wastes in Synroc: a current appraisal," *Nuclear and Chemical Waste Management*, Vol. 2, pp.287-305, 1981.

[7]. Aubin-Chevaldonnet, "Synthèse, caractérisation et étude du comportement sous irradiation électronique de matrices de type hollandite destinées au confinement du césium radioactif", thesis, Lab. Chimie Appliquée Etat Solid,

Université Pierre et Marie Curie – PARIS VI, Paris, Nov. 2004.

[8]. A. Byström and A. M. Byström, "The crystal structure of hollandite, the related manganese oxide minerals and α-MnO2," *Acta Crystallographica,* Vol. 3, pp. 146-154, 1950.

[9]. R.W. Cheary, "An analysis of the structural characteristics of hollandite compounds," *Acta Crystallographica*, Vol. B42, pp. 229-236, 1986.

[10]. D.S. Filimonov, Z.-K. Liu and C.A. Randall, "Synthesis and thermal stability of a new barium polytitanate compound, Ba1.054Ti0.946O2.946," *Materials Research Bulletin*, Vol. 37, pp. 467-473, 2002.

[11]. J.E. Post, R.B. Von Dreele and P. R. Buseck, "Symmetry and cation displacements in hollandites: structure refinements of hollandite, cryptomelane and priderite," Acta Crys, Vol. B38, pp. 1056-1065, 1982.

[12]. J. Vicat, E. Fanchon, P. Strobel and D.T. Qui, "The structure of K1.33Mn8O16 and cation ordering in hollandite-type structures", Acta Cryst, vol. B42, pp. 162-167, Apr. 1986.

[13]. J. Zhang and C.W. Burnham, "Hollandite-type phases: Geometric consideration of unit-cell size and symmetry," *American Mineralogist*, Vol. 79, pp. 168-174, 1994.

[14]. F. Angeli, P. McGlinn and P. Frugier, "Chemical durability of hollandite ceramic for conditioning cesium," *Journal of Nuclear Materials*, Vol 380, pp. 59–69, 2008.

[15]. V. Aubin-Chevaldonnet, D. Caurant, A. Dannoux, D. Gourier, T. Charpentier, L. Mazerolles and T. Advocat, "Preparation and characterization of (Ba,Cs)(M,Ti)8O16 (M = Al3+, Fe3+, Ga3+, Cr3+, Sc3+, Mg2+) hollandite ceramics developed for radioactive cesium immobilization," *Journal of Nuclear Materials*, Vol 366, pp. 137-160, 2007.

[16]. A.Y. Leinekugel-le-Cocq, P. Deniard, S. Jobic, R. Cerny, F. Bart and H. Emerich, "Synthesis and characterization of hollandite-type material intended for the specific containment of radioactive cesium," *Journal of Solid State Chemistry*, Vol 179, pp. 3196-3208, 2006.

[17]. V. Aubin-Chevaldonnet, P. Deniard, M. Evain, A.Y. Leinekugelle-Cocq-Errien, S. Jobic, D. Caurant, V. Petricek and T. Advocat, "Incommensurate modulations in a hollandite phase Ba-x(Al,Fe)2xTi8-2xO16 intended for the storage of radioactive wastes: a (3+1) dimension structure determination," Z. Kristallogr, Vol 222, pp. 383-390, 2007.

[18]. M.L. Carter, E.R. Vance, D.R.G. Mitchell, J.V. Hanna, Z. Zhang and E. Loi, "Fabrication, characterization, and leach testing of hollandite, (Ba,Cs)(Al,Ti)2Ti6O16," *Journal of Materials Research*, Vol. 17, pp. 2578-2589, 2002.

[19]. E. Bart, G. Leturcq and H. Rabiller, "Iron-substituted Barium Hollandite Ceramics for Cesium Immobilization, Environnemental Issues and Waste Management Technologies in the Ceramic and Nuclear Industries IX *Part I,"*

Ceramics for Waste or Nuclear Applications, Vol. 155, pp. 11-20, 2012.

[20]. M.L. Carter, E.R. Vance, G.R. Lumpkin and G.R. Loi, "Aqueous dissolution of Rb-bearing hollandite and Synroc-C at 90 °C," *Materials Research Society Symposium Proceedings*, Vol. 663, pp. 381-388, 2000.

[21]. H. Rabiller, F. Bart, F.Miserque, G. Leturcq, D. Rigaud, Leaching behavior of hollandite ceramics for cesium immobilization, ATALANTE, Nimes, Juin 2004.

[22]. S.E. Kesson, and T. J. White, "Radius ratio tolerance factors and the stability of hollandites," *Journal of Solid State Chemistry*, Vol. 63, pp. 122-125, 1986.

[23]. F. Aouchiche, N. Kamel, Z. Kamel, S. Kamariz, Y. Mouheb, D. Moudir, "Synthèse et caractérisation d'une céramique de confinement du Cs, de formule chimique K0.28Ba0.76 Cu0.9Ti7.10O16," Internal Report, November 2013.

[24]. Philips X'Pert High Score Package, Diffraction Data CD-ROM, International Center for Diffraction Data, Newtown Square, PA, 2004.

[25]. D.M. Strachan: "Glass dissolution: Testing and modelling for long-term behavior," *Journal of Nuclear Materials*, Vol. 298, pp. 69-77, 2001.

[26]. JCPDS, PCPDFwin. Diffraction Data CD-ROM. International Center for Diffraction Data, Newtown Square, PA, 2004.

[27]. C. Fillet and Nicolas Dacheux, Matrices céramiques pour conditionnements spécifiques, Dossier Techniques de l'Ingénieur bn3770, Ed. Techniques de l'Ingénieur, Paris, France, 2011.

[28]. G. Leturcq, P. Mcglinn, C. Barbé, M.G. Blackford and K.S. Finnie, "Aqueous alteration of nearly pure Nd-doped zirconolite (Ca0.8Nd0.2ZrTi1.8Al0.2O7), a passivating layer control," *Applied geochemistry*, Vol. 20, pp. 899-906, 2005.

[29]. G. Leturcq, T. Advocat, K. Hart, G. Berger, J. Lacombe and A. Bonnetier, "Solubility study of Ti,Zr-based ceramics designed to immobilize long-lived radionuclides," *American Mineralogist*, Vol. 86, pp. 871–880, 2001.

[30]. D. Bregiroux, "Synthèse par voie solide et frittage de céramiques à structure monazite," thesis, faculté des sciences et techniques, Université de Limoges, France, Novembre 2005.

[31]. N. Kamel, H. Ait amar and S. Telmoune, "Study of the dissolution of three synthetic minerals: zirconolite, y-britholite and mono-silicate fluorapatite," *Annales de chimie et science des matériaux*, Vol. 32, pp: 547-559, 2007.

[32]. B. Shabalin, Y. Titov, B. Zlobenko and S. Bugera, "Ferric titanous hollandite analogues — Matrices for immobilization of Cs-containing radioactive waste: Synthesis and properties," *Mineralogy*, Vol. 35, pp. 12-18, 2014.

[33]. T. Suzuki-Muresan, J. Vandenborre, A. Abdelouas, B. Grambow and S. Utsunomiya, "Studies of (Cs,Ba)-hollandite dissolution under gamma irradiation at 95 °C and at pH 2.5, 4.4 and 8.6," *Journal of Nuclear Materials*, Vol. 419, pp. 281–290, 2011.

[34]. A.G. Solomah, P.G. Richardson and A.K. McIlwain, "Phase identification, microstructural characterization, phase microanalyses and leaching performance evaluation of SYNROC-FA crystalline ceramic waste form," *Journal of Nuclear Materials*, Vol. 148, pp. 157-165, 1987.

[35]. Z. Klika, Z. Weiss, M. Mellini and M. Drabek, "Water leaching of cesium from selected cesium mineral analogues," *Applied Geochemistry*, Vol. 21, pp. 405–418, 2006.

RESEARCH ARTICLE

Biogas production from sewage sludge as a distributed energy generation element: A nationwide case study for Turkey

Suleyman Sapmaz[1],* (iD), Ibrahim Kilicaslan[2] (iD)

[1] Kocaeli University, Energy Systems Eng. Dept. Umuttepe Campus 41380 İzmit, Kocaeli, TURKEY
[2] TÜBİTAK Marmara Research Center, Gebze, Kocaeli, TURKEY

ABSTRACT

Sewage sludge is outcome of the wastewater treatment process. It contains hazardous biological and chemical compounds that need to be stabilized. Anaerobic digestion is among the stabilization methods of sewage sludge. Digestion process destroys organic fraction of sewage sludge and produces biogas (%65 Methane, %34 CO_2 and etc.). Biogas is burned in internal combustion engines to produce electricity. Digested residue can be used fertilizer. In this study, the total electricity production that can be obtained by anaerobic digestion of all wastewater treatment plants throughout the country is examined. Main objective of this study is preliminary evaluation of energy potential of biogas from sewage sludge anaerobic digestion. Since Wastewater Treatment Plants are distributed in the various regions of a city, above mentioned biogas plants should be considered as distributed generation equipment. Use of small scale energy production plants near the consumers is called distributed generation. Energy transmission losses and related infrastructure cost can be reduced or delayed by means of distributed generation. Within a smart grid approach, mentioned plants can support electricity grid. They can also serve as local emergency power plants. As a nationwide scenario WWTP are evaluated. Biogas energy capacity potential of 234 plants is calculated. Capacities less than 100 kWe are assumed to be non-feasible due to scale economy. It is evident that 91 plants can be installed with an average capacity of 660 kWe.

Keywords: Biogas, sewage sludge, distributed generation, waste to energy

1. INTRODUCTION

Global warming directs mankind to think energy and environment together. Most of the harmful emissions are produced by energy plants. There are two effective strategies to decrease emissions; increasing energy efficiency either in supply and demand side and exploitation of renewable energy sources.

Electricity supply system of a country should transmit clean, cheap, reliable energy. Energy should be available in every case. The planning of the energy mixture is dependent on countries' domestic resources. Primary energy sources are fossil fuels (coal, natural gas, fuel oil, biomass), renewables (hydroelectric, solar, wind, geothermal, biogas) and nuclear energy.

Centralized, conventional fossil fuel based power plants fulfills the major part of global energy production. Coal and natural gas are primary sources of electrical energy production. Coal causes high rate of emissions harmful to environment. Natural gas is not present in every country. However, natural gas being a trade material, it is also a political source. That affects energy security of countries.

Centralized energy production requires installation of high capacity transmission lines. As the technology and urbanization increases so the energy requirement. This causes risks of failure in the network. Development of new technologies also decreases the cost of small scale energy systems. Distributed generation (DG) approach encourages relatively lower capacity (<10MW) power plant installations in the energy demand area. By this aspect, transmission losses are prevented. When combined heat and power (CHP) systems are used for energy production, waste heat of process can also be used and hence increase system energy efficiency. DG

can be used as emergency power supply in case of contingencies with the islanding capabilities [1].

In this study energy production potential of sewage sludge (SS) from waste water treatment plants (WWTP) is investigated. Biogas (from anaerobic digestion of SS) based electrical energy potentials are calculated. Since the most of the WWTP are located near the urban areas and distributed to different locations of a city, these plants can be considered as DG units. Evaluation results are discussed from nationwide DG aspect.

Capacity and properties of 234 existing and operational WWTP's are investigated. Information about WWTPs are compiled from public report of KAMAG Project named as "Management of Residential/Urban WWT Sludge Project", (Project number 108G167).

2. ENERGY PRODUCTION FROM SEWAGE SLUDGE

India's Solid fraction SS contains organic material. This organic material is combustible. SS calorific value is generally between 10-14 MJ kg^{-1} [2-4] and sometimes may reach 17 MJ kg^{-1} [5-7]. Combustion and anaerobic digestion are well investigated Waste to Energy (WtoE) approaches for Sewage Sludge (SS) [3, 6, 8-15, 16-18]. Direct combustion or co firing with coal or biomass is common energy production solution. Fertilizer recovery from ashes of SS [19, 22] is another option. Organic fraction of the sludge solids is digested by means of bacterial activity in special digesters resulting biogas production. Produced biogas can be converted to electrical energy in Gas Engines. Other emerging technologies to exploit energy from SS are gasification, pyrolysis and hydrothermal carbonization [17, 23, 24-31, 32]. In this study biogas option is selected as it is a mature technology. Digested stable material can be converted to fertilizer depending of composition. This approach supports recycle of biomass in natural environment.

3. RESEARCH METHODOLOGY

Design methodology for a single stage, high rate mesophilic anaerobic digester is given as summary [8] and as detailed [32] in the literature. Main measures
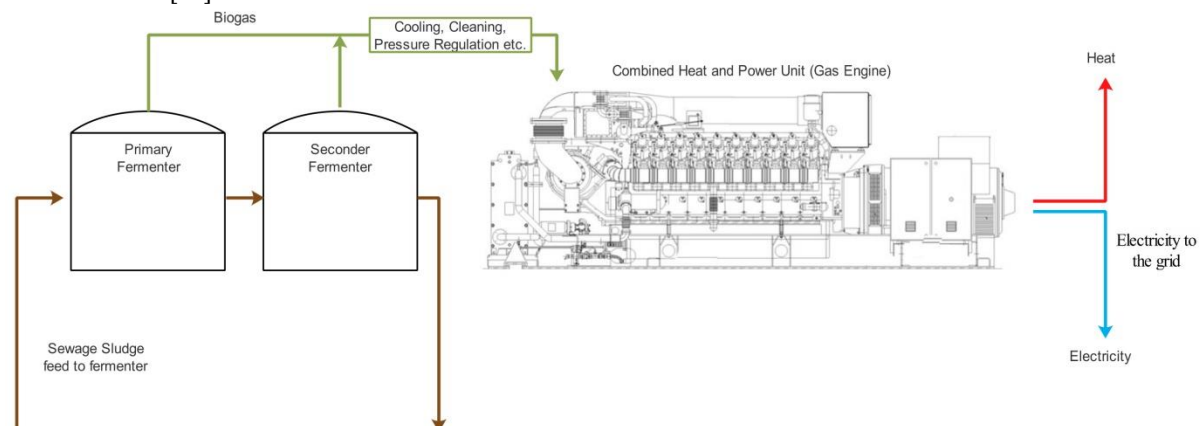
of energy potential of a SS are wastewater feed (Q, m^3 day^{-1}) and biodegradable COD (kg m^{-3}). Within an anaerobic digestion process; pH, alkalinity, temperature, and retention times affect the rates of the different steps of the digestion [8]. Full design of a biogas plants require analysis of WWTP process and effluent values, area requirement etc. In this study rather than a case specific full design study a preliminary potential calculation performed. Biogas potential calculation methodology conducted according to [32]. Information of WWTP are collected from public report of KAMAG Project (108G167) Management of Residential/Urban WWT Sludge [33].

Biogas is a product of digestion of organic matter in the solid phase of the sludge. Biodegradable COD is the measure of organic matter in the sludge. Biodegradable COD loading to digester can be calculated using Equation (1). Total volatile solid production per day is calculated with Equation (2).

$$COD_b \ Load = COD_b * Q \tag{1}$$

In Equation (1) COD_b is the ratio of biodegradable COD in sludge, (kg COD m^{-3} sludge). Q is the wastewater flow, m^3 day^{-1}.

$$P_x = Y * Q / (1 + k_d * SRT) \tag{2}$$

In Equation (2), Y (=0,08) and k_d (0,02< k_d <0,04 for mesophilic conditions) are the yield coefficient and endogenous coefficient respectively. Yield coefficient is the ratio of volatile solids production per COD_b (g VSS g^{-1} BOD). k_d is constant and accepted as 0.03 [32]. SRT is sludge residence time (days) in the digester. In the mesophilic conditions, for SRT values above 12–13 day; changes in volatile solids destruction increase are rather small [8]. Hence the SRT is accepted as 13 days. Methane (CH_4) gas production per day is calculated according to Equation (3).

$$V_{CH4} = 0.40 * (COD_b \ Load * C) - 1.42 * P_x) \tag{3}$$

Biogas composition of AD of sewage sludge is %50-75 CH_4, %24-40 CO_2, %1-2 H_2O and relatively small amount of H_2S, N_2, H_2, O_2 also present [2]. As an averaging approach, Methane rate in biogas can be accepted as %65. Regarding to this value, total biogas production can be calculated using Equation (4).

$$V_{biogas} = VCH_4 / 0.65 \tag{4}$$

Fig 1. Energy conversion in a biogas plant

Table 1. Constant Parameters

Parameter	Value	Unit
Specific gravity of water	1.02	-
Solid content of sludge	5	%
SRT	13	days
Density of water	1000	kg m^{-3}
COD$_b$	0.3	kg m^{-3}
Waste conversion rate - C	50	%
Yield coefficienct - Y	0.08	-
Endogenous coefficient - k$_d$	0.03	-
Methane content of biogas	65	%
Methan conversion rate	40	%

Internal combustion engines, fuel cells, micro gas turbines are main devices for the electrical conversion of biogas. Internal combustion engine (gas engine) is selected as conversion device for the evaluation. Electrical conversion efficiency of a gas engine is %35. Biogas energy input can be calculated using methane gas calorific value, 35.8 MJ N^{-1} m^{-3}. Biogas Plant electrical capacity can be calculated according to Equation (5).

$$E_{biogas}=H_{CH4}*0.35 \tag{5}$$

4.   RESULTS

Anaerobic digestion of organic waste produces two valuable products biogas and digestate that can be used as fertilizer [3]. Digestate is produced during anaerobic digestion and it is a valuable product in terms of nutrients [34]. In this study energy potential of 234 WWTP in case of an anaerobic digester biogas production plant installation calculated using Equation (1)-(5). On the theoretical basis energy content of organic matter present in municipal wastewater, is higher than the energy requirement of the WWT process [35]. However, in practice WTPs are not a negligible source of greenhouse gases (GHG). In this regard, the collection of biogas from anaerobic digestion of sludge and energy recovery is an option for the reduction of GHG emissions [3].

Total potential energy capacity is found to be 60 MWe electricity. Total proposed plant number is 93. Energy production units located on WWTPs can be considered as distributed generation elements. Distributed generation of electricity by anaerobic digestion means that urban districts could be self-supporting in terms of electricity, heat and cooling [36]. Total potential capacity is 0.06% of country's installed capacity. Despite that the value is rather small in numbers, by using electricity and heat together overall utilization efficiency could reach to 90% causing an important save of GHG emission [36]. Average potential capacity of proposed plants is 660 kWe.

Fig 2 shows capacity of every plant with descending order. Plant size distribution is stable. High capacity

(above 1 MWe) plants (listed in Fig 4) are located in the crowded cities.

Fig 3. Shows regional distribution of power plants. Energy potential depends on WWTP processing capacity and population. Marmara is the most urbanized region thus the highest potential capacity is calculated. Even the plant counts are high in the Akdeniz, Ege and Karadeniz regions total potential capacity is relatively small. This can be conclusion the fact that Akdeniz and Ege are touristic regions so the settlements are small and Karadeniz region is a highland so the settlements are distributed and small.
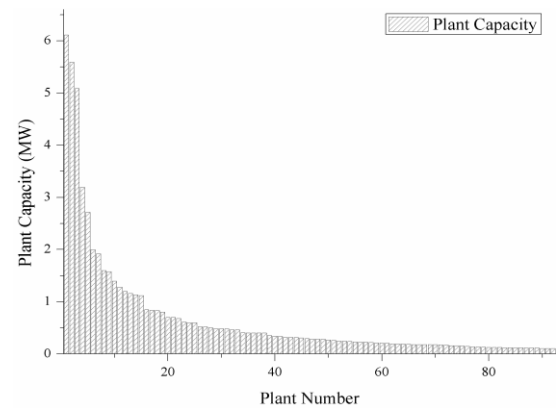

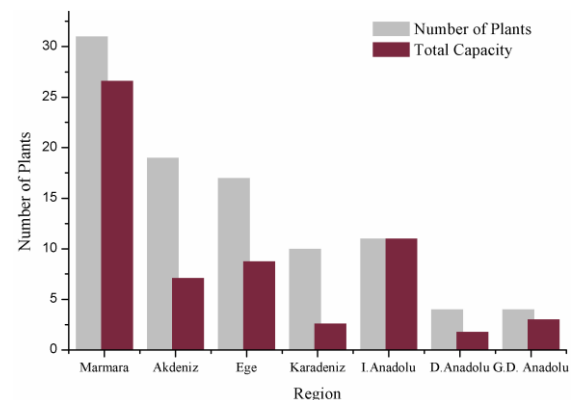**Fig 2.** Distribution of capacity ranges of proposed biogas power plants

Fig 3. Regional distribution and capacity of plants

Capacity and names of 15 plants whose capacity are higher than 1 MWe are listed in Fig 4. 7 of 15 plants are located in the İstanbul -the most crowded city of Turkey. Other 8 plants are also located in the biggest cities of country. There is also options for increasing the energy potential of plants like co-digestion of SS with various organic waste. Co-digestion is an anaerobic digestion method with at least two different wastes that are mixed and digested together. Among the options for additional waste for co-digestion, landfill leachate and organic fraction of municipal solid waste are proved to increase biogas production rate [34].

Among the advantages of the DG is support of supply during the peak load conditions. SS based biogas plant energy production generally do not fluctuate. This is an important advantage over solar and wind systems. There are also constraints for the integration of distributed generation like price of electricity, power

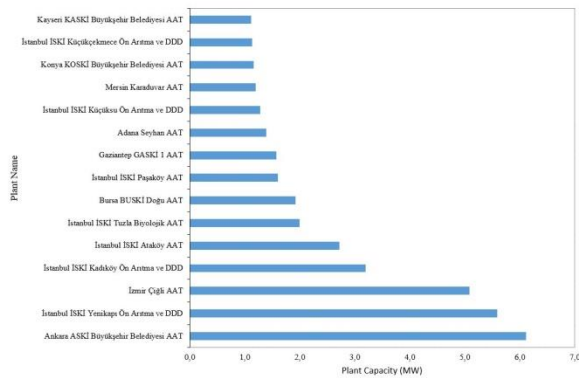quality, infrastructure requirements, and technical performance [37].

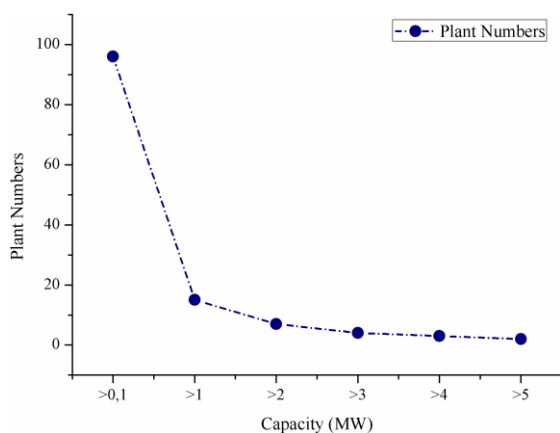**Fig 4.** List of plants with a capacity of more than 1 MWe

Fig 5. Capacity distribution of proposed plants

5. CONCLUSIONS

Sewage sludge is a valuable source rather than a waste. Exploitation of energy potential of this abundant resource can be accomplished by various methods including biogas production. In this study electricity production by using biogas plants is investigated for all of WWTPs of the country. 91 of the 234 plants are found to be feasible (electrical capacity >100 kWe) for biogas installation regarding potential electricity capacity. Regarding the wastewater flowrate %95 of total capacity can be used in electricity production. As an alternative option, power demand fluctuations in peak hours can be managed with built in biogas storage units.

For the non-feasible group of plants, installation of regionally centralized combustion plants can be analyzed. Collected sludge can be dried and combusted to produce electricity. Further studies should be conducted on two aspects: Feasibility analysis of proposed biogas plants with region specific SS properties values and economical aspects and preliminary design of common combustion plants for small scale plants sludge in every city.

REFERENCES

[1]. Z. Abdmouleh, A. Gastli, L. Ben-Brahim, M. Haouari and N. A. Al-Emadi, "Review of optimization techniques applied for the integration of distributed generation from renewable energy sources," *Renewable Energy*, Vol. 113, pp. 266–280, 2017.

[2]. I.F.S. Dos Santos, R.M. Barros and G.L. Tiago Filho, "Electricity generation from biogas of anaerobic wastewater treatment plants in Brazil: An assessment of feasibility and potential," *Journal of Cleaner Production*, Vol. 126, pp. 504–514, 2016.

[3]. A.T.A. Felca, R.M. Barros, G.L. Tiago Filho, Ivan F. S. Santos and E.M. Ribeiro, "Analysis of biogas produced by the anaerobic digestion of sludge generated at wastewater treatment plants in the South of Minas Gerais, Brazil as a potential energy source," *Sustainable Cities and Society*, Vol. 41, pp. 139-153, 2018.

[4]. M.C. Samolada and A.A. Zabaniotou, "Comparative assessment of municipal sewage sludge incineration, gasification and pyrolysis for a sustainable sludge-to-energy management in Greece," *Waste Management*, Vol. 34, pp 411-420, 2014.

[5]. T. Murakami, Y. Suzuki, H. Nagasawa, T. Yamamoto, T. Koseki, H. Hirose and S. Okamoto, "Combustion characteristics of sewage sludge in an incineration plant for energy recovery," *Fuel Processing Technology*, Vol. 90, pp. 778–783, 2009.

[6]. D. Lechtenberg and H. Diller. Alternative Fuels and Raw Materials Handbook for the Cement andLime Industry, Vol 1. MVW Lechtenberg Projectentwicklungs- undBeteiligungsgegelschaft. Düsseldorf, Germany, 2012.

[7]. J. Sadhukhan, "Distributed and micro-generation from biogas and agricultural application of sewage sludge: Comparative environmental performance analysis using life cycle approaches," *Applied Energy*, Vol. 122, pp. 196–206, 2014.

[8]. L. Appels, J. Baeyens, J. Degrève and R. Dewil, "Principles and potential of the anaerobic digestion of waste-activated sludge," *Progress in Energy and Combustion Science*, Vol. 34, pp. 755–781, 2008.

[9]. V. Paolini, F. Petracchini, M. Carnevale, F. Gallucci, M. Perilli, G. Esposito, M. Segreto, L.G. Occulti, D. Scaglione, A. Ianniello and M. Frattoni, "Characterisation and cleaning of biogas from sewage sludge for biomethane production," *Journal of Environmental Management*, Vol. 217, pp. 288–296, 2018.

[10]. C. Bougrier, J. P. Delgenès and H. Carrère, "Effects of thermal treatments on five different waste activated sludge samples solubilisation, physical properties and anaerobic digestion," *Chemical Engineering Journal*, Vol. 139, pp. 236–244, 2008.

[11]. K. Gorazda, B. Tarko, S. Werle and Z. Wzorek, "Sewage sludge as a fuel and raw material for phosphorus recovery: Combined process of gasification and P extraction," *Waste Management*, Vol. 73, pp. 405-415, 2018.

[12]. S. Werle and R. K. Wilk, "A review of methods for the thermal utilization of sewage sludge: The Polish perspective," *Renewable Energy*, Vol. 35, pp. 1914–1919, 2010.

[13]. A. Sever Akdağ, A. Atımtay and F.D. Sanin, "Comparison of fuel value and combustion characteristics of two different RDF samples," *Waste Management*, Vol. 47, pp. 217-224, 2016.

[14]. G.K. Parshetti, Z. Liu, A. Jain, M.P. Srinivasan and R. Balasubramanian, "Hydrothermal carbonization of sewage sludge for energy production with coal," *Fuel*, Vol. 111, pp. 201–210, 2013.

[15]. M. Ragazzi, E.C. Rada and R. Ferrentino, "Analysis of real-scale experiences of novel sewage sludge treatments in an Italian pilot region," *Desalination and Water Treatment*, Vol. 55, pp. 783–790, 2015.

[16]. Y. Cao and A. Pawłowski, "Life cycle assessment of two emerging sewage sludge-to-energy systems: Evaluating energy and greenhouse gas emissions implications," *Bioresource Technology*, Vol. 127, pp. 81–91, 2013.

[17]. J. Werther and T. Ogada, "Sewage sludge combustion," Progress in Energy and Combustion Science, Vol. 25, pp. 55–116, 1999.

[18]. S. Donatello and C.R. Cheeseman, "Recycling and recovery routes for incinerated sewage sludge ash (ISSA): A review," *Waste Management*, Vol. 33, pp. 2328–2340, 2013.

[19]. I. Kliopova and K. Makarskiene, "Improving material and energy recovery from the sewage sludge and biomass residues," *Waste Management*, Vol. 36, pp. 269–276, 2015.

[20]. K. Gorazda, B. Tarko, Z. Wzorek, H. Kominko, A.K. Nowak, J. Kulczyck, A. Henclik and M. Smol, "Fertilisers production from ashes after sewage sludge combustion – A strategy towards sustainable development," *Environmental Research*, Vol. 154, pp. 171–180, 2017.

[21]. H. Weigand, M. Bertau, W. Hübner, F. Bohndick and A. Bruckert, "RecoPhos: Full-scale fertilizer production from sewage sludge ash," *Waste Management*, Vol. 33, pp. 540–544, 2013.

[22]. M. Tomasi Morgano, H. Leibold, F. Richter, D. Stapf and H. Seifert, "Screw pyrolysis technology for sewage sludge treatment," *Waste Management*, Vol. 73, pp. 487–495, 2017.

[23]. N. Gao, J. Li, B. Qi, A. Li, Y. Duan and Z. Wang, "Thermal analysis and products distribution of dried sewage sludge pyrolysis," *Journal of Analytical and Applied Pyrolysis*, Vol. 105, pp. 43–48, 2014.

[24]. V. Frišták, M. Pipíška and G. Soja, "Pyrolysis treatment of sewage sludge: A promising way to produce phosphorus fertilizer," *Journal of Cleaner Production*, Vol. 172, pp. 1772–1778, 2018.

[25]. H.S. Kambo and A. Dutta, "A comparative review of biochar and hydrochar in terms of production, physico-chemical properties and applications," *Renewable & Sustainable Energy Reviews*, Vol. 45, pp. 359–378, 2015.

[26]. N. Mills, P. Pearce, J. Farrow, R. B. Thorpe and N. F. Kirkby, "Environmental & economic life cycle assessment of current & future sewage sludge to energy technologies," *Waste Management*, Vol. 34, no. 1, pp. 185–195, 2014.

[27]. A. Kumar and S.R. Samadder, "A review on technological options of waste to energy for effective management of municipal solid waste," *Waste Management*, Vol. 69, pp. 407–422, 2017.

[28]. B. Groß, C. Eder, P. Grziwa, J. Horst and K. Kimmerle "Energy recovery from sewage sludge by means of fluidised bed gasification," *Waste Management*, Vol. 28, pp. 1819–1826, 2008.

[29]. S. Werle, "Modeling of the reburning process using sewage sludge-derived syngas," *Waste Management*, Vol. 32, no. 4, pp. 753–758, 2012.

[30]. L. Fiori, D. Basso, D. Castello and M. Baratieri, "Hydrothermal carbonization of biomass: Design of a batch reactor and preliminary experimental results," *Chemical Engineering Transactions*, Vol. 37, pp. 55–60, 2014.

[31]. M. Escala, T. Zumbühl, C. Koller, R. Junge and R. Krebs, "Hydrothermal carbonization as an energy-efficient alternative to established drying technologies for sewage sludge: A feasibility study on a laboratory scale," *Energy and Fuels*, Vol. 27, pp. 454–460, 2013.

[32]. Metcalf & Eddy et al., Wastewater engineering: treatment and resource recovery.

[33]. Committee, "Management of Residential/Urban WWT Sludge" 2010. Available: http://webdosya.csb.gov.tr/db/cygm/editordosya/IP_1.pdf [Accessed: May. 31, 2018].

[34]. H. Guven, M. S. Akca, E. Iren, F. Keles, I. Ozturk and M. Altinbas, "Co-digestion performance of organic fraction of municipal solid waste with leachate: Preliminary studies," *Waste Management*, Vol. 71, pp. 775–784, 2018.

[35]. H. Ozgun, H. Guven, R. Kaan Dereli, I. Ozturk, I. Isik and M. Evren Ersahin, "Energy recovery potential of anaerobic digestion of excess sludge from high-rate activated sludge systems for co-treatment of municipal wastewater and food waste," *Energy*, Vol. 172, pp. 1027–1036, 2019.

[36]. S. Evangelisti, P. Lettieri, R. Clift and D. Borello, "Distributed generation by energy from waste technology: A life cycle perspective," *Process Safety and Environmental Protection*, Vol. 93, pp. 161–172, 2015.

[37]. G. Allan, I. Eromenko, M. Gilmartin, I. Kockar and P. McGregor, "The economics of distributed energy generation: A literature review," *Renewable & Sustainable Energy Reviews*, Vol. 42, pp. 543–556, 2015.

Environmental Research & Technology

RESEARCH ARTICLE

The effects of fertilization on the green tea elements

Ertugrul Osman Bursalioglu[1,*] (iD)

[1]Bioengineering Department, Faculty of Engineering, Sinop University, Sinop, TURKEY

ABSTRACT

Camellia sinensis, which is widely used as a beverage in our country and in the world, has various beneficial effects on human health due to its various components. Farmers use chemical fertilizers to get more products. However, the use of more chemical manure may cause some problems in terms of environmental pollution and human health. Due to the lack of some nutritious minerals in the soil, various manure ingredients are used for better cultivation and growth. In this study, in order to investigate the effect of use of manurate on tea plant on 5 different soils in Rize, the concentrations of 18 elements in the leaves were analyzed using the ICP-MS device. When manure was used in tea, the concentration of Li, Mg, K, Al, Ca, Cr, Mn, Fe, Cu, Zn, As, Se, Cd, Pb elements increased and Na, Co, Ni, Hg values decreased.

Keywords: Camelia sinensis, element, environmental pollution, green tea, ICP MS, manure

1. INTRODUCTION

The tea plant is a perennial plant of the genus Camellia of the Theaceae family, which is green in all seasons, usually grown in high regions. Tea is the second most commonly drank liquid on earth after water. It is being consumed socially and habitually by people since 3000 BC [1]. The tea plant is grown in at least 30 countries, in various parts of Asia, Africa and the Middle East. There are 2 varieties of Camellia sinensis, *Camellia sinensis* variety tea (Chinese tea) grown in China, Japan and Taiwan and *Camellia sinensis* variety assamica (Assam tea) which is common in south and southeast Asia. Chinese tea varieties are grown in Turkey as well [1, 2].

Green tea contains many ingredients; such as enzymes, polyphenols, alkaloids, nitrogen compounds, caffeine, essential oils, carbohydrates, pigments, vitamins, organic acids, aroma-forming substances, and minerals [3-5]. Epigallocatechin gallate (EGCG), a group of catechins, is a very effective antioxidant, believed to be a crucial substance in the therapeutic properties of green tea [6, 7]. In addition to green tea is a medical plant widely used by local people in India, China, Japan and Thailand for a long time [8, 9]. From this point on; some of the ingredients obtained from the tea are said to be beneficial to human health [1].

It was determined that tea plants have antioxidant, anticancer, antiaging, and anti-inflammatory effects [10-12]. Several studies have tried to prove that regular use of green tea is preventive against some chronic diseases. Green tea is protective against coronary heart diseases, diabetes [13], various types of cancer such as stomach and colorectal [8, 14], breast, throat, prostate [15]. Also, green tea has been shown to be effective in regulating bone density, preventing obesity, protecting against UV rays, preventing hemolysis, aging and cognitive disorders [8, 14].

In this study, it is aimed to determine the effect of the fertilization on concentration of 18 elements in the green tea leaves grown at 5 different region in Rize, Turkey. This study further investigate decreasing the amount of chemical fertilizers or searching alternative fertilizer methods.

2. MATERIALS & METHOD

2.1. Supply of plant samples

Rize; in the highest part of the Eastern Black Sea region 400 20'east and 410 20' between the northern latitudes, is located in northeastern Turkey. The pH of

the soil where green tea is collected is around 3.14-5.88. The average annual rainfall over 2000 mm, the dispersion of rain by month should be regular, at least 70 % relative humidity and soil. Tea is collected three times in a year. First collection is in May, second is in July, and the third is in August-September. Green tea with and without manure in the soil were collected in five separate regions in an area of 2 kilometer from–Rize, in Turkey (5 fertilized and 5 unfertilized tea leaves were taken from this region (Table 1)). Manure content is that: N, NH_4-N, P, K, in 50 kg package. 60-70 kg of manure per hectare is applied at the end of March.

Table 1. Situation of manure in the tea fields

Field	Situation of fertilization
1	10 years fertilized
2	10 years fertilized
3	10 years fertilized
4	10 years fertilized
5	10 years fertilized
6	10 years unfertilized
7	10 years unfertilized
8	10 years unfertilized
9	10 years unfertilized
10	10 years unfertilized

Green tea samples (five) used in our tests were collected from a tea garden at the first collection periods in May 2018. Leaves on top branches of tea plants were collected, placed in a sealed plastic bag and immediately transferred to laboratory. Before extraction, an extensive literature search was carried out to find out the most effective and suitable extraction procedure. Green tea leaves were liofilised by Telstar LyoQuest (P: 0.2 milibar, 24 hours) and stored -20°C. Situation of manure in the tea fields are detailed in Table 1.

2.2. Preparation of ICP-MS Standards and Solutions

Firstly, for the measurement of Co, Se, Na, Mg, K, Ca, Mn, Fe, Cu, Zn, Al in tea leaves standard solutions were prepared. For the measurement of alkali metals (Ca, Mg, Na, K) to be healthy, standards should be prepared as ppm (mg/L) and others (Cd, Pb, Hg, As, Fe, Mn, Co, Ni, Cu, Zn, Al, Cr, Ag, Se, V, Be, Ba, Tl, U, Ga, Li, Rb, Cs, Sr, Sb) should be prepared in ppb (μg/L) level. The standards used are as follows: 1000 ppm(mg L^{-1}=μg mL^{-1}) Ca, Mg, Zn, Sb :10 ppm Mix Cd, Pb, As, Fe, Mn, Co, Ni, Cu, Zn, Al, Cr, Ag, Se, V, Be, Ba, Tl, U, Ga,Li, Na, Ca, Mg, K, Rb, Cs, Sr : 10ppm Hg.

HNO_3 %1: Ultra-pure water is filled in half of a 250 ml glass tube. 2.4 ml HNO3 added to the line up to 220 ml with pure water. Preparation of 1ppm stock solution containing 27 elements and 100 ppb Hg: 1mL 10 ppm Agilent 8500-6940 2A mixture and 0.1mL 10 ppm Agilent 8500-69400-Hg is added to the test tube. Then 8ml pure water is added on it. Preparation of 100 ppm Ca+Mg stock solution: 1mL Ca 1000 ppm (μg mL^{-1}, mg

L^{-1}) (Merck170308) mixture and 1mL 1000 ppm Mg (Merck170331) is added to the test tube. Then 8ml pure water is added on it.

In this study, green tea samples were collected from an area of throughly 600-650 meters above sea level in Rize. Green tea with and without manure in the soil were collected in five separate regions in an area of 2 kilometer.

2.3. ICP MS test procedure

Fresh tea leaves were dried for 24 hours and then placed in a microwave. Microwave acid digestion procedure was as follows: Place a TFM vessel on the balance plate, tare it and weight of the sample. Introduce the TFM vessel into the HTC safety shield. Add the acids; if part of the sample stays on the inner wall of the TFM vessel, wet it by adding acids drop by drop, then gently swirl the solution to homogenize the sample with the acids. Close the vessel and introduce it into the rotor segment, then tighten by using the torque wrench. Insert the segment into the microwave cavity and connect the temperature sensor. Run the microwave program to completion. Cool the rotary by air or by water until the solution reaches room temperature. Open the vessel and transfer the solution to a marked flask.

Measurements of multi elements in the tea leaves were performed using the Agilent 7700x ICP-MS. The samples were directly put into the ICP-MS system using a standard peristaltic pump with Tygon pump tube (internal diameter of 1.02 mm) and ASX-520 automatic sampler. Analyses were executed in time resolve analysis mode using an integration time of 3 ms for all stages. A rinse solution containing 1% nitric acid was used to provide sample washing during each stage. The general settings of the Agilent 7700x system are detailed in Table 2. Our analysis conforms to the EPA 6020 standard.

Table 2. Agilent 7700x operating conditions

Parameter	Value
Forward power	1550 W
Carrier gas flow rate	0.8 L min^{-1}
Make-up gas flow rate	0.32 L min^{-1}
Spray chamber temperature	2 °C
Sampling depth	8.0 mm
ORS^3 helium gas flow rate	5.0 mL min^{-1}

3. RESULTS & DISCUSSION

Environmental pollution is one of the most important factors that threaten life.Unconsciously used chemical fertilizers for more products in agriculture threaten the all living life balance. On the other hand, this chemical manure content has a negative effect on substance cycles in nature. These two basic problems cause us to think seriously about plant growth and the use of chemical manure for more products.

Black tea is a very popular drink in our country. In other words; the tea in the cup is consumed more by the people, in some parts of our country than the water in the cup in some periods of their lives. In this study, the concentrations of 18 elements in the leaves

were analyzed by using the ICP-MS device in order to investigate the effect of use of manure on tea plant on 5 different soils in Rize. The results of multi-element analysis in green tea leaf samples are given in the table below (Table 3).

Table 3. Data obtained in the ICP-MS system for tea samples (Conc. ($\mu g\,kg^{-1}$))

Tea Sample	Li (7) ($\mu g\,kg^{-1}$)	Na (23) ($\mu g\,kg^{-1}$)	Mg (24) ($\mu g\,kg^{-1}$)	Al (27) ($\mu g\,kg^{-1}$)	K (39) ($\mu g\,kg^{-1}$)	Ca (43) ($\mu g\,kg^{-1}$)
1	538.31	48261.53	2858044.18	1433023.60	9430681.03	4319273.87
2	696.97	365311.74	3703355.89	1196247.78	10820696	5739499.9
3	915.39	37036.43	3054146.19	2120700.14	8954240.97	9133760.17
4	631.95	56964.90	4712793.90	1832648.62	13737686.45	4759987.55
5	855.69	90178.81	7649338.47	2322422.2	13328255.74	14332095.96
6	1249.88	84986.14	6410117.56	2128400.91	OR	10181722
7	1395.75	71966.72	4832051.20	2113987.87	13097179.86	9829438.59
8	1418.62	72487.78	4668564.63	2449992.61	13626183.08	8345042.71
9	1119.53	84070.92	5324989.32	2223668.84	OR	8362212.11
10	1015.54	86106.70	5408671.66	4959969.27	15901676.71	11947958.53

Tea Sample	Cr (52) ($\mu g\,kg^{-1}$)	Mn (55) ($\mu g\,kg^{-1}$)	Fe (56) ($\mu g\,kg^{-1}$)	Co (59) ($\mu g\,kg^{-1}$)	Ni (60) ($\mu g\,kg^{-1}$)	Cu (63) ($\mu g\,kg^{-1}$)
1	239.74	662183.89	169897.82	384.45	2507.57	5734.8
2	263.42	966069.37	197261.76	1341.56	17348.78	9495.98
3	239.82	2265836.92	155366.13	1447.82	6611.97	7700.24
4	208.13	1220090.79	145927.31	600.76	4424.51	9947.87
5	459.2	2542646.86	374634.94	565.0	6777.47	14350.9
6	544.28	2210857.5	360111.3	1991.41	9153.17	12074.01
7	306.14	1401290.32	253158.02	526.02	5491.92	7651.1
8	529.83	1329223.5	295800.81	462.74	8608.98	10111.01
9	497.27	1865493.72	288011.43	442.35	7011.39	11825.69
10	483.25	1492773.55	354691.9	303.29	3335.16	8392.27

Tea Sample	Zn (66) ($\mu g\,kg^{-1}$)	As (75) ($\mu g\,kg^{-1}$)	Se (82) ($\mu g\,kg^{-1}$)	Cd (111) ($\mu g\,kg^{-1}$)	Hg (201) ($\mu g\,kg^{-1}$)	Pb (206) ($\mu g\,kg^{-1}$)
1	23143.03	47.31	112.04	40.87	266.08	242.7
2	47753.29	46.72	122.48	58.73	165.25	255.93
3	23564.54	53.48	91.15	69.95	138.08	159.78
4	39132.2	63.47	120.29	52.79	144.09	146.23
5	88585.36	78.26	121.29	47.34	218.03	281.97
6	72518.39	66.04	149.09	142.49	189.09	358.4
7	43158.06	69.32	119.88	101.0	162.74	359.72
8	32342.94	68.95	121.85	58.36	192.36	475.53
9	46319.52	84.03	127.5	49.93	147.62	363.98
10	45629.9	91.65	156.12	83.63	142.05	561.65

When manure was used in tea, the concentration of Li, Mg, K, Al, Ca, Cr, Mn, Fe, Cu, Zn, As, Se, Cd, Pb elements increased and Na, Co, Ni, Hg values decreased (Fig 1) (Fig 2). As a result of the use of manure required for

tea, a change was observed due to the binding of minerals.

Taskin and his colleagues (2015) stated the following results regarding a study: K ; about 21. 106 ($\mu g\ kg^{-1}$), Ca; about 1685. 105 ($\mu g\ kg^{-1}$), Mg; about 22. 106 (μg

kg^{-1}). In our study; concentration of K was measured at lower than this value in tea with manured, concentration of Ca was measured in some places less than this value and concentrations of Magnesium measured at lower than this value (Fig 3) (Taskin et al. 2015). The graph of our study of Ca, Mg and K values is shown below.

The comparison of the average values of the 18 elements in the green tea leaf with and without manured is given in the graph below (Fig 4). Decrease in concentration of elements; it can be attributed to the inability of the tea plant to get them enough from the soil.
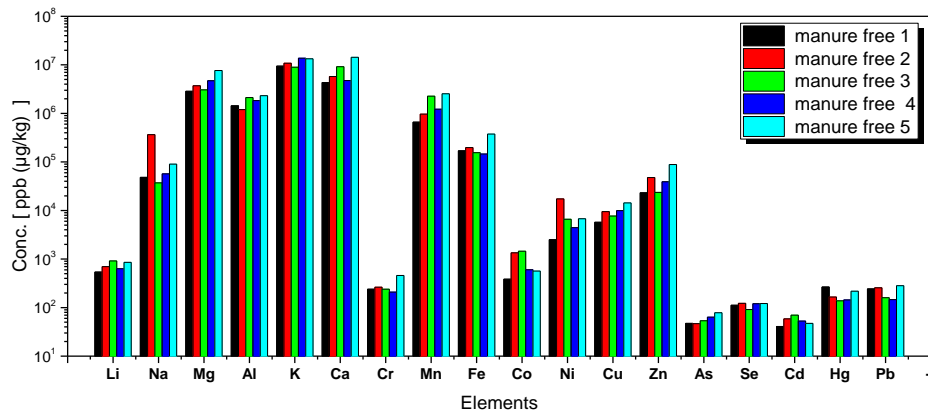

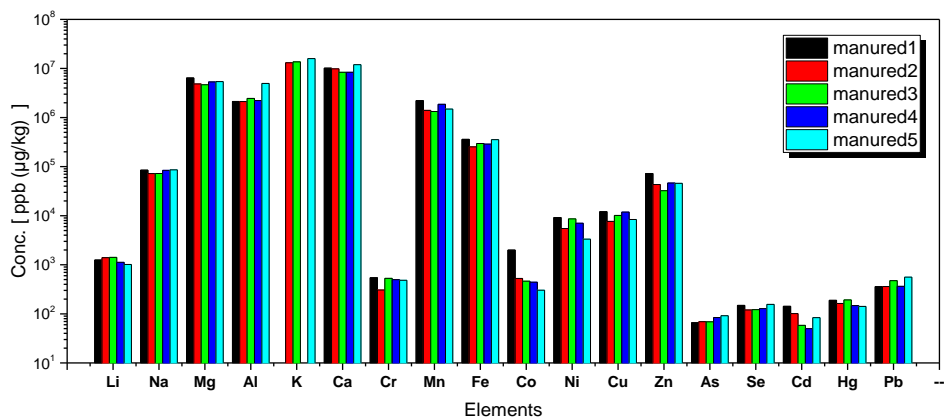**Fig 1.** The element concentrations in the tea grown in unfertilized soils

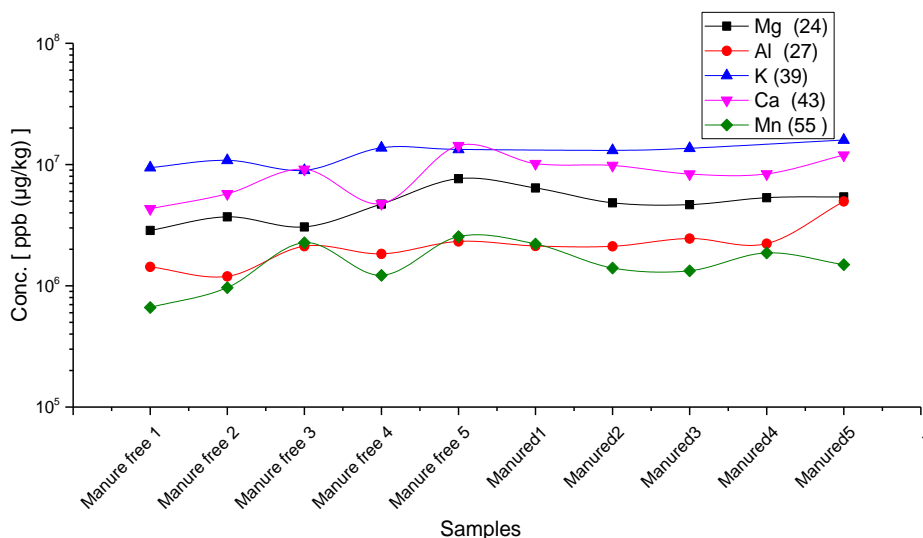**Fig 2.** The element concentrations in the tea grown in fertilized soils

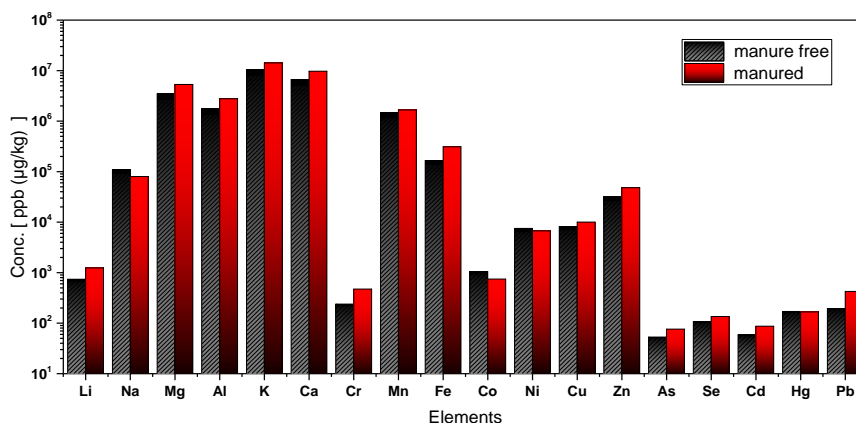**Fig 3.** The changes in some elements concentrations in tea samples

Fig 4. Comparison of element concentrations in two tea groups

4. CONCLUSIONS

The difference in the physical growth of this chemical fertilizer usage to the tea plant should be compared very well in terms of human health and benefit and harm. When this aspect of the study is examined, more and different studies are required. The increase in the concentration of elements in green tea leaves may suggest that the soil may be rich in these elements or may be due to use of manurate. After this study, a larger scale study will be planned. It is designed to include examples of the three tea cultivation periods (May, July, August-September) from other cities of the Black Sea region and the use of other manurate samples.

REFERENCES

[1]. A.B. Sharangi, "Medicinal and therapeutic potentialities of tea (Camellia sinensis L.) ," *Food Research International*, Vol. 42 (5-6), 529–535, 2009.

[2]. K.P. Biswas, "Description of tea plant. In Encyclopaedia of Medicinal Plants," *New Dehli: Dominant Publishers and Distributors*, pp. 964-966, 2006.

[3]. F. Hoffmann, M. Manning, Herbal Medicine and Botanical Medical Fadsi New Yark: The Haworth Press pp. 202. 2005.

[4]. A. Szymczycha-Madeja, M. Welna and P. Pohl, "Elemental analysis of teas and their infusions by spectrometric methods," *Trends in Analytical Chemistry,* Vol. 35 (12), 169–171, 2012.

[5]. B.E Sumpio, A.C. Cordova, D.W. Berke-Schlessel, F. Qin and Q.H. Chen, "Green tea, the Asian Paradox, and cardiovascular disease," *Journal of the American College of Surgeons*, Vol. 202 (1), 813-820. 2006.

[6]. M. Demeule, J. Michaud-Levesque, B. Annabi, D. Gingras, D. Boivin, J. Jodoin, S. Lamy, Y. Bertrand and R. Beliveau, "Green tea catechins as novel antitumor and antiangiogenic compound," *Current Medicinal Chemistry & Anti-cancer Agents*, Vol. 2 (4), 441–63, 2002.

[7]. F.K. Maiti, J. Chatterjee and S. Dasgupta, "Effect of green tea polyphenols on angiogenesis induced by angiogeninlike protein," *Biochemical and Biophysical Research Communications*, Vol. 308 (1), 64–, 2003.

[8]. V.V. Chopade, A.A. Phatak, A.B. Upaganlawar and A.A. Tankar, "Green tea (Camellia sinensis): Chemistry, traditional, medicinal uses and its pharmacological activities- a review," *Pharmacognosy Reviews*, Vol. 2 (3), 157-162, 2008.

[9]. P. Namita, M. Rawat and J.V. Kumar, "Camellia Sinensis (Green Tea," *Global Journal of Pharmacology*, Vol. 6 (2), 52-59, 2012.

[10]. S. Hsu, "Green tea and the ski," *Journal of The American Academy of Dermatology*, Vol. 52 (6), 1049-1059, 2005.

[11]. H.R. Kim, R. Rajaiah, Q.L. Wu, S.R. Satpute, M.T. Tan, J.E .Simon, B.M. Berman and K.D. Moudgil "Green tea protects rats against autoimmune arthritis by modulating disease-related immune events," *Journal of Nutrition*, Vol. 138 (11), 2111-2116, 2008.

[12]. G. Park, B.S. Yoon, J.H. Moon, B. Kim, E.K. Jun, S. Oh et al. "Green tea polyphenol epigallocatechin-3-gallate suppresses collagen production and proliferation in keloid fibroblasts via inhibition of the STAT3-signaling pathway," *Journal of Investigative Dermatology*, Vol. 128 (10), 2429-2441, 2008.

[13]. S. Sarıca, Ü. Karatas and M. Diktas, "Çay (Camellia sinensis) İçerigi Metabolizma ve Saglık Üzerine Etkileri, Antioksidan Aktivitesi ve Etlik Piliç Karma Yemlerinde Kullanımı," *GOÜ Ziraat Fakültesi Dergisi*, Vol. 25 (2), 79-85, 2008.

[14]. I.A. Ross, "Tea common names and its uses". In Medicinal Plants of the World. 3 rd Vol. New Jersey: Humana Press. pp. 1-19. 2005.

[15]. M.X. Doss, S.P. Potta, J. Hescheler and A. Sachinidis, "Trapping of growth factors by catechins: a possible therapeutical target for prevention of proliferative diseases," *Journal of Nutritional Biochemistry*, Vol. 16 (5), 259–266, 2005.